Aspects of Humic and Fulvic Acid Chemistry

by

Michael Patterson

A Doctoral Thesis submitted in partial fulfilment of the requirements for the award of

Doctor of Philosophy

of the Loughborough University of Technology

January 1995

Research supervisor: Dr P. Warwick

"The most important thing
is not to stop questioning."

Albert Einstein

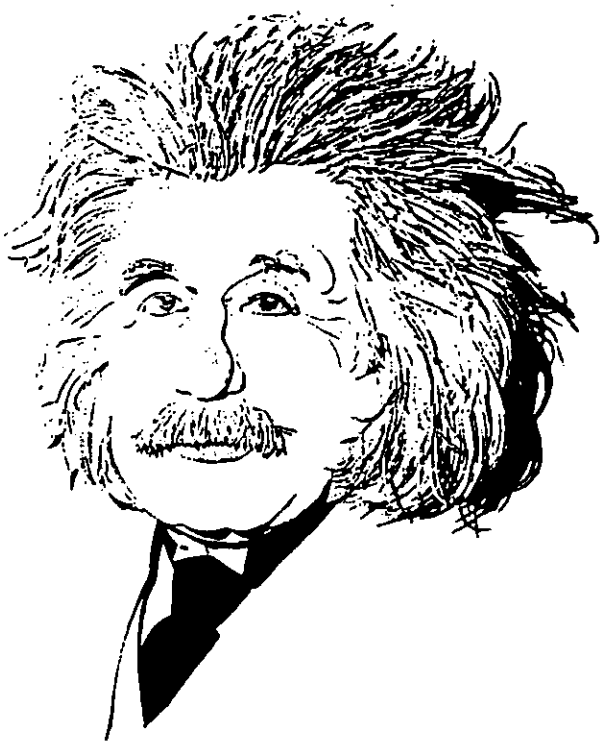

ACKNOWLEDGEMENTS

I would like to thank numerous people who have both helped and supported me since I started my Ph.D as a young inexperienced chemist all those years ago.

I cannot express in words my unending gratitude to Dr Peter Warwick who made everything possible and then was a constant support throughout. His knowledge, understanding, patience and experience has never ceased to amaze or drive me ever forward.

I would also like to express my sincerest gratitude to every member both past and present of the Radiochemistry group at Loughborough University and all the friends that I have in Loughborough (R.Hooper etc.) who all helped to make the time I spent at Loughborough most excellent.

Especial thanks go to John Cobb, Ian Mason, Ian Barwick, Tony Hall, Linda Sands and Christine Bartropp, although no longer together the *'OLD'* group will still live on.

I must also mention the unquestioned support that I have been given by both Hilary Chaning Pearce and my Mother. Thankyou All

ABSTRACT

Humic and fulvic acids are present in all environmental waters and are known to combine with environmental contaminants and pollutants producing water soluble complexes. These complexes may be much more mobile than the unassociated contaminant through the environment because of groundwater and surface water movement. Therefore, of considerable interest, is to determine the characteristics and contaminant complexing ability of these materials.

Most investigations of the complexing abilities of humics have been conducted on material which has been extracted from natural waters. The resulting solid humic material is then redissolved in an aqueous solution of known chemical composition. Part one of this thesis describes work designed to ascertain whether the extraction procedure alters the properties of the material, thus invalidating the results obtained from e.g. stability constant measurements. Experiments showed that the material was not altered and that measurements of stability constants using extracted material were valid. Part Two describes the development of an ion-exchange resin technique for measuring stability constants. Stability constants for the reaction of humic with nickel and europium were measured by this technique. The thesis also contains an account of the investigation and development of a method for investigating metal-humic interactions by fluorescence spectrophotometry. Competition reactions with calcium have also been investigated.

CONTENTS

Chapter One

Introduction

1.1 HUMICS – BACKGROUND

Humic substances are an ubiquitous and preponderant part of the aquatic and terrestrial environment. These complex natural materials have been studied and researched by soil scientists, chemists and numerous other scientists for over two centuries. Methods of extracting humic substances have been found in works by Achard in 1786. He obtained a dark precipitate of humic acid by treating soil with alkali. However, the name humic was not used until somewhat later, in fact it was probably Sausore who first used the term humus in 1804 (1, 2). Humic materials are heterogeneous mixtures of organic substances generally yellow to black with high molecular masses and melting points. They are named and classified according to their solubility in water. Humin is the fraction that is insoluble in water at all pH values. Humic acid is the fraction that is soluble at pH values above 2, whilst fulvic acid is the fraction that is soluble at all pH values. Other methods which have been employed in an attempt to define more specifically the fractions include their adsorption characteristics, hydrophobic character and anionic character. However, no better classification system has been found than that based on their solubility in water. Recently, there has been escalating interest in humic substances by scientists from a diversity of disciplines outside the realms of soil science. Chemists, biologists, geochemists, environmental scientists and medical researchers are now intrigued by the nature, role and application of humic substances in their particular fields of interest, for example the health effects arising from the chlorination of municipal drinking water containing low concentrations of humic substances (3, 4). As well as their presence and role in diverse environments, humic substances are also important because they serve as a major reserve of organic carbon in both soils and aquatic environments for the global carbon cycle (5). Although different aspects of humic substances have been carefully and extensively studied by many scientists for many years, their work has not yet culminated in a fundamental or even general understanding of the geochemical role, origin, mechanism of reaction or formation of humic substances.

However, information on the nature and the geochemical implication of these substances has been slowly and steadily accumulating over the years.

To date there are several basic questions which remain unanswered: What is the precise nature of humic substances? How are they formed? How do they react with metals and other organic materials? Answers have been suggested but no concrete conclusions have been reached.

1.2 ORIGINS OF HUMICS

The precise chemical nature and properties of humic substances depend to some extent on the environment in which they are found, e.g. soil, peat bog, surface water, groundwater, lakes, streams and oceans.

Two main theories prevail, one being that they are derived from the lignified tissue of plant residues and the second that they were formed from simpler components, i.e. sugars or phenols. Maillard (6) worked extensively on this concept of reducing sugars and amino acids to form brown nitrogenous products akin to humics. Maillard's concept that humic substances represented products formed by chemical reactions of simple compounds is in close agreement with some modern views of humus formation. However, Trusor's concept of humification (7) comes even closer to present day concepts. In a series of studies on the biochemistry of humus formation, Trusor postulated the following sequence in the humification process:

(i) hydrolytic decomposition of plant remains with the synthesis of simple substances of aromatic nature;
(ii) oxidation of the latter by microbial enzymes to form hydroxy quinones;
(iii) condensation of the quinones into dark coloured products (humic substances).

Both Maillard and Trusor theories depend on the enzymatic activity of microorganisms.

The view that lignin was a precursor to humics was advanced by Hobson and Page (8), Waksman (9) and others. It was this theory that was generally adopted and had a dominating influence on humus chemistry for decades. However, by the mid 20th century, the lignin theory of humus formation, popularized only two decades earlier by Waksman et al had been rejected by most researchers. The view gradually became accepted that humic and fulvic acids were formed by a multistage process that included:

(i) decomposition of all plant components, including lignin, into simpler monomers;
(ii) metabolism of the monomers with an accompanying increase in the soil biomass;
(iii) repeated recycling of the biomass carbon (and nitrogen) with synthesis of new cells;
(iv) concurrent polymerization of reactive monomers into high-molecular weight-polymers (10) (7).

The general consensus of opinion involves polyphenols synthesized by microorganisms which polymerize alone or in the presence of amino acids. Overall it is probable that a different mechanism or combination of mechanisms predominate in different environments. Whichever mechanism predominates, it is sure to be a dynamic process involving competing formation and degradation reactions and local concentration of humic substances usually vary seasonally with the climatic conditions.

1.3 GROUNDWATER AND SURFACE WATER HUMICS

The present investigation is primarily concerned with the chemistry of humic substances, found in groundwater and surface water.

From a study of several groundwaters, Thurman (11) concluded that the concentration of humic substances in groundwater is generally very much less than in surface water, being of the order of the equivalent of only 1mg l^{-1} of carbon. It is this fact that makes it difficult to investigate humics in groundwater quantitatively, since large amounts of water would be required to produce sufficient quantities of humic material for analysis. However, one hypothesis as to the origin of groundwater is that it originates in overlying soils. Soil interstitial waters leach organic matter from the soil and transport it into the aquifer. The humic material is transported from the oxidizing environment of the soil to the reducing environment of the aquifer where it is modified. If the modification was only slight then it would be possible to use surface water as an analogue to groundwater, and to some extent this is the case. The groundwater humics investigated, generally had more carbon but less oxygen and colour than surface water humics. However, groundwater and surface water humics were found to be similar in carboxyl (COOH) content, molecular masses and in binding constants for copper.

1.4 GENERAL CHEMICAL PROPERTIES OF HUMICS

The term 'general' is used to denote the fact that no one precise chemical property is quantitatively identical from one humic to another, and thus generates bands of experimental ranges. It is apparent that humic substances consist of a widely heterogeneous mixture of compounds for which no single structure can be given. In addition each fraction (humic acid, fulvic acid etc.) has come to be regarded as being made up of a series of molecules of different sizes, few, if any, having precisely the same structural configuration or array of reactive functional groups.

In contrast to humic acids, fulvic acids contain higher oxygen but lower carbon content and they contain considerably more acidic functional groups, which can all be accounted for in known functional groups (COOH, OH, C=O); however, a higher proportion of the oxygen in humic acid occurs as a structural component of the material (ether, ester linkage). Also, it would appear that the concentration of acidic functional groups in fulvic acids are substantially higher than in other naturally occurring organic polyelectrolytes.

1.5 STRUCTURAL FEATURES OF HUMIC SUBSTANCES

An exact structure for the humic substance has not been found. However, as the resolution of analytical instruments has improved over the years, results obtained allow us to comment on, though not define, the structure of a humic.

We know that the core, or dominant, structure is predominantly aliphatic and not aromatic, as was theorized for decades. Data from ^{13}C NMR has shown that only $\approx$ 15% of carbon in fulvics and $\approx$ 30% of carbon in humics is present in aromatic structures.

All evidence shows that fulvics have molecular weights of approximately 1000 Daltons and a radii of gyration of less than 10 Å, and that humics have molecular weights of approximately 3000 Daltons and a radius of gyration of 10-20 Å i.e. humics are larger than fulvics. The shape, however, is dependent on pH, ionic strength, concentration of humic, net charge on the molecule and molecular hydrogen bonding. The carbon core of the molecule is highly substituted with oxygen containing functional groups. The major contribution being carboxyl groups with minor amounts of phenolic and methoxy groups. Nitrogen is also a definite component of both humics and fulvics with approximately one nitrogen atom per molecule in fulvic acid and 2-3 per molecule in humic, but not all the

molecules may actually possess a nitrogen atom. The amount of α-amino acid is not known but it is thought to be one third of the total nitrogen.

Kleinhempel (12) proposed a structure as shown in Figure 1.1 which incorporates some of the above mentioned characteristics and could be a structure of a humic substance.

1.6 METAL INTERACTION

The ability of humic substances to form stable complexes with polyvalent cations has been well established (13) (14) (15). Whether in all cases genuine complexes are formed is still the subject of debate. However, this 'complexation' facilitates the mobilization, transport and deposition of various trace metals in the aquatic and terrestrial environment. Some of the trace metals, notably copper, iron, manganese, molybdenum and zinc, are essential for plant growth and in that respect the process of migration of metals via humics is very favourable. However, there are situations in which this process of mobilization and migration could prove to be hazardous.

1.6.1 Proposed mechanisms

Schnitzer (16) and Gamble et al (17) postulated that two types of reactions are involved in metal-humic substance interaction. The most important one involves both OH and COOH groups. A reaction of lesser importance involves the COOH groups only. The two reactions are as shown in Figure 1.2.

The formation of phthalate-type complexes (lower reaction) is likely because humic acids have been shown to contain carboxyl groups located on adjacent positions of aromatic rings (18). Positive proof of the salicylate-like ring interaction (top reaction) has yet to be found.

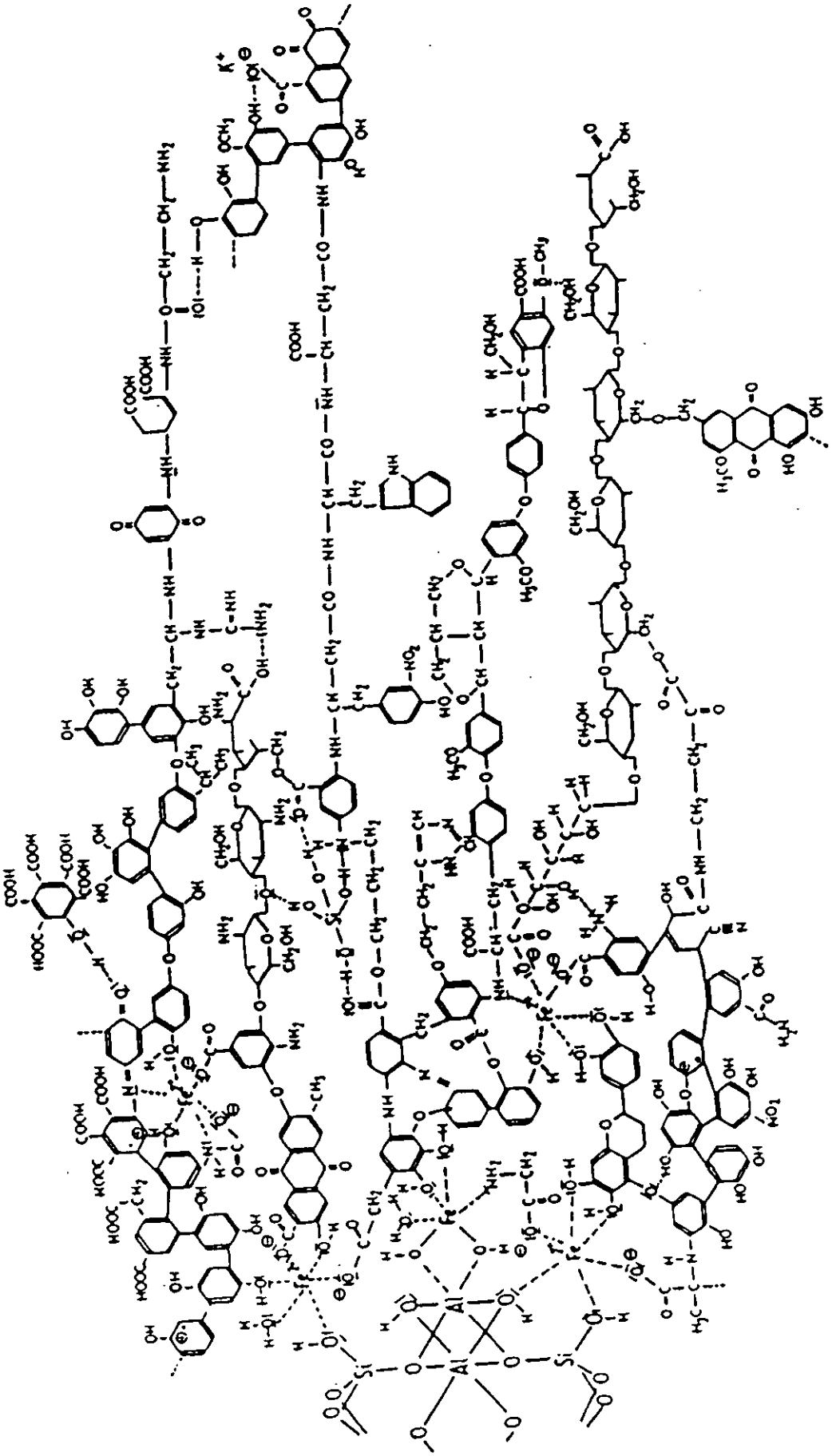

Fig 1.1 Theoretical schematic of a humic molecule

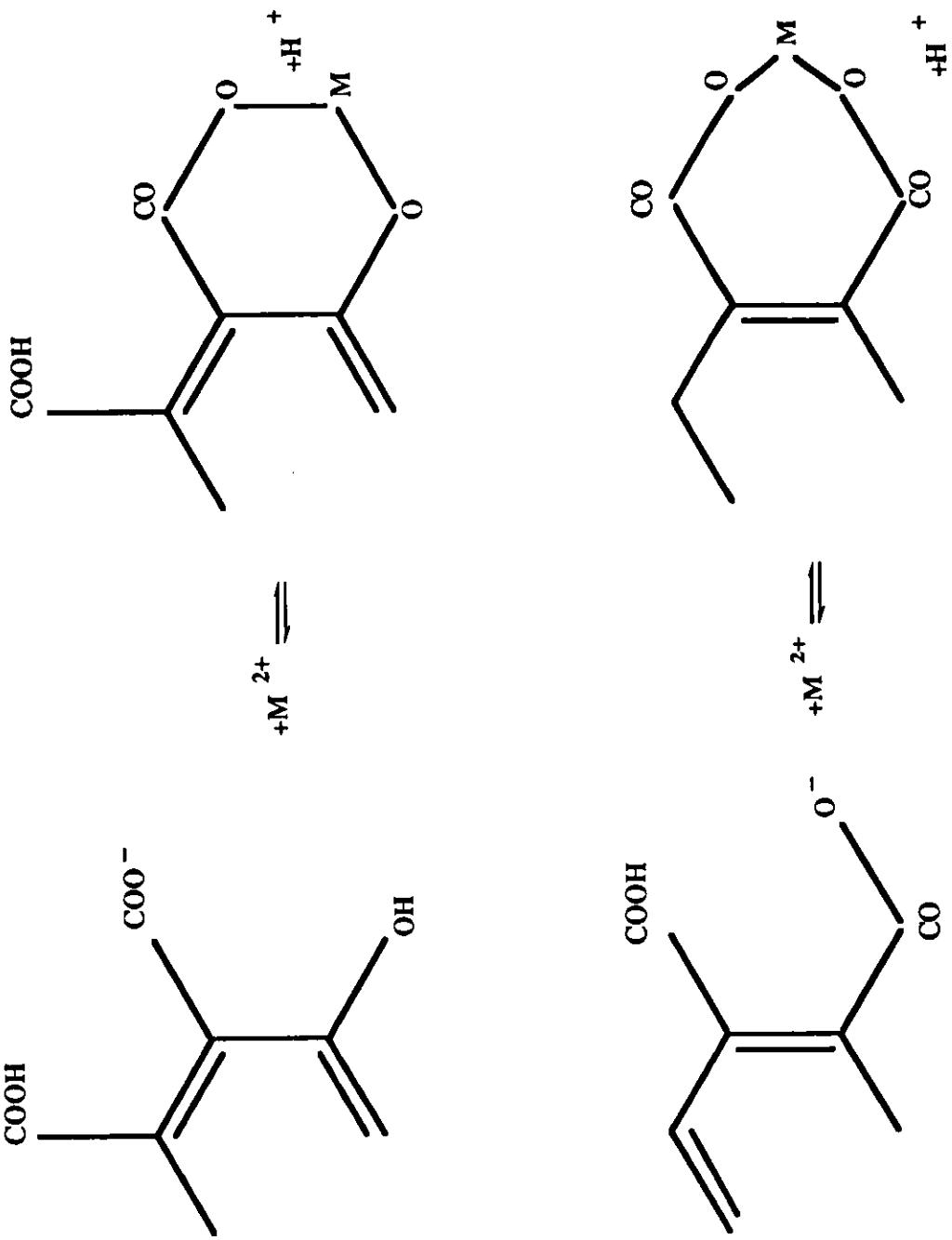

Fig 1.2 Theoretical binding of a site to a metal

1.6.2 Complexation of metals by humic materials

1.6.2.1 Simple ligand systems

Consider the reaction of M metal with L ligand:

$$mM^{x+} + nL^{y-} \rightleftharpoons M_mL_n^{(mx-ny)}$$

the overall thermodynamic stability constant (K_{mn}) for the complex M_mL_n (omitting charges) is given by:

$$K_{mn} = \frac{\{M_mL_n\}}{\{M\}^m \{L\}^n}$$

where the { } are used to denote the thermodynamic activity (not the concentration) of each chemical species. Thermodynamic activity can be related to concentration through the use of the activity coefficient

$$\{M\} = \gamma_M [M]$$

where[ ] denotes the concentration of M, and γ_M is the activity coefficient of the metal ion M.

This allows the stability constant to be expressed in terms of concentrations and activity coefficients

$$K_{mn} = \frac{(\gamma_{MmLn})[M_mL_n]}{(\gamma_M)^m [M]^m \quad (\gamma_L)^n [L]^n}$$

defining

$$K_{mn,c} = \frac{[M_mL_n]}{[M]^m [L]^n}$$

allows us to write

$$K_{mn} = \frac{(\gamma_{MmLn})}{(\gamma_M)^m (\gamma_L)^n} \cdot K_{mn,c} \qquad (C1)$$

the quantity $K_{mn.}$ is the concentration quotient and its value is dependent on the ionic concentration of the solution, unlike the true thermodynamic constant which is independent of all solution conditions. A simplified version of the Debye - Huckel theory gives the relationship between the activity coefficient (γ_i) of species i and the ionic concentration (I). For dilute solutions (I < 0.1) at 25°C.

$$\log \gamma = -0.5 \; z^2 \sqrt{I} \qquad (C2)$$

where

γ – activity coefficient

I – ionic strength = $0.5 \sum_1 c_i z^2_i$

c_i - concentration of ion i

z, z_i - charge on ion (i)

combining equations C1 and C2 for a 1:1 complex gives

$$\log K_{mn} = \log K_{mn} + 0.5 \sqrt{I} \; |2 Z_M Z_L|$$

Thus values of $\log K_{mn}$ are predicted to decrease as the ionic strength (I) increases, the effect being most pronounced for complexes that are formed from multi-charged metal ions and ligands. That is, complexes become effectively weaker as the ionic strength of the system increases.

1.6.2.2 The Humate system

Consider the case of the homologous complexant, i.e. humic material. The reaction may be written in simple terms where metal M reacts with ligand Hu (omitting charges)

$$xM + yHu = M_x Hu_y$$

The equilibrium constant is given by:

$$K^{th} = \frac{\{M_x Hu_y\}}{\{M\}^x \{Hu\}^y}$$

again K^{th} is the true thermodynamic equilibrium constant as a function of activities ({ }).

The above relationship is in a form analogous to that of simple ligands. However, determining complexation parameters is more difficult than in the simple ligand case and numerous problems exist, due to the character of the homologous complexant. However, it is expected that the humic material will conform to the same trends of stability constant change with ionic strength as with the simple metal ligand case.

(1) Humic materials are macromolecules with a range of molecular weights. This means that expressing concentrations in terms of molecular concentrations is flawed, so many workers use a mass per unit volume, whilst others use concentration of complexing sites available on the humic molecules.

(2) Humic materials are polyfunctional macromolecules. The reaction can occur between a metal M and complexing sites -S, but several additional effects, herein called secondary effects, can influence the complexation process. These effects arise from the complicated structures and complexing site availability. Let us consider the coordinating site (-S) on the molecule as the group of atoms (-COOH, $-NH_2$, -φ-OH) which directly participate in bonding to form a complexed site, and complexing ligand (-L) on the molecule that includes all the -S sites and their environments (electric, steric etc.). The environment in which a site -S is situated can exert considerable influence on the stability of a complex, through

complex, through secondary effects. These can be split into three categories for homologous complexants.

a) Polyfunctional properties

i) diversity in the nature of -S. In contrast to a simple ligand, homologous complexants possess different types of coordinating sites.

ii) the electronic environment about -S. Within a given macromolecule two identical sites can be found bound to different organic or inorganic components which exert through inductive, mesomeric factors, different electronic environments which can either aid or deter complexation.

b) Conformational properties

The steric environment depends on the steric conformation of the complexant, which for homologous complexants can vary with the chemical condition of the medium, such as ionic strength, pH and complexing ion content. The conformation is also dependent on hydration-dehydration processes and the formation of hydrogen bonds and metallic bridging, which in turn is dependent on site occupation, i.e. site occupation is dependent on site conformation, and vice versa. Thus, depending on conditions, humics tend towards linearity, with no internal bonding, or spherical, with a large amount of internal structure and bonding implying that the complexation sites can be readily accessible or completely inaccessible, depending on the conformation.

c) Polyelectrolyte properties

The homologous complexants sites have been characterised into two types, minor or weak sites and major or strong sites. These sites will be ionised to various extents, depending on their pKa. At natural water pHs (5-9) the major complexing sites are often ionised, thus creating localised electric fields which influence the entire stability of an M-S complex regardless of site type. The net charge on a

humic material at natural pHs is negative which facilitates electrostatic interaction between the metal cation and the humic molecule as positive ions swarm around the negative surface.

With humic materials all the properties a, b and c are important when considering metal interaction and it is these properties which create the major difficulties in trying to understand complexation behaviour. Also, this array of properties means that the equilibrium constants that are generated are 'average conditional equilibrium constants', which can only be quoted for the conditions which are prevalent at the time of measurement.

Although not true thermodynamic constants the equilibrium constants that are generated are of use in computer models to predict metal binding in natural systems.

1.6.3 Interpretation of metal-humic experimental data

Although there are numerous methods (12) by which experimental data can be interpreted ,a discrete ligand model and continuous distribution model will only be described in this report, since these have been used to interpret experimental data obtained during this work.

1.6.3.1 Discrete ligand models

This model is based on the simple case described previously where one metal (M) complexes with one site type (S_i) on the humic molecule to give the metal complex (MS_i). Quantitatively, the complexation is governed by the stability constant (K)

$$K = \frac{[MS_i]}{[M]\,[S_i]} \qquad 1.1$$

Theoretically , the metal complexation site type (S_i) may be:

1) a free site i.e. one which is not occupied by a metal or a proton

$$M + S_i^- \rightleftharpoons M\text{-}S_i$$

2) already occupied by a proton

$$M + H\text{-}S_i \rightleftharpoons M\text{-}S_i + H^+$$

3) already occupied by a metal

$$M + M'\text{-}S_i \rightleftharpoons M\text{-}S_i + M'$$

The metal exchange reaction depends primarily on the relative stability constants of the metal site reaction. Irrespective of the above three reactions, the total possible site concentration for i sites is given by the sum of the three possible interactions

$$C_{si} = [S_i] + [HS_i] + [MS_i] \qquad 1.2$$

where C_{si} is the total concentrations of the i site,
$[S_i]$ and $[HS_i]$ are the concentrations of sites not bound to the metal and
$[MS_i]$ is the concentration of the sites bound to metal.

The expression for the stability constant in equation 1.1 may then be re-written to provide a conditional stability constant for the i sites, K'_i :

$$K'_i = \frac{[MS_i]}{[M]\ \{C_{si}-[MS_i]\}} \qquad 1.3$$

where [M] is the free metal concentration and
$[MS_i]$ is the bound metal concentration.

Unfortunately the single value of K, derived from equation from 1.3, does not adequately describe the complexation ability of a single humic or fulvic material. Humic and fulvic acids are made up of numerous site types in various chemical and electrical environments, suggesting that a number of K values are needed to describe fully the humic material's complexing ability. Perdue and Lytle (19) point out that since different sites have different affinities for any given metal, then the value of K'_{av} cannot be constant and will change with site occupancy.

Consider the bonding of the metal to a particular site type in terms of the site occupancy factor (θ)

$$\text{where } \theta = \frac{[MS_i]}{C_{si}}$$

From equation 1.3

$$[MS_i] = K.[M]\{C_{si} - [MS_i]\}$$

$$= K.[M].C_{si} - K.[M].[MS_i]$$

therefore

$$[MS_i] + K.[M].[MS_i] = K.[M].C_{si}$$

$$[MS_i]\ (1 + K.[M]) = K.[M].C_{si}$$

$$[MS_i] = \frac{K.[M].C_{si}}{(1 + K.[M])}$$

therefore

$$\theta = \frac{[MS_i]}{C_{si}} = \frac{K.[M].C_{si}}{(1 + K.[M])} \Big/ C_{si}$$

Therefore the site occupancy for the i sites is

$$\theta = \frac{K\,[M]}{1 + K\,[M]} \qquad 1.4$$

The expression for the stability constant in equation 1.1 may then be re -written to provide an average conditional stability constant for all sites, K'av:

$$K'av = \frac{[MS]}{[M]\ \{C_S - [MS]\}}$$

or this can be written in terms of the total metal concentration C_M as:

$$K'av = \frac{C_M - [M]}{[M]\ \{C_S - (C_M - [M])\}} \qquad 1.5$$

where C_S is the concentration of all sites

C_M is the total metal concentration

[M] is the total free metal concentration

Thus for the whole system $\bar{\theta}$, which is usually called the formation function, is given by

$$\bar{\theta} = \frac{\sum_i \theta_i C_{Si}}{\sum_i C_S} \qquad 1.6$$

or

$$\bar{\theta} = \frac{C_M - [M]}{C_S} \qquad 1.6'$$

Combination of equations 1.5 and 1.6' gives

$$K'_{av} = \frac{\bar{\theta}\, C_S}{[M]\{C_S - \bar{\theta}\ C_S\}}$$

Rearranging gives

$$\text{ie } \frac{\bar{\theta}}{[M]} = K'_{av} - K'_{av}\,\bar{\theta} \qquad 1.7$$

This is a simple form of the Scatchard equation (20) which predicts a linear relationship between $\bar{\theta}$ /[M] and $\bar{\theta}$ if K'_{av} is constant. If K'_{av} is not constant the Scatchard plot will be a curve. As a curve has an infinite number of possible tangents that can be drawn on it, an infinite number of K' values would be produced. Thus for humic and fulvic metal complexation analysis certain assumptions must be made. The assumptions being that only two types of site exist: major or strong sites and minor or weak sites.

Combining equations 1.4 and 1.6 and the number of sites is assumed to be two, then the formation function becomes:

$$\bar{\theta} = \left(\frac{K'_{av1}\,[M]}{1 + K'_{av1}\,[M]}\right)\frac{C_1}{C_S} + \left(\frac{K'_{av2}\,[M]}{1 + K'_{av2}\,[M]}\right)\frac{C_2}{C_S}$$

and from this equation the four complexation parameters K_{av1}, K_{av2}, C_1 and C_2 are obtained. Sense dictates that a better fit to the curve can be obtained by increasing the value of i, but the improvement is deemed mathematically unsound (21). Perdue and Lytle (19) also pointed out that since K_{av1}' and K_{av2}' are not constant then the Scatchard derived values have no thermodynamic significance, and are in fact only curve fitting parameters. But these curve fitting parameters or Scatchard

derived K_{avl}' values can be used to predict the degree of complexation of metals by humic materials, within the experimental range of C_M and C_S values used in their derivation. In practice, Scatchard derived parameters have practical value but no chemical significance in terms of individual sites. Several refinements to the discrete ligand approach are well documented (22)(23)(24). Sposito (25) has developed a model which is based on the hypothesis that the overall reaction of a trace metal with a dissolved humic material could be based on an equivalent set of non interacting organic ligands, e.g. Lysine, ornothine. etc., whose reaction with trace metals are well characterised thermodynamically and whose functional groups are relevant to humic materials.

1.6.3.2 Continuous distribution models

Humic materials are generally considered as being polyfunctional polyelectrolytic heterogeneous mixtures of organic material bound together into one macro molecule. As stated previously there are a large number of sites in a large number of environments, with different steric and electronic interactions associated with each ligand. As metal loading increases the charge distribution and steric structure could alter, thus site availability and occupancy will change continuously with metal load. It is this assumption that prompted Altmann and Buffle (26) to argue that a stability constant will probably vary continuously with metal loading and is probably best described as a differential function. This replaces the concept of determining numerous discrete K values, with an ever changing function which produces a continuous variation in K values which exist within the analytical window about C_M and C_S. Such theoretical considerations have led several continuous distribution models to be developed, e.g. normal distribution model affinity spectrum model and the differential equilibrium function model. These models are fundamentally similar to Scatchard analysis with a metal combining

with a site. However, the complexity of the maths required for the interpretation has increased.

Normal distribution model

Perdue and Lytle (19) originally suggested a Gaussian distribution to describe the pattern of site types within the humic material, with a mean log K value and a standard deviation of log K's from that mean position.

i.e. $$\frac{C_{S1}}{C_S} = \frac{1}{\sigma\sqrt{2\pi}} e^{-1/2\left(\frac{\mu - \log k'}{\sigma}\right)^2} d \log k \qquad 1.10$$

σ is the standard deviation of the distribution of log K values about μ the mean log K′ value.

$\frac{C_{S1}}{C_S}$ is the mole fraction of ligand sites in the interval d log K′.

If this Gaussian distribution for the sites is then combined with the formation function from equation 1.6 an equation is generated which links the simple summation of log K′ derived from equation 1.6 to a continuously varying integral, i.e.

$$\bar{\theta} = \frac{1}{\sigma\sqrt{2\pi}} \int_{-\infty}^{+\infty} \left(\frac{10^j [M]}{1 = 10^j [M]}\right) e^{-1/2\frac{(\mu - j)^2}{\sigma}} dj$$

$$j = \log k'$$

the theoretical values of $\bar{\theta}$ can now be generated for different values of [M].

The theoretical values of $\bar{\theta}$ can be compared with the experimental values derived

from ($\bar{\theta} = C_M - [M] / C_S$). A non linear regression technique is used to generate an optimum set of μ and σ values. It was found that the gaussian distribution model was better than the Scatchard model, when predicting complexation parameters for metal humic material interaction that were outside the analytical window used in the experimental investigation.

Affinity spectrum model

The fundamental difference between the normal distribution and affinity spectrum model is that there is no initial assumption made concerning the shape of the distribution. It is then possible to substitute various functions into the equation to allow different distributions to be analysed for compatibility. Thus the affinity spectrum can be written as

$$\theta = \int_{-\infty}^{\infty} \left(\frac{10^j [M]}{1+10^j [M]} \right) N(j)\ dj$$

N(j) is the unknown or the selected distribution function

Affinity spectra are derived from the binding data using a second order approximation of the above equation . Peaks in an affinity spectrum correspond to inflections in the experimental formation function (27)(28). Each peak in the distribution indicates the most probable log K value controlling metal binding in a particular region of the formation function and the area under the peak determines the concentration of the most probable ligand. The approach has been used by Shuman et al (29) who studied copper interaction with estuarine humics.

Differential Equilibrium Function (DEF) model

The original DEF was proposed by Gamble (30) and later refined by Altmann and Buffle (26). As the titration progresses the site will either be near saturation (strong sites) or almost completely free (weak sites). The relatively small change in site filling (d[HxS]) at any given stage of the titration gives a relatively small change in the amount of complex formed (d[MS]). Thus the stability constant will change as a function of these small incremental changes and can be written as

$$*K' = \frac{d[M]}{[M]\ d[HxS]}$$

*K' is the DEF derived conditional stability constant.

The DEF and average K'_{av} can be related as shown by Gamble (31) and Buffle (32) by

$$*K' = \frac{d\left[(\bar{K}'_{av} (1-\bar{\theta}) \right]}{d\bar{\theta}}$$

by plotting $K'_{av}(1-\bar{\theta})$ against $\bar{\theta}$, *K' can be obtained from the curve as the slope for each value of $\bar{\theta}$. However the formation function $\bar{\theta}$ is given by:

$$\bar{\theta} = \frac{[MS]}{C_S}$$

which means that Cs is required to calculate $\bar{\theta}$. The Cs value for a humic material is difficult to determine and if generated from Scatchard data can be seen, at best, as a crude approximation. Thus an alternative relationship which allows *K values to be deduced without knowledge of Cs was proposed by Buffle (32) i.e.

$$*K' = \frac{\alpha}{C_M} \left\{ \frac{1 - \frac{\alpha - 1}{\alpha} \frac{d \ln C'_S}{d \ln \alpha}}{1 + (\alpha - 1) \frac{d \ln [C_M / C'_S]}{d \ln \alpha}} \right\} \qquad 1.8$$

where $\alpha = [M]t / [M]$

C'_S = the concentration of humic material used in the experimental titration and is expressed in the experimentally determinable units g L^{-1}

As there is no sample dilution C's is constant thus the numerator is 1

Initially the experimental data is manipulated to yield values of the functions ln [Mt]/{p}(where p is the concentration of ligand used in g L^{-1}) and ln [Mt]/[M] (ln α). A graph of ln [Mt]/{p} is plotted against ln α. The equation of the resulting curve is then generated using the computers internal curve fittng program. This function represents the function d ln $[C_M/C's]$ / d ln α in the Buffle equation above. The equation can then be solved for different values of C_M to afford values of log *K'. This is then plotted against [Ms]/TOC to give the distribution equilibrium function for the system under investigation. The role of various parameters on the *K' values can be determined by generating DEF plots for systems in which the parameter of interest i.e. Ionic strength , pH temperature etc. is the only variable(12).

Advantages and disadvantages of Continuous Distribution Models.

The main advantage of the continuous models approach is that the function is calculated without knowledge of the complexation capacity of the ligand, it is this value that is impossible to know with any degree of certainty (33). The curves that are generated are continual distributions of stability constants. These continuous distributions of stability constants contrast with the two constants that are generated with the discrete ligand approach which is a somewhat oversimplification of the

situation. The distribution models also allow for substitution of statistical functions which allows the equation to be solved algebraically (34)(35). Altmann and Buffle(33) argue that the DEF is a promising means of describing the underlying cumulative site distribution and may eventually help in the elucidation of the chemical nature of the background sites. The disadvantages include the complexity of the affinity spectrum approach due to the mathematical transformations involved (36). The binding power of a site depends on the product of $K_i C_{si}$ and not just K_i. Also, the complexity of the functions involved makes it difficult to incorporate continuous distribution models into computer speciation codes. However, it has been achieved in the MINTEQA2 program for Perdue's model.

1.6.4 Predictive computer modelling of metal-humic interactions

Although there are numerous computer codes available (37) for modelling metal-humic interactions only a discrete ligand code (Spositos) and a continuous distribution code (MINTEQA2) will be considered in this report

1.6.4.1 Spositos discrete ligand model

Sposito and Mattigod (25) makes the assumption that all the sites present on a humic molecule behave in an identical fashion to that observed for mixtures of simple ligands. In other words, the sites behave as independent ligands and the extent of interaction, with any given metal, is simply governed by the concentrations of the various types of site present and the corresponding stability constants. Sposito et al (25) identified certain classes of known organic acids whose proton dissociation constants fall into a range observed for sewage sludge derived fulvic acid; these acids were then used to simulate the humic molecule. The acids used to simulate the humic acid system are shown in table 4.32.

Table 4.32

Ligands

Benzene sulphonic acid

Salicylic acid

Phthalic acid

Citric acid

Maleic acid

Ornothine

Lysine

Valine

Arginine

The model is incorporated into the speciation code SOILCHEM. However due to the unavailability of this program the model was inputted into the PHREEQE speciation code. To allow this to be carried out the data must be presented in a form that PHREEQE can assimilate. This is achieved by inputting all the known stability constants for the metal in question and for the various organic acid ligands.

1.6.4.2 MINTEQA2

This computer model is an adapted mineral equilibrium model which has been modified to include a composite ligand submodel. This new submodel computes the complexation of various metals with natural dissolved organic matter. This is in essence based on work of Dobbs et al (38) which treats dissolved organic matter as a complex material consisting of many different types of monoprotic acid sites. The concentration of these ligands is normally distributed with respect to there log K values for proton and metals (39). The mean log K values for various metals with

dissolved organic matter, from the Suwannee river, have been determined by lanthanide ion probe spectroscopy (40). A database of trace metal reactions with Suwannee river organic matter and their mean log K values are included in the submodel. To make the model more versatile the model also contains an added subroutine PRODEFA2 which enables the ligand database to be expanded by the user, as it allows the user to define new composite ligand reactions, and thus tailor the program to their specific need.

1.7 AIMS AND OBJECTIVES OF THE STUDIES REPORTED IN THIS THESIS.

In 1990 a project, funded by Her Majesty's Inspector of Pollution, Department of Environment, commenced and was concerned with answering the question ***"does extraction of humic and fulvic acids from natural waters alter their physical and chemical properties?"***. This study was important because almost every reported investigation of the metal binding properties of these acids had been conducted using extracted acids and, clearly, if their properties change during or after extraction, measuring the metal binding properties of these extracted acids would not provide a faithful representation of their binding properties in natural waters. The project consisted of three parts

1 the collection of a suitable environmental water,

2 a comparison of physical and chemical properties of in-situ and extracted humic and fulvic acids, and

3 a comparison of the metal binding properties of in-situ and extracted humic and fulvic acids.

The work carried out to satisfy points 1 and 2 are reported in this thesis. This work was completed in 1992.

Also reported in this thesis is an investigation of europium and nickel binding to Aldrich sodium humate. Many investigations have used the Schubert method to determine stability constants for metal-humic reactions but the method, as generally applied, only provides a single stability constant. A modification of the Schubert method which allows the data to be represented as a Scatchard plot is investigated. This novel approach produces two stability constants, one representing the average of the weak binding sites and the other representing the average of the strong binding sites. A comparison of the use of ion-exchange resins in column and batch experiments is also reported. The data obtained in these experiments were used to compare two models currently used for metal binding.

The third part of this thesis is concerned with an investigation of synchronous fluorescence spectrometry for investigating metal-humic binding and for investigating competition reactions between metals and calcium for humic binding sites. The justification for this work was that, even after years of investigating these reactions, a non-invasive and simple technique is still required to quantitate these reactions.

Chapter Two
Water Collection and Treatment

2.1 LOCATION OF SURFACE WATER SAMPLES IN DERBYSHIRE

Although it would have been preferable to use a groundwater in these studies, the low amounts of humic and fulvic acid present in groundwaters make experimental procedures difficult. As groundwater humics and surface water humics are similar, differing only in the increased organic content of surface water, it was decided to collect and extract the humic material from a suitable source of surface water.

Discussions with the Severn Trent Water Authority indicated that the catchment area around the Howden Reservoir in the Derbyshire Peak District contained large areas of peatland and bog. They also indicated that the run off tributary rivers which serve the lake were high in dissolved organic matter. Accordingly, on 15th November 1990, this area was visited and samples of water were collected.

Initially a remote site on high ground at the head of the Howden Reservoir was selected and a hole was dug 18 inches into the peat. The hole filled rapidly with surface run off water. A sample of this water was collected for analysis. A second sample was collected from the Upper Misden Clough lower down the same hillside. The pH of the water was 4.5 and the temperature 8°C. The samples were returned to the lab within a few hours of collection for filtering. Initially the samples were passed through a coarse filter paper to remove plant debris so that the second stage of filtering would be easier. The samples were then filtered through Gelman 0.45μm filter membranes held in special filter units. The sample taken from the hole was extremely difficult to filter and several membranes were needed. Duplicate samples and controls were sent to the National Rivers Authority's Analytical Laboratories, Meadow Lane, Nottingham, for total organic carbon analysis.

The results are given below in Table 2.1.

Table 2.1 Total organic carbon content of first visit samples

Sample		TOC (mg L^{-1})
Hole water	1	112
Hole water	2	109
Clough water	1	18
Clough water	2	20
Tap water		2
HPLC water		4

2.2 ESTIMATION OF HUMIC ACID AND FULVIC ACID CONTENT

The pH of a sample of the Clough water was converted to pH < 1 by the addition of concentrated hydrochloric acid and the humic acid precipitate filtered off. The UV absorbance of the water at 254 nm was measured before and after pH adjustment to obtain an estimate of the humic to fulvic acid ratio. The results shown below assume the absorbance at 254 is attributable to the humic and fulvic acid alone.

Absorbance of Clough water before adjustment = 0.33

Absorbance of Clough water after adjustment = 0.19

$$\therefore \text{Fulvic acid content} = \frac{0.19}{0.33} \times 100 = 58\%$$

$$\therefore \text{Humic acid content} = 100\% - 58\% = 42\%$$

2.3 DERBYSHIRE REVISITED

After the promising results of the first visit a second visit was made to the Howden

catchment area. Samples from a variety of locations were taken to obtain the humic/ fulvic material content in the general area. Eight locations were sampled. All the samples were either permanent standing or flowing water samples as the subsurface samples were difficult to manipulate in the laboratory.

pH of all samples	4.5
Temperature of all samples	5°C

On returning to the lab the samples were filtered through 0.45μm membranes using filter membrane assemblies. The eight samples were sent along, together with two controls, for total organic carbon analysis at the NRA laboratories, Nottingham. The results are shown below in Table 2.2.

Table 2.2 Total organic carbon of second visit samples

Sample sites	TOC (Mg l^{-1})
1	7.1
2	9.7
3	6.3
4	9.2
5	4.6
6	6.8
7	7.1
8	7.0
9 Research grade H_2O unfiltered	<0.5
10 Research grade H_2O filtered	11.0

Some Conclusions

1. The dissolved organic material concentration has decreased between the two visits, due to:

a) recent heavy rainfall causing dilution, and possibly

b) seasonal slowing of humification process.

2. No significant differences were observed between the bulk reservoir samples and the other samples. Thus the bulk sample was used for a trial extraction.
3. Progression up the hillside produced higher levels of dissolved organic material.
4. The total organic content results of the filtered and unfiltered HPLC were a cause of concern and are explained in Section 2.5.2.

2.4 TRIAL EXTRACTION OF BULK HOWDEN RESERVOIR SAMPLE

2.4.1 DEAE pretreatment

The extraction was carried out according to a procedure developed originally by Miles, Tuschall and Brezonik(41). 50g of DEAE cellulose (Whatman 52) was placed in 1l of 0.5M hydrochloric acid for one hour and gently stirred. The cellulose was then filtered through a Buchner funnel and washed with deionised water. The cellulose was then placed into 1l of 0.5M sodium hydroxide and left for one hour again with gentle stirring. The cellulose was filtered and washed until the pH was neutral. The pretreated cellulose was stored at 4°C in the dark.

2.4.2 Extraction

To a filtered sample of Howden Reservoir water (23 litres) was added 40g of the pretreated DEAE cellulose. The pH was checked and found to be 6.5 so no adjustment was made as optimum recovery of humic / fulvic from waters occurs at approximately pH 6 (54). The mixture was stirred gently for 3 hours. After overnight settling, the clear supernatant was siphoned off. UV adsorbance measurement of the supernatant indicated an extraction of ≈ 80% of the original organic content. The brown precipitate slurry of DEAE cellulose / humic fulvic material was packed into a glass column (24cm x 4.5cm ID), plugged with glass wool. The column was rinsed with 250cm^3 of distilled water and then eluted with

500ml of 0.1M sodium hydroxide, followed by 250cm^3 of 1M sodium hydroxide. From the colour of the column it was judged that most of the humic/fulvic material had now been desorbed from the cellulose. The elution fractions were combined, mixed thoroughly and divided into approximately equal volumes.

One half was stored after pH adjustment to 7, the other half was adjusted to pH 1 to precipitate the humic acid. The small amount of precipitate was centrifuged off after standing overnight. UV measurements at 254 nm indicated that the supernatant which contains the fulvic acid represented 60% of the sample organic content. The solid humic acid and the fulvic acid solution were stored for characterisation studies, as mentioned earlier.

Conclusions

80% of the dissolved organic material in the original water samples was extracted on the DEAE column. 40% of the extracted organic matter was found to be humic acid and 60% fulvic acid.

2.5 THIRD VISIT TO DERBYSHIRE

2.5.1 Sampling

The third visit took place after spells of heavy rain and snowfall, which could have diluted the humic fulvic material content of the Howden Reservoir water. Accordingly a new site was chosen, which from the colour of the water alone seemed to indicate a high dissolved organic matter approaching that found on the first visit. The new location was a small isolated clough on Hallam Moor, approximately half a mile from Moscar (GR 235875), 6 miles from the Howden Reservoir site. On this occasion 10 vats were filled and a total of 230 litres of water collected all from the same small section of the Clough.

The sampling conditions were as follows:

pH of samples	~ 4.0
Temperature of samples	~ 3.5°C
Weather	– sunny, cold
Date	– 4th January 1991

the water was returned to the lab for 0.45 μm filtration.

2.5.2 Membrane filtration

The proximity of the Derbyshire location allowed filtration of the samples to commence within 3 hours of collection. This was essential since as well as removing colloidal material, membrane filtration arrests bacterial changes.

Discussion with Gelman Sciences, who supplied the filter membranes, revealed that the membranes previously used contained an organic wetting agent. This material was responsible for the high total organic carbon values in the control samples highlighted earlier. Further discussions with Gelman indicated that they were aware of this problem and had recently introduced into this country a purpose made groundwater filtering capsule, which met the requirements of the US environmental protection agency. The capsules contain a 0.45μm membrane made of polysulphone which is inherently hydrophilic and is not treated with a wetting agent. When used in conjunction with a peristaltic pump these capsules rapidly filtered 20 litres of water before needing to be changed. Consequently all subsequent filtration was conducted using these filtering capsules.

2.5.3 Extraction of moorland water

The extraction procedure developed earlier was applied to eight of the ten vats, i.e.

≈ 200 litres. The two unused vats were to be used for the in-situ studies. After discussion with Whatman it was revealed that pretreated DEAE cellulose was now available, so this was used instead of undertaking the laborious pretreatment stage as was outlined in the trial extraction. To each of the eight vats was added 50g of the pretreated cellulose and the vats were shaken gently. Absorbance measurements of the supernatant after several hours indicated 70% of the organic content of the water had been extracted. So a further 20g of DEAE cellulose was added, increasing the extraction efficiency to 80%. The extraction efficiency was calculated from the absorbance data as shown below.

Average absorbance at 300nm of vats 1 and 2	0.287
Average absorbance at 300nm of vats 3-10 after treatment	0.054

$\therefore$ Average extraction efficiency = 81%

As stated previously vats 1 and 2 were retained without DEAE addition and were to be used for the in-situ studies.

2.5.4 Column elution

The clear supernatant liquids in vats 3-10 were siphoned off and the residual brown slurry poured into a glass column (24 x 4.5cm ID) plugged with glass wool. The humic fulvic material was eluted from the column with 250cm^3 of 0.5M sodium hydroxide followed by 250cm^3 of 1M sodium hydroxide (equivalent of 3-4 bed volumes). The fractions from all the columns were collected into four one litre aliquots. The pH of the aliquots was rapidly lowered to approximately pH 3 with A.R.G. hydrochloric acid to avoid oxidation of the humic/fulvic material which is known to occur at high pH's.

2.5.5 Treatment of eluates

Three of the four one litre aliquots had their pH's adjusted to approximately 0.6 and were left to allow the humic acid to precipitate out. After two days the humic acid was separated by centrifuging the sediments and membrane filtration of the supernatant, the precipitate was washed with distilled water. The solid humic acid extracts were combined and freeze dried. The filtrates were combined to give approximately three litres of fulvic acid solution, which was stored in the fridge at pH 0.6. The remaining one litre sample of mixed humic acid / fulvic acid was treated with sodium hydroxide to give a pH of 6.5 and this mixture was also stored in the fridge.

The samples contained varying amounts of sodium chloride as a result of elution with sodium hydroxide and pH adjustment with hydrochloric acid.

2.6 PREPARATION OF STOCK SOLUTIONS FOR CHARACTERISATION EXPERIMENTS

The stock solutions to be used throughout the characterisation experiments were as follows:

(i) Moorland water (in-situ and x4)
(ii) Fulvic acid extract (FA)
(iii) Humic acid extract (HA)
(iv) Mixed humic and fulvic acid extract (HA/FA)
(v) Aldrich humic acid (AHA)
(vi) Aldrich sodium humate (NaA)

The abbreviations in brackets will be used throughout the rest of the report to indicate the material being used.

The AHA and NaA are well characterised materials and were used as semi-

reference materials. Working stocks were prepared as follows:

(1) Moorland water (in-situ and x4)

For some direct studies on the moorland water 'in-situ' material was used, i.e. moorland water simply filtered through 0.45μm membranes.

However, to facilitate detection in the complexation experiments the moorland water was pre-concentrated by rotary evaporation. 1 litre samples of the filtered in-situ water were evaporated to 250ml. The rotary evaporation was carried out at 33°C to avoid thermal decomposition, and structural alterations, to the humic and fulvic compounds. The final solutions were 0.45μm filtered. During evaporation the pH dropped from 3.8 to 3.5. Complexation decreases with pH so a small amount of NaOH was added to bring the final pH to an arbitrary value of 6.3. At this pH complexation is significant but complications arising from formation of hydroxy species remain minimal with the metals investigated. This concentrated water was known as x4 water.

(ii) Fulvic Acid Extract Solution and Solid (FA)

Working stock solutions of extracted fulvic acid were prepared by diluting 200ml aliquots of the original extract, with HPLC water to a final volume of 1 litre. The pH was simultaneously adjusted to 6.3 and the final solutions were 0.45μm filtered. A sample of solid fulvic acid was prepared as follows. 25ml fulvic extract solution was mixed with 5g of the hydrophobic resin, SM7 Bio-Beads™ (Bio Rad) and left to stand for several hours. The slurry was packed into a glass column. The column was then washed with methanol to regenerate the Biobeads and remove the fulvic material. The methanol was then removed by evaporation to leave 36mg of residue which was believed to contain solid fulvic acid. This residue was placed in an oven at 105°C and left for 3 hours. 19mg of a yellow residue was produced.

(iii) Humic Acid Extract Solution (HA)

The working stocks of extracted humic acid were prepared by dissolving weighed amounts of solid freeze dried HA in a little NaOH solution, followed by pH

adjustment to 6.3, and making up to exactly 1 litre. These solutions were also 0.45μm filtered.

(iv) Mixed Humic and Fulvic Acid Extract Solution (HA/FA)

The working stock solutions of the mixed extracted humic and fulvic extract were produced in an identical fashion to the fulvic acid solutions, i.e. five fold dilution, pH adjustment to 6.3 and 0.45μm filtered.

(v) Aldrich Humic Acid Solution (AHA)

A concentrated solution of Aldrich sodium humate was prepared in distilled water then treated with concentrated AR hydrochloric acid to reduce the pH to below 1. After standing for several hours the precipitated HA was filtered off and washed with water. The process was repeated, i.e. re-dissolution in NaOH, precipitation and washing. The final HA product was freeze dried. Solutions containing weighed amounts, e.g. 60 mg of this re-precipitated HA, were prepared with pH adjustment to 6.3 and 0.45μm filtration.

(vi) Aldrich Sodium Humate (NaA)

Solutions of NaA were simply prepared by taking weighed amounts of the commercial solid as required, followed by the usual pH adjustment and filtration.

The analyses of the working stock solutions carried out by NRA are presented in Table 2.4. In most cases the ratio of concentrations can be explained in terms of the dilutions and the pH adjustments made.

Table 2.4 Analyses of working solutions

	In situ	x4	FA	HA	HA/FA	AHA	
pH	3.8	6.3	6.3	6.3	6.3	6.3	
Chloride	11	86	4100	123	5350	33	mg/l
Bromide	-	-	7.0	<0.25	2.4	-	mg/l
Alkalinity as $CaCO_3$	<2	-	-	-	43	10	mg/l
Ammonia as N	.03	0.130	0.28	0.17	0.22	0.090	mg/l
Nitrite as N	<.01	0.013	0.01	0.032	0.02	0.057	mg/l
Calcium	3	21	<5	<5	<5	<1	mg/l
Magnesium	1.7	14	<5	<5	<5	<0.1	mg/l
Sodium	5	48	2624	95	3040	25	mg/l
Potassium	1.4	4.1	0.4	0.4	0.4	<0.1	mg/l
Total Hardness as $CaCO_3$	10	107	<15	<15	<15	<1	mg/l
Sulphate	29	122	153	74	218	123	mg/l
Phosphate as P	<0.05	<0.05	<0.05	<0.05	<0.05	<0.05	mg/l
Silica	6.5	40	2.2	0.21	3.15	<0.1	mg/l
Fluoride	.06	0.33	<0.05	<0.05	<0.05	<0.05	mg/l
Total Oxidised Nitrogen	<0.5	0.5	<0.5	<0.5	<0.5	<0.5	mg/l
Total Organic Carbon	7.9	26	43.5	25.5	73	25.0	mg/l
Total Inorganic Carbon	-		<0.5	3.5	-	-	mg/l
Boron	.014	51	10	25	10	<10	mg/l
Molybdenum	<.0025	<0.01	<0.01	<0.01	<0.01	<0.01	mg/l
Uranium	-	<0.5	-	-	-	-	mg/l
Lithium	-	<0.1	<0.01	<0.01	<0.01	<0.1	mg/l
Strontium	.019	0.08	<0.01	<0.01	<0.01	<0.01	mg/l
Iron	790	3200	1530	109	2000	510	µg/l
Manganese	201	1780	73	<10	83	<10	µg/l
Aluminium	360	330	810	34	1150	204	µg/l
Vanadium	<10	<10	<50	<50	<50	<10	µg/l
Lead	<5	<5	<5	<5	<5	<5	µg/l
Chromium	<2	<2	<2	<2	<2	<2	µg/l
Copper	18	63	43	<10	20	20	µg/l
Nickel	<5	10.3	22.0	<5	19.5	<5	µg/l
Zinc	50	65	275	<10	265	<10	µg/l
Cadmium	<0.5	0.53	2.0	<0.5	<0.5	<0.5	µg/l
Barium	59	300	30	<10	18	<10	µg/l
Cobalt	3	<10	<10	<10	<10	<10	µg/l
Electrical Conductivity at 20°C	125	420	10100	340	12400	108	µS/cm

Chapter Three

Characterisation of natural water samples

3.1 CHARACTERIZING THE MATERIAL

Almost every analytical technique has at some time been used in the investigation of humic substances. However, only those techniques used during this study will be discussed in this report.

3.1.1 Spectroscopic Studies – UV-Visible Spectroscopy

In many instances ultraviolet / visible (uv-vis) spectroscopy is a valuable tool in the identification of chromophoric functional groups on discrete organic molecules. But even a simple, two component mixture may make the interpretation of a uv-vis spectrum difficult from a functional group point of view, so one can appreciate the enormity of the problem when attempting to glean any valuable functional group information from the uv-vis spectra of humic substances. The uv-vis spectra of humic substances is generally featureless (42) (43) (44) (45) (18), with the intensity of the absorption increasing towards shorter wavelengths. It has been stated that while absorption spectra do not provide detailed information on their chemical structure, the similarity of their spectra suggests that we are dealing with compounds with similar basic structure. Due to the absence of absorption maxima, no meaningful qualitative information can be obtained from spectra. However, it is possible to obtain useful information by employing other strategies. Examples include the estimation of concentration of dissolved humic substance in water based on Beer's law (i.e. absorbance is linearly related to concentration) and an estimate of the degree of humification using the E_4/E_6 ratio, i.e. the ratio of absorbance at 465nm to that of 665nm (7). Also Chen et al (46) present a very convincing argument for a relationship between E_4/E_6 and molecular weight. Chen et al state that the higher the ratio, the lower the molecular weight. However, due to the difficulty in measuring and obtaining reproducible results at 665nm other workers have proposed other absorbance ratios. For the example the E_2/E_3 ratio (ratio of absorbance at 250nm to that at 365nm) (47) which has the same relationships to molecular weight and humification as the E_4/E_6, but is more easily

measured because of the low absorbance at 665nm. Characteristically humics should have low ratios showing high molecular weight and higher humification and fulvics should have high ratios showing the inverse.

Finally, quantitative uv-vis spectroscopy has been applied to several studies of metal complexation by humic materials, especially in conjunction with chromatographic separation techniques (44) (18).

3.1.2 Spectroscopic Studies – Fluorescence

Humic substances are known to fluoresce (48) (42). In order to fluoresce, humic molecules must first absorb some uv-vis radiation. As such, fluorescence suffers from similar limitations as those of uv-vis spectroscopy. Schnitzer (42) and Schnitzer and Khan (44) review the literature on the use of spectrofluorimetry in the study of humic substances. The inapplicability of fluorescence to the direct determination of functionality in humic substances is apparent from these reviews. Although a detailed interpretation cannot be given as to functionality of the molecule, fluorescence is still a powerful technique and can be used quantitatively. Excitation is usually effected at wavelengths between 325 and 427nm (49), and fluorescence emission occurs between about 400-500nm.

Attempts have been made to differentiate between humics from different environments based on fluorescence spectra (50) and the fluorescence has been used in complexation studies using the quenching effect of increasing amounts of added metal to determine complexation constants (51). Plechanov (52) states that the slope of the curve of fluorescence intensity versus the concentration, even for fractions of the same material, will be inversely proportional to the molecular weight used. Fluorescence will be discussed in more detail in chapter five.

3.1.3 Molecular mass determination

Various methods have been used to determine number and weight average molecular masses based on Colligative properties, eg osmometry, depression of

freezing point and elevation of boiling point. However, such methods suffer once again from the drawback that humic substances are mixtures. Accordingly methods which attempt to fractionate, whilst determining molecular mass distribution, have been widely applied. These methods include ultrafiltration, gel permeation chromatography, and ultra centrifugation. There are no well defined ranges into which the molecular size of a humic or fulvic fall but, in general, humic acids are larger than the corresponding fulvic acid.

3.1.4 Ultrafiltration

Using a variety of polymeric materials and manufacturing processes, filters can now be prepared which have a known controlled pore size ranging from several micrometres to a few nanometres in diameter. Membranes with pore sizes at the lower end of the range can be used to filter molecules in solution on the basis of molecular size and this process is referred to as ultrafiltration. Membranes are manufactured by a variety of companies (eg Amicon, Millipore, Sartorius) with nominal molecular weight cut off values ranging from 50 to 100 000 daltons with numerous filters within this range. If the ultrafiltration membranes are used over a set molecular weight range, ie 500-100 000 daltons and in a set sequence, ie highest to lowest molecular weight cut off, then it is possible to determine the distribution of molecular masses of a given sample. Practically ultrafiltration is a very simple technique. Typically a solution of the sample is placed in the pressure cell with the membrane supported at the base of the cell. Pressure is applied to the cell by means of an inert gas and the solution is stirred constantly with a stirrer bar suspended just above the membrane. This is to help prevent clogging of the membrane, and to ensure a uniform distribution of solute molecules. However, the pore size within the membranes is not completely uniform so that the molecular weight cut off is not as sharp as it might be. Manufacturers quote that 90% or more of spherical uncharged solute molecules of that molecular weight will be retained. It has also been observed that charged particles interact with the membrane leading

to a sorption effect which can interfere with the filtration process. In addition the filtration process depends on both the pressure and concentration gradient (53). As the volume of the solvent in the cell decreases, the concentration of larger molecular size solutes in the cell increases, resulting in a breakthrough of larger molecular size solutes. Buffle et al (54) recommended that the filtration volume should never exceed 90% of the initial total volume. Nevertheless, the method is of value, giving operational molecular mass distribution.

3.1.5 Gel permeation chromatography (Gel filtration)

Gel permeation chromatography utilizes a synthetic gel matrix of cross linked polymers which have pores of approximately uniform size. The method then utilizes the fact that different sized particles travel through such a matrix at different rates which are proportional to the size of molecule in question. It is thought that for similar compounds size is proportional to molecular weight. If the system is calibrated with molecules of known molecular weight it is possible to create a calibration graph of logarithm of molecular weight against K_{av}. Where K_{av} is the fraction of the stationary gel volume which is available for diffusion of a given solute species and defines solute behaviour independently of bed dimensions and packing. Thus knowing the elution volume and thus K_{av} of an unknown species, the molecular weight can be theoretically calculated using the following relationship:

$$K_{av} = \frac{V_t - V_e}{V_t - V_o}$$

Most workers use Sephadex gels and an aqueous solvent system. However, Swift and Posner (55) reported interaction of humics with Sephadex, due to both electrostatic effects and adsorption effects. These sorption problems make the interpretation of results, which should be based exclusively on size effects,

difficult. These workers recommended, that in order to minimise such problems, separation should be carried out in a basic buffer eluant, with relatively high ionic strength, eg 1M tris buffer at pH 9. A further complication is that humic molecules are believed to aggregate to a varying extent depending on pH and ionic strength, hampering interpretation of results. A final problem is the lack of realistic standards for humic materials. The column should be calibrated with standards of similar chemical constitution to the substance under study, but no such standards exist for humic substances and therefore, globular proteins or polysaccharides have to be used. Despite these drawbacks and difficulties, because of its simplicity, gel filtration has been much used, much trusted technique and numerous workers utilize gel permeation chromatography (56) (57) (58) (59) (52).

3.1.6 Ultracentrifugation

Ultracentrifugation continues to be the most reliable means of determining the molecular weight values for dissolved humic materials. The two major techniques for molecular weight determination are sedimentation velocity and approach to equilibrium. Archibald (60) and Cameron et al (61) determined that whole humic acid samples are usually too polydisperse to yield reliable molecular weight measurement by sedimentation velocity ultracentrifugation. However, with an advance in technology it has been possible to obtain results for molecular weight distribution using a modified technique (62) (63). The main advantage of this technique is that matrix interactions are almost negligible. The technique is sufficiently sensitive to allow detection on samples of organic concentration 2mg l^{-1} to 40mg l^{-1} and the technique is purely dependent on molecular weight as opposed to molecular weight and size. This means that no preconcentration is needed. However, the cost and lack of availability of the equipment needed deters most investigators. Also, the suppression of intermolecular charges is essential. This is achieved by the addition of an electrolyte (64) and studies where this has not been done should be disregarded.

3.1.7 Elemental analysis

Before any approximate molecular structure can be postulated, it is essential that elemental analysis of the humic material is carried out. Traditional methods of organic elemental analysis including catalytic combustion followed by absorption of gases, Dumas and Kjeldahl techniques, etc. can be applied to humic materials. Elements determined include carbon, hydrogen, oxygen, nitrogen, sulphur, phosphorus and halogens. However, once again elemental analysis also suffers limitations as humic materials are dynamic mixtures of compounds and the results need careful interpretation. The most serious problem that affects elemental analysis is lack of reproducibility. Source, extraction and fractionation procedure all change the elemental composition slightly so most compositions fall within certain ranges :

	Humic %	Fulvic %
C	53.8-58.7	40.7-50.6
H	3.2-6.2	3.80-7.0
O	32.8-38.3	39.7-49.8
N	0.8-4.3	0.9-3.3
S	0.1-1.5	0.1-3.6

For humic substances it is not the actual percentage of element present that is important. Of more importance are certain elemental ratios which give the key to structure or material type, ie soil and aquatic humics have a H/C ratio clustered around 1.0, but lake and sedimentary humics have somewhat higher H/C ratios (65). It is the ratios of H/C, O/C and N/C that prove to be useful in many ways:

1) To identify types of humic substance;
2) To monitor structural changes of humates in soils and sediments;
3) To devise structural formulae for humates.

3.1.8 Determination of acidic functional groups

Numerous descriptions of methods of analysis of the acidic functional groups of humic substances have been published (66) (44) (18). The published methods include direct titration, discontinuous titration, indirect titration, thermometric titration, non-aqueous titration, irreversible reactions of acidic hydrogens and so on. The two most commonly described methods are the barium hydroxide method for the determination of total acidity, and the calcium acetate exchange method for the determination of carboxyl groups, both of which are classified as indirect potentiometric titration methods.

3.1.9 Total acidity determination

One must conclude that the total acidity of a sample refers to all acidic hydrogens that react with a specified reagent under a specified set of experimental conditions. It is apparent that a good method must involve equilibration of the sample with a reagent of high pH in order for even the weakest acid to react. However, this introduces two serious experimental problems. Firstly, it is difficult to accurately determine how much base has reacted with the humic substance in the presence of the extreme concentration of base that is needed to reach the high pH. Secondly, equilibration should be achieved as quickly as possible to avoid base catalysed site reactions that might alter the apparent total acidity of the sample. The two preferred methods for acidity determination are direct titration and the barium hydroxide method. The direct titration method involves the titration of a solution of the humic material dissolved in a basic solution, i.e. sodium hydroxide, under an inert atmosphere, titrated with a standard acid. This gives the acidity directly. The barium hydroxide method was originally designed for use with coals and was adapted for humic substance research (44). The method involves the addition of excess standard barium hydroxide to the humic material. Any precipitate is removed after an equilibration period under nitrogen, and the excess barium hydroxide is titrated with standard hydrochloric acid to pH 8.4. The pH of the

reagent is greater than 13 so all the acidic protons ions can be expected to have reacted. The results indicate total acidity. This is an example of an indirect titration.

3.1.10 Carboxyl content

The carboxyl content of humic material is often determined using the calcium acetate exchange method. The humic material is treated with an excess of standard calcium ethanoate. The acetic acid which is released is equivalent to the number of carboxyl groups present. After equilibration under nitrogen the product is filtered and the filtrate titrated against standard sodium hydroxide. However, the method is somewhat empirical, Perdue et al (67) showed that if sodium acetate is used instead less H^+ ions are released. Perdue et al concluded that calcium acetate may be releasing H^+ ions from other groups in addition to carboxyl groups. Again, the carboxyl titration results should be treated as operational results.

3.1.11 Phenolic content

There is no simple appropriate potentiometric method for determining phenolic groups exclusively. Consequently they are generally calculated as the difference between the total acidity and the carboxyl content. This generally means that they tend to be overestimated. A check that can be applied is to relate the phenolic content to the aromatic content, if it is known or can be estimated.

Table 1.2 Typical acid content of humic and fulvic acids

Acidity	HA(meq/g)	FA(meq/g)
Total acidity	7.1 - 8.9	9.6 - 16.6
COOH acidity	4.5 - 5.9	6.5 - 10.7
Phenolic acidity	2.2 - 3.7	1.0 - 4.7

3.2 Experimental

3.2 UV Visible Spectrophotometric Studies

3.2.1 Apparatus

1 cm path length quartz cuvettes and a Philips P8600 scanning ultraviolet visible spectrophotometer were used throughout the investigation.

3.2.2 Initial Beer's Law and pH Investigation using Aldrich sodium humate

To determine the concentration range over which Beer's Law holds for a typical humic material, 50 mg of Aldrich sodium humate (NaA) was dissolved in distilled water and made up to one litre in a volumetric flask.

From this solution nine other solutions of concentrations from 5mg l^{-1} to 45mg l^{-1} were prepared in distilled water. The ultraviolet and visible absorption spectra of each solution were recorded from 210nm to 665nm. The measurements were repeated with the same concentrations of sodium humate dissolved in 0.01M and 0.1M sodium hydroxide solution.

Figure 3.1 contains the calibration curves showing absorbance at 254nm plotted against dissolved sodium humate concentration in mg l^{-1}. All graphs show that Beer's law is obeyed over the concentration range investigated and that the absorption at 254nm is only slightly affected by increasing the pH of the solution.

To investigate the absorbance at lower pH values, a sample of the stock solution was placed in a 50ml beaker. The pH was lowered by the addition of 1M hydrochloric acid and the spectra measured after each addition of acid. The volume change was

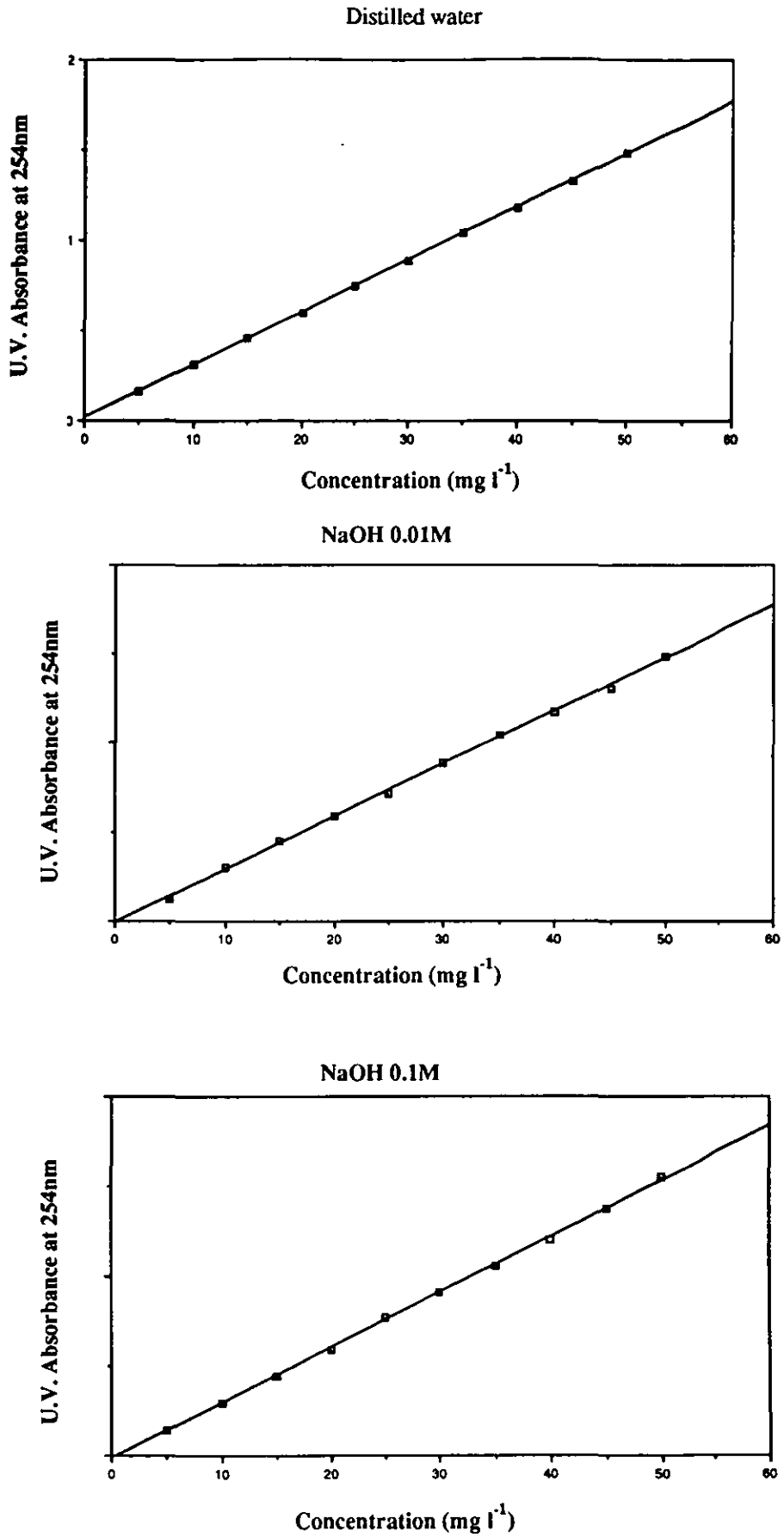

Figure 3.1 Aldrich sodium humate Beer's Law UV calibration plots at 254nm

negligible. Figure 3.2 shows that the absorbance at 254 nm changes only slightly within the pH range 2.5 to 7.

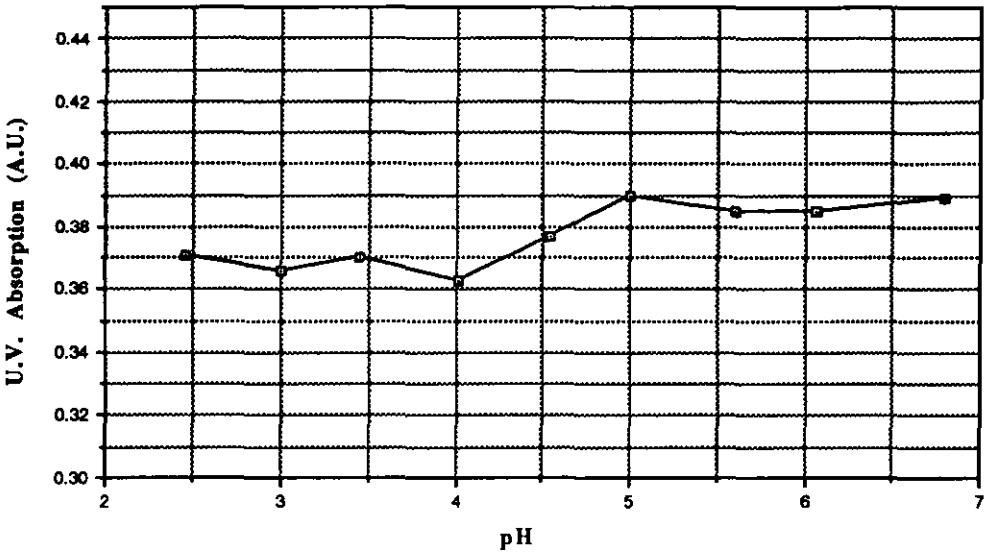

Figure 3.2 Effects of pH on the UV absorption at 254nm of Aldrich sodium humate

3.2.3 Investigation of UV-Visible spectrophotometric properties of HA, FA, HA/FA, NaA and in-situ material

The total organic carbon content (mg C l^{-1}) of the stock solutions of FA, HA, HA/FA and in-situ water are shown in Table 2.4. These solutions were diluted with phosphate buffer made up to pH 6.5 then sodium chloride added at 1% wt/vol to provide solutions of similar ionic strength. A solution containing 84 mg l^{-1} of NaA in the same phosphate buffer solution was also prepared. The absorbance of all solutions were measured between the wavelengths of 210 nm and 665 nm. The spectra were similar and the spectrum for HA/FA is presented as an example in Figure 3.3.

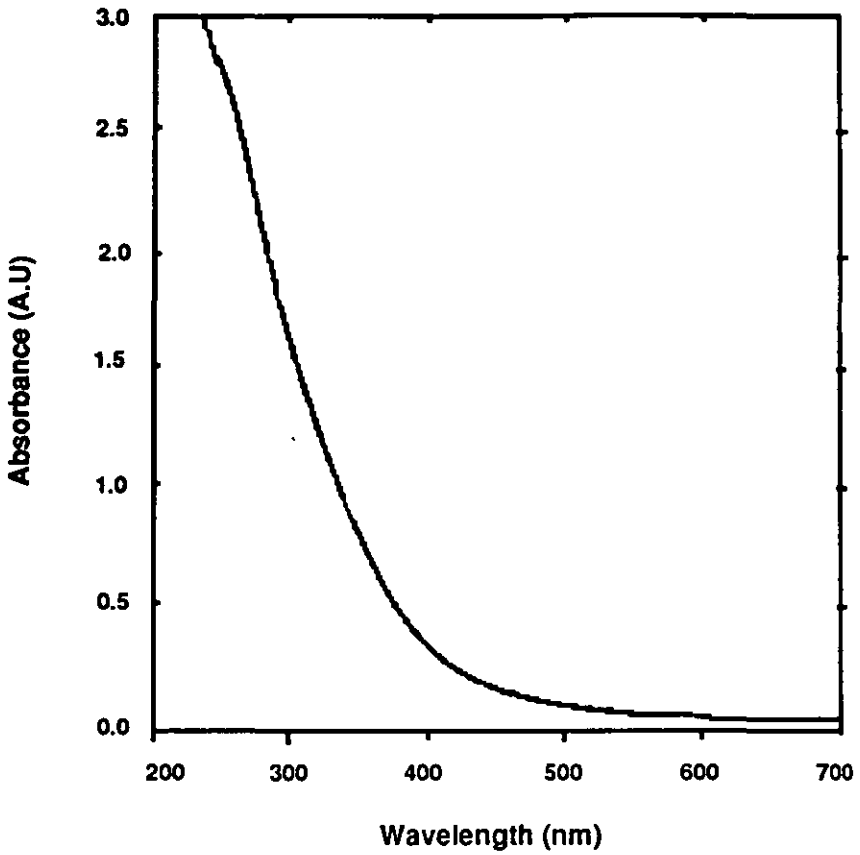

Figure 3.3 UV visible absorption of HA/FA

These solutions were progressively diluted and Figure 3.4 shows the results of plotting the absorbance at 254nm as a function of the organic concentration in each solution. It may be concluded that the absorbance at 254nm remains proportional to organic carbon concentration up to about 50mg C l^{-1} for all types.

The absorptivities were calculated to be

FA	0.0475	l mg^{-1} cm^{-1} (TOC)
HA	0.0755	
HA/FA	0.0430	
NaA	0.0535	
In situ	0.0398	

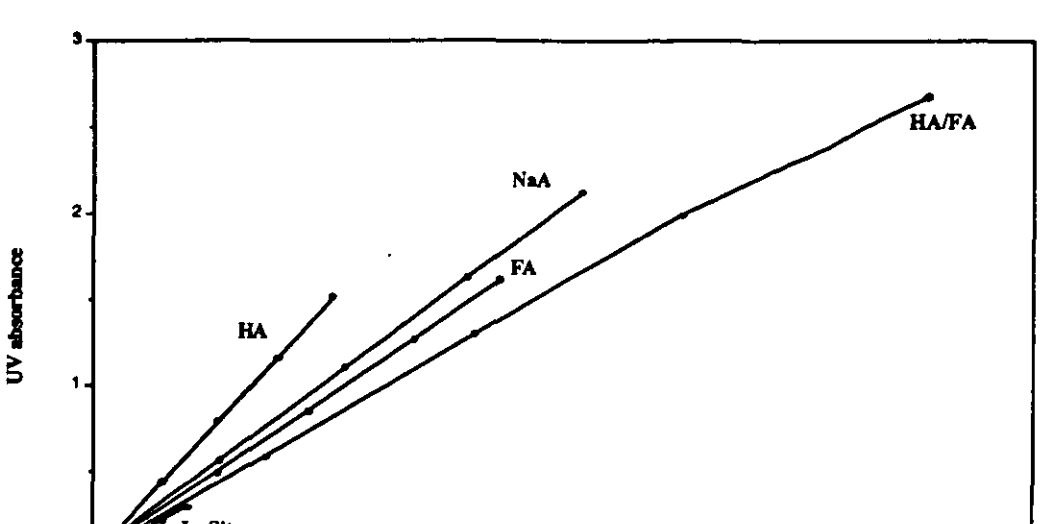

Figure 3.4 Extract and in-situ Beer's Law Calibration plots at 254nm

3.2.4 E_4/E_6 and E_2/E_3 determinations

Figures 3.5 and 3.6 show plots of the E_4/E_6, E_2/E_3 ratios of the various solutions as a function of the organic carbon content of each solution. As stated earlier the higher the ratio the lower the molecular weight and the lower the degree of humification. Figure 3.5 shows that it is difficult to determine a relationship between the different solutions using the E_4/E_6 ratio because the ratios were erratic and scattered. However, plotting the E_2/E_3 ratios as a function of TOC for each solution (Figure 3.6) produced the qualitative results anticipated. The FA solution showed the highest E_2/E_3 ratio since it has the smallest range of molecular weights and the lowest degree of humification. The two humic solutions gave the lowest ratios and the HA/FA and in-situ mixtures produced ratios which are in between those observed from the FA and HA solutions.

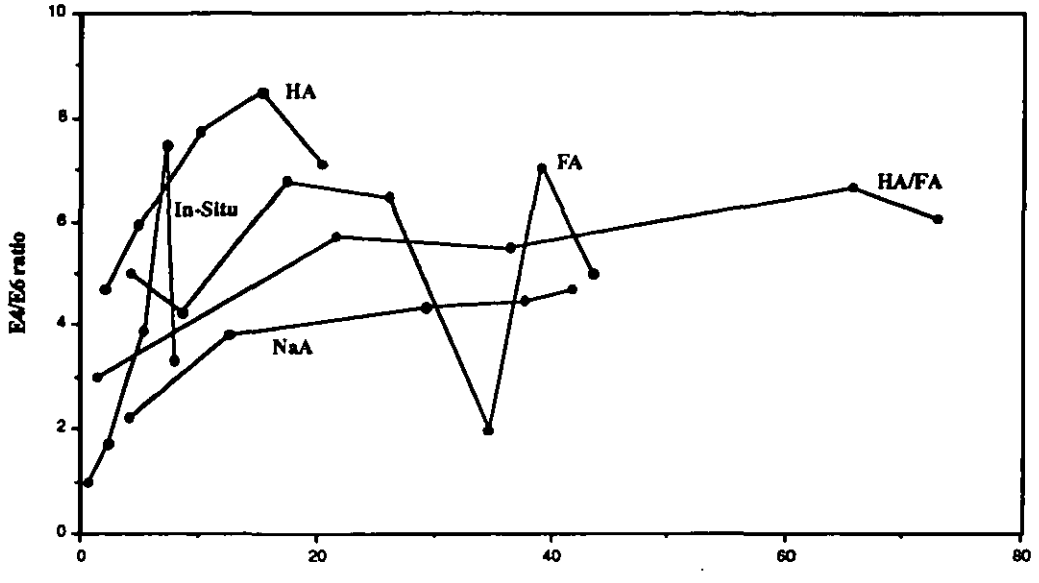

Figure 3.5 Variation of E_4/E_6 ratio with Total Organic Carbon content

3.2.5 Discussion of UV-Visible spectrophotometric results

The ultraviolet visible absorption studies show that:

1. The absorbance at 254 nm can be used to quantitate solutions of humic acid and fulvic acid at least up to a TOC concentration of 50mg l^{-1}. The absorptivities follow the trend: HA > NaA > FA > HA/FA > In-situ. From the absorptivities of the extracted fulvic acid (69% of in-situ TOC) and extracted humic acid (31% of in-situ TOC), the predicted absorptivity at 254nm of the in-situ material is

$$= \frac{(69 \times 0.0475) + (31 \times 0.0755)}{100} \text{ l mg (TOC)}^{-1} \text{ cm}^{-1}$$

$$= 0.0572 \text{ l mg (TOC)}^{-1} \text{ cm}^{-1}$$

This value is 1.4 times greater than the measured value which initially suggests that the absorptivity of the humic / fulvic molecules may have changed during the

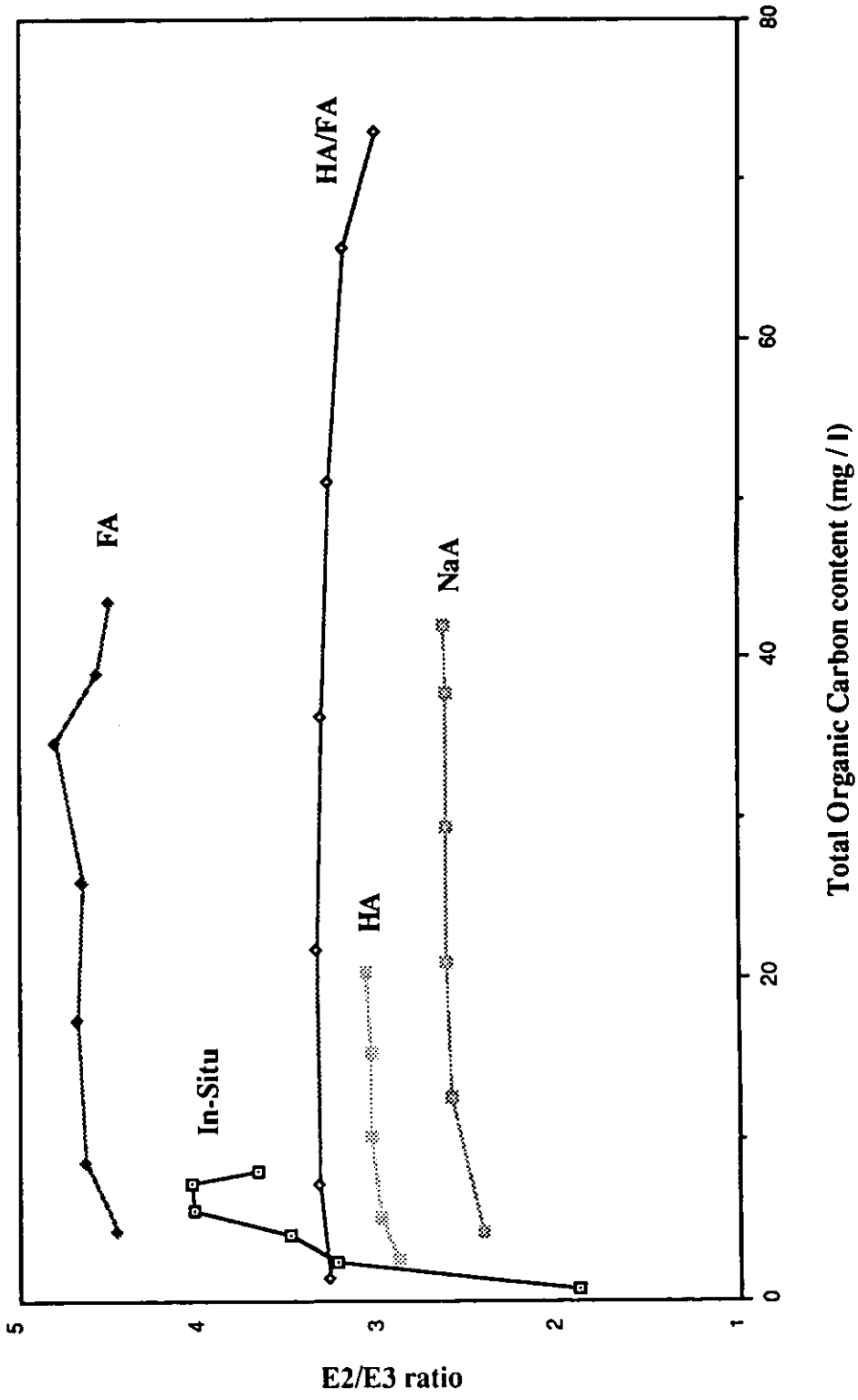

Figure 3.6 Variation of E2/E3 ratio with Total Organic Carbon content

extraction. However, the in-situ and HA/FA results are similar, which suggests that they have not.

2. The E_4/E_6 ratio is irreproducible

The E_2/E_3 ratio is subject to less scatter and the measurement of the E_2/E_3 ratio for the different materials gave results as expected. The calculated E_2/E_3 ratio for the in-situ material is

$$= \frac{(69 \times 4.7) + (31 \times 3.1)}{100}$$

$$= 4.20$$

This value corresponds to the two highest values shown by the in-situ water and is 1.25 times the average E_2/E_3 ratio of the HA/FA mixture.

3.3 FLUORESCENCE SPECTROPHOTOMETRIC STUDIES

3.3.1 Apparatus

The fluorescence measurements were made using a Hitachi model F-4000 spectrophotometer equipped with a 150w Xenon lamp and an R372F photomultiplier tube employing a band pass setting of 5nm. The samples were allowed to dark-adapt for 2 minutes prior to measurement. The cell holder was maintained at 25°C using a flow of thermostatted water.

The same solutions as those prepared in sections 3.2.2 and 3.2.3 were used for the fluorescence studies.

3.3.2 Preliminary Fluorescence Investigation of NaA

Calibration curves of maximum fluorescence intensity (arbitrary units) against

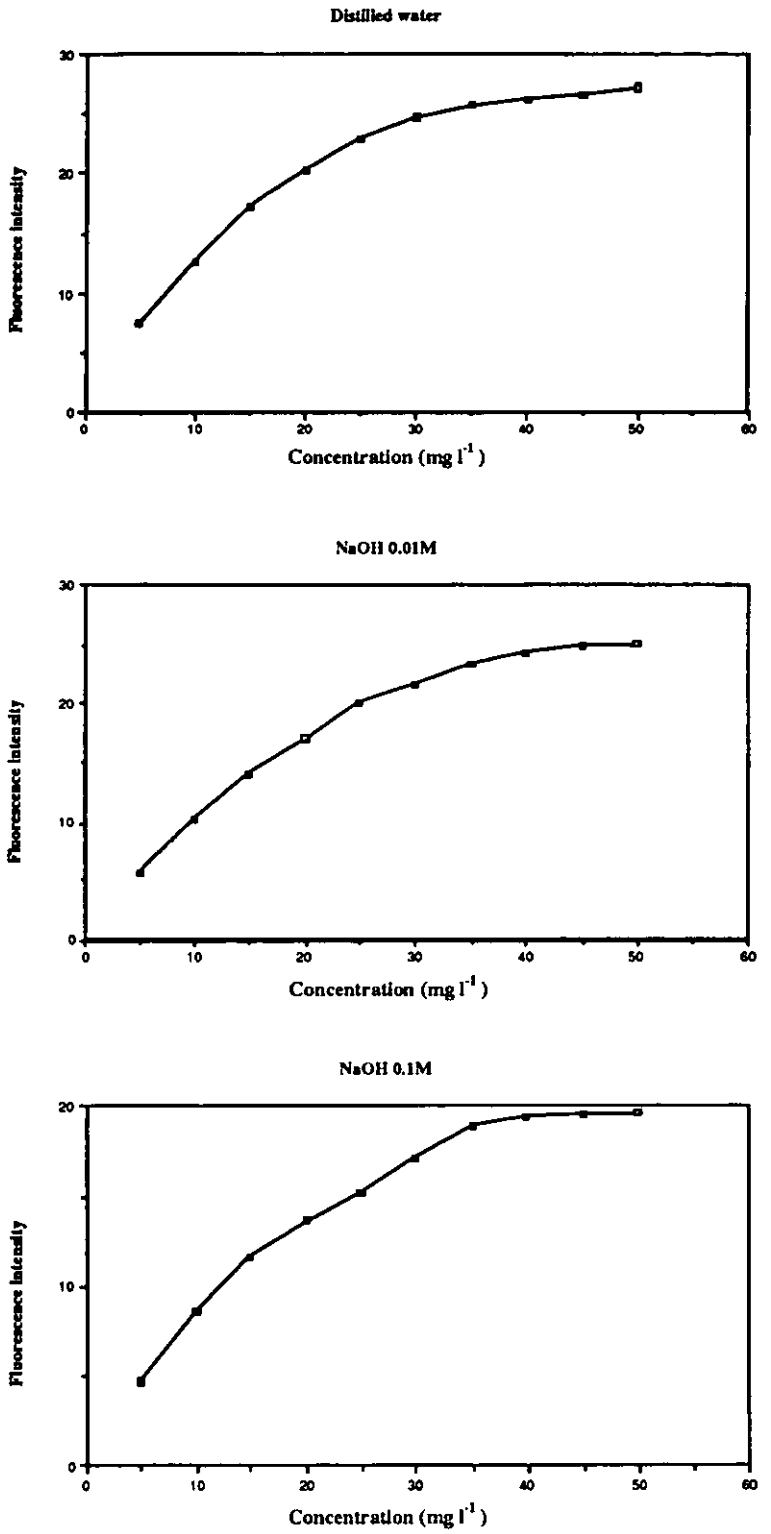

Figure 3.7 Aldrich sodium humate fluorescence calibration plots

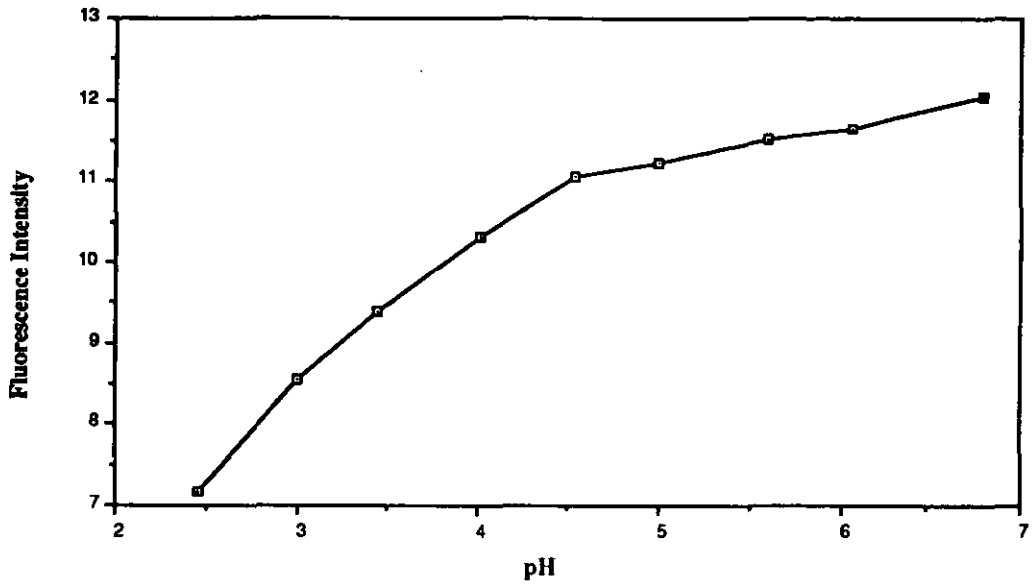

Fig 3.8 Effect of pH on the fluorescence intensity of Aldrich sodium humate

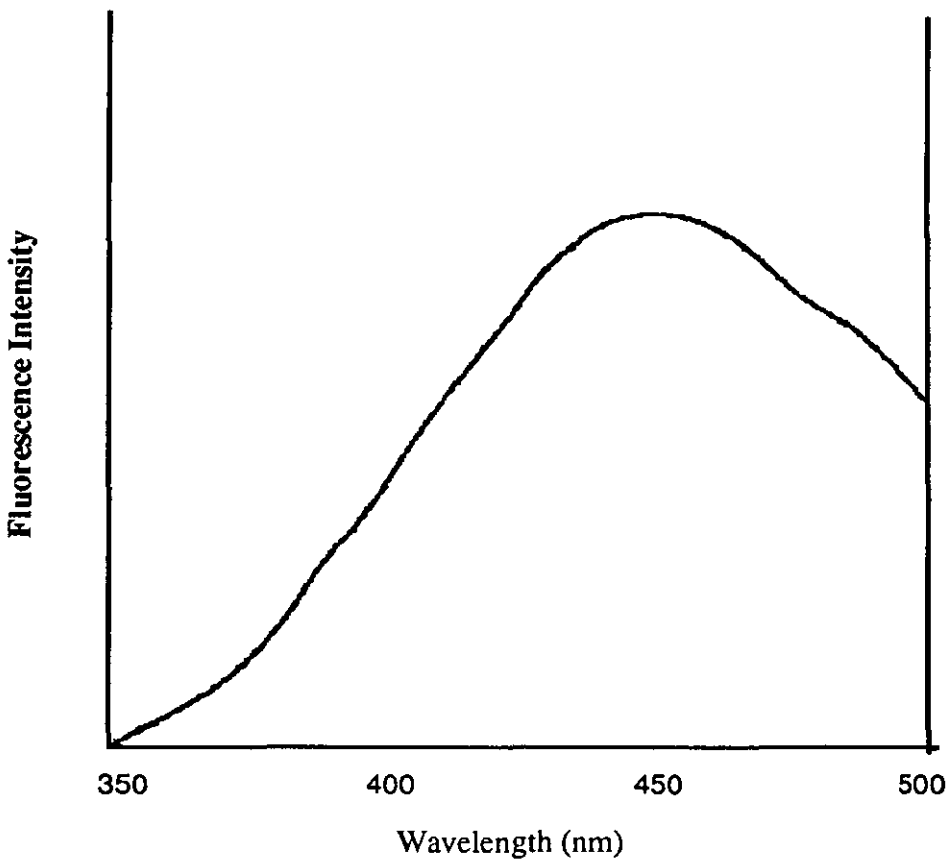

Fig 3.9 The fluorescence emission spectrum of HA/FA using λ_{ex} 350nm

TOC (mg l^{-1}) for NaA in distilled water, 0.01M and 0.1M sodium hydroxide solution are shown in Figure 3.7. An excitation wavelength of 350nm was used.

Figure 3.8 shows further effects of pH on fluorescence intensity of NaA dissolved in distilled water.

3.3.3 Investigation of fluorescence spectrophotometric properties of HA, FA, HA/FA and in-situ material

The fluorescence scans from 350nm to 500nm for HA, FA, HA/FA and the in-situ materials were similar and a typical result, the HA/FA mixture is shown in Figure 3.9. The excitation wavelength was 350nm.

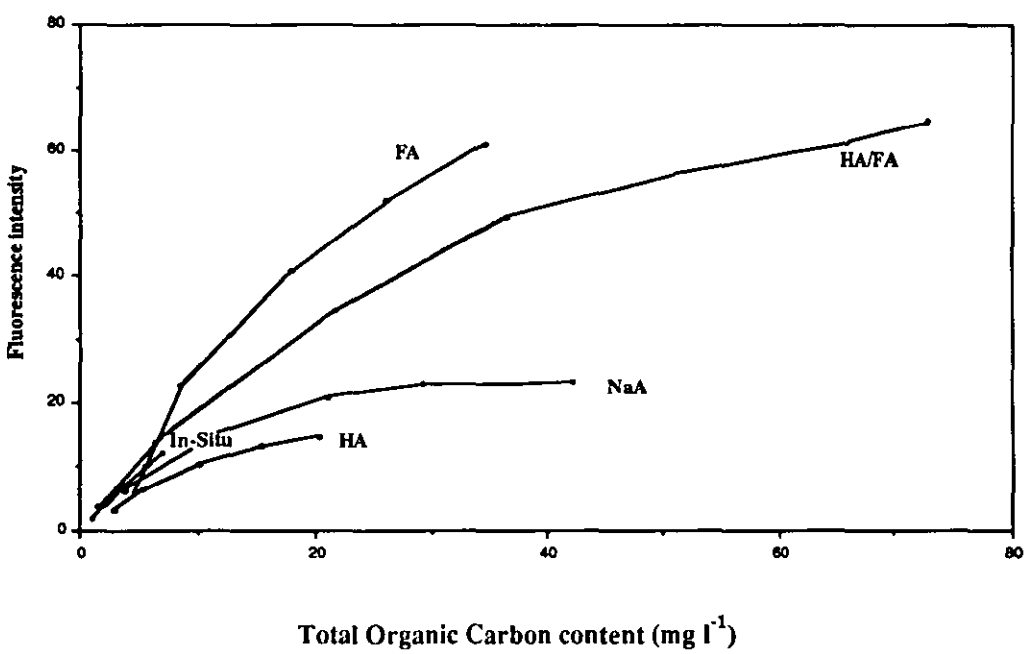

Figure 3.10 Extract and in-situ fluorescence calibration plots

3.3.4 Discussion of fluorescence results

Figure 3.10 shows the maximum fluorescence intensity of all the solutions including NaA plotted as a function of the total organic carbon content of each solution. These results show that the fulvic acid samples have the highest fluorescence per unit total organic carbon. The two humic substances (extracted humic acid and sodium humate) have the lowest fluorescence intensities per unit total organic carbon and the in-situ and the humic/fulvic mixture lie in between. The graph shows that fluorescence is linearly related to concentration below 20mg $C\,l^{-1}$. Noting that the measured fluorescence intensities of the various materials at a TOC of 20 mg l^{-1} are FA 46.25, HA 17.5, HA/FA 34.3, NaA 20, in-situ 34.3, the calculated value for the in-situ material is

$$= \frac{(69 \times 46.25) + (31 \times 17.5)}{100}$$

$$= 37.33$$

which is very similar to the measured value for the in-situ and HA/FA materials. This calculation suggests that the fluorescence properties of the humic materials and hence groups responsible for the fluorescence do not change significantly during extraction.

Plechanov (65) suggested that the slope of a curve of fluorescence intensity against concentration is inversely proportional to the molecular weight of the material. Detailed inspection of the early linear sections of the calibration plots in Figure 3.10 demonstrate this phenomenon. The two shallow slopes, which belong to the humic materials, are associated with the highest molecular weight materials. The fulvic and the humic / fulvic mixed have almost identically high slopes which correspond to the lowest molecular weights. The in-situ lies in between the two extremes. However, this information can only be used qualitatively to place the materials in molecular weight order.

3.4 ULTRACENTRIFUGATION

Ultracentrifugation used in this study was carried out by Dr. A Wilkinson (1992), Department of Biochemistry and Molecular Biology, Manchester University. The procedure was applied to determine the average molecular weight of species present in NaA, HA, FA HA/FA mixture and in in-situ material. A Beckman L8 - 70 ultracentrifuge, fitted with an ultraviolet scanner covering an absorbance range of 0 to 1.0 at 280nm was used. The output was sent to a Beckman recorder, giving a trace of absorbance versus radius. Samples were analysed in a cell fitted with 12mm double sector aluminium filled EPON centrepiece and plain quartz windows. The rotor was a Beckman 4 Place Titanium AnFTi.

For this technique to be successful, the sample to be analysed must have an absorbance at 254nm between 1 and 2. In order to comply with this requirement, the in-situ material was concentrated by rotary evaporation to yield an absorbance of 1.352. The TOC and absorbance values of the five samples are given in Table 3.2.

Table 3.2 Properties of samples provided for Ultracentrifugation

Sample	UV Absorbance at 254nm (a.u.)	Organic Content (mg C l^{-1})
FA	1.583	43.50
HA	1.607	25.50
HA/FA	1.500	73.00
NaA	1.702	73.00
in-situ (rotary evaporated)	1.352	45.36

The samples were diluted with a solvent containing 0.1M phosphate buffer pH 6.9, 0.1M NaCl + 1% sucrose, 0.05% sodium azide. The sucrose helped to prevent convective mixing due to the small concentration gradients obtained from the low weight concentrations in the cell. Samples were placed in one sector of the cell centrepiece and the solvent in the other. The absorbance measured by the instrument was the difference between the two sectors. The fluid column length was approximately 1.1cm. The results are shown in Table 3.3.

Table 3.3 Centrifugation Results

Solution	Molecular weight (Daltons) (immediate dilution)	Molecular weight (Daltons) (bulk of sample)
FA	2587 ± 346	1375 ± 23
HA	6073 ± 585	2725
HA/FA	2223 ± 352	1960
NaA	5700 ± 320	2000
In-situ (rotary evaporated)	2805 ± 249	1429 ± 40

3.4.1 Discussion of the ultracentrifugation results

Ultracentrifugation, unlike ultrafiltration and gel permeation chromatography, does not suffer to the same extent from problems related to molecular dimensions. Therefore ultracentrifugation may be the most accurate technique for determining molecular weights. If the molecular weights obtained after immediate dilution are considered, the results show that the two humics (HA and NaA) have the highest (and similar) molecular weights and the fulvic material has the smallest molecular weight. The molecular weight of the in-situ material lies in between these two

extremes. The humic / fulvic mixture seems anomalously low but when the limits of error are taken into account the molecular weight of this mixture of materials may lie between the two extremes.

The molecular weights designated 'bulk of the sample' are as to be expected. The humic (bulk) has a molecular weight of about 2725 Daltons. Using the 69:31 ratio the predicted in-situ is 1794, which can be compared with the value of 1429 actually measured and the 1960 value for mixed HA/FA. However, the value of 1429 may have been a low estimate, since evidence was obtained for a reasonably discrete group of larger molecules which did not contribute to the final value quoted for the rotary evaporated water, due to their rapid sedimentation.

3.5 ULTRAFILTRATION

30 ml of a solution of NaA (pH 6.3, ionic strength regulated with sodium chloride to 1%) was placed into an Amicon 8050 stirred ultrafiltration unit, above a filter membrane (45mm in diameter cut from a 150mm membrane disc). The unit was assembled and a positive pressure of nitrogen (70 bar) was applied.

The first 5ml collected from the cell was discarded, the next 10ml was kept for analysis and the remaining 15mls were discarded. The membrane filter was changed after each run for the next pore size membrane and the experiment repeated.

The membrane pore sizes were:

Membrane Code	Filtrate Size
YC05	<1nm
YM1	~1nm
YM5	<1.3nm
YM10	<1.7nm
YM30	<2.1nm
YM100	<5nm

All filter membranes were soaked in sodium chloride (5%) solution then in distilled water (3-4 changes of water), and finally washed with distilled water before use.

Measuring the ultraviolet absorbance at 254nm of the initial solution and of the filtrate enables the calculation of the percentage total organic content of the filtrate. From the percentages determined for each filter size, the percentage organic material passing through each filter can be calculated.

The ultra-filtrations were repeated with the in-situ material, HA, FA, HA/FA mixture. The results are presented in Table 3.4.

Table 3.4 Percentage material passing through filters with the stated pore sizes

Filtrate size	In-situ (rotary evaporated)	HA/FA	HA	FA	NaA	NaA *
<1nm	4.50	2.70	1.90	2.40	1.30	-
~1nm	9.00	11.01	8.74	9.13	5.87	4.9
1.3nm	32.43	28.00	19.67	35.40	11.86	-
1.5nm	36.04	57.12	51.09	67.00	26.66	33.3
2.1nm	39.64	84.03	83.06	89.50	57.89	54.3
5nm	63.06	96.00	96.72	95.60	80.85	-

* Results obtained by Peachy and Williams (68) included for comparison.

3.5.1 Discussion of the ultrafiltration results

The molecular weight cutoffs of the membranes stated for proteins were inappropriate for humics and fulvics so only size ranges were considered. The size distribution results show that the two humic materials (HA and NaA) have a higher proportion of larger sized molecules, ie only 19.67% and 11.86% pass through the 1.3nm membrane. The fulvic acid has the smallest molecular size range (35% passes through the 1.3nm membrane) and the humic / fulvic mixed has an intermediate size range. The in-situ material appears to be larger, which can be explained if the in-situ organic material is partially aggregated. Calculations were made to obtain the weighted average mean sizes of the various materials. The results given in Table 3.5, suggest that in-situ molecules are larger. The 69:31 ratio of FA to HA predicted an average size of only 1.511nm. However, the measured average value of 3.131 arose because of the existence of the discrete group of larger molecules in the rotary evaporated water first observed in the ultracentrifugation experiments.

Table 3.5 Average 'particle' size (Ultrafiltration)

Sample	Average Size (nm)
FA	1.351
HA	1.868
HA/FA	1.808
NaA	2.663
In-situ (Rotary evaporated)	3.131

3.6 SIZE EXCLUSION CHROMATOGRAPHY

Sephadex G50 size exclusion gel was used throughout this investigation. The gel has a fractionation range of between 1 500-30 000 Daltons for proteins.

2g of the untreated gel was placed into a beaker of 1% sodium chloride and left at room temperature for 3 hours to swell. When swollen, the gel was placed into a K9/ 30 gel column (Pharmacia, UK) and eluted with a mobile phase of 1% (wt -vol) sodium chloride solution at a flowrate of 4.4 ml hr^{-1}. Samples were introduced on to the column using a 1ml injection loop. The mobile phase that eluted from the column was monitored and the absorbance at 254nm recorded continuously. The mobile phase was also fraction collected and the ultraviolet and visible absorption spectra and fluorescence spectra of each fraction obtained.

3.6.1 Calibration experiments

To estimate the molecular weight of an unknown, from the volume of mobile phase required to elute the unknown from the column, the column was calibrated with molecules of known molecular weight. In this study globular proteins were used, although it is accepted that they are probably inappropriate as standards for humic and fulvic acid molecular weight determinations.
The compounds used for molecular weight calibration of the column were:

Calibrant	Molecular Weight
Blue dextran	> 1 000 000
Chymotryptsinogen A	25 000
Ribonuclease A	13 700
Sodium Acetate	82

Blue dextran was used to determine the voids volume (V_0), ie the mobile phase volume required for an unretained material to pass through the column. Sodium acetate was used to determine the total column volume (V_t), ie the volume of mobile phase required to elute a material which is expected to completely penetrate the pores of the gel. A material which elutes in a volume which is greater than that of the total volume must undergo adsorption on the gel and therefore the molecular weight of the material cannot be correlated with its elution volume.

The peak elution volume (V_e) of each compound was determined from the ultraviolet trace and K_{av} calculated from the following relationship

$$K_{av} = \frac{V_t - V_e}{V_t - V_o}$$

Table 3.6 shows the elution volumes, the K_{av} values and the logarithms of the molecular weights of the calibrants.

Table 3.6 Sephadex G50 Calibration Data

Compound	Elution volume ml	K_{av}	log MW
Blue dextran	7.42	0.00	>6.0
Chymotryptsingen A	9.45	0.19	4.4
Ribonuclease A	11.25	0.37	4.2
Sodium Acetate	17.77	1.00	1.9

The plot of K_{av} against the logarithm of molecular weight is shown in Figure 3.11.

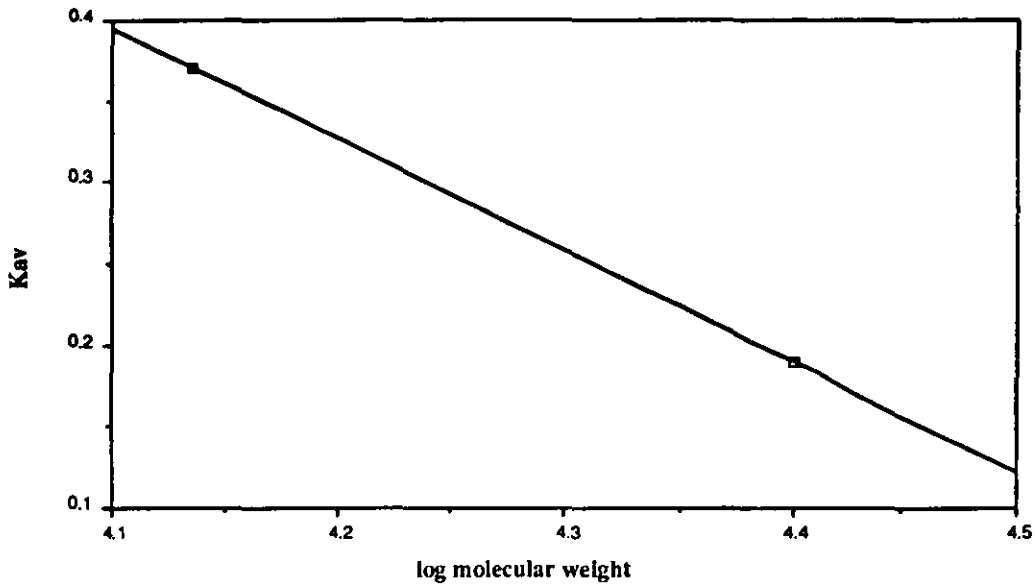

Figure 3.11 Sephadex G50 molecular weight calibration plot

3.6.2 Gel chromatographic analysis of HA, FA , HA/FA, NaA and x4 in-situ material

1ml samples of the x4 water, NaA, FA, HA and HA/FA were passed through the column. The peak elution volume of each material was determined using a UV detector and the ultraviolet visible absorption spectra and fluorescence spectra of each fraction recorded.

Figures 3.12 to 3.16 show the 254nm elution chromatograms of these species.

Table 3.7 shows the calculated peak molecular weight of each species derived from the measured K_{av} values.

Table 3.7 Sample Molecular Weights (Gel Filtration)

Species	K_{av}	Peak Molecular Weight
x4 water	0.913	1860
NaA	0.980	1463
FA	0.947	1646
HA	0.947	1646
HA/FA	0.913	1860

Two distinct peaks were observed in the elution profile (Figure 3.12) of the in-situ material. One peak was eluted near the voids volume (molecular weight >30 000 Daltons) of the column. This peak was not fluorescent. The other peak was eluted later and corresponded to a molecular weight of approximately 1900 Daltons. The elution profile of the NaA (Figure 3.13) showed one major peak at 1500 Daltons with a very minor peak around the voids volume. The elution profile of the extracted FA (Figure 3.14) did not show a peak around the voids volume. The elution profile of the extracted HA (Figure 3.15) showed a reduction in the peak eluted around the voids volume. The HA/FA mixture (Figure 3.16) showed only a small shoulder on a main peak at the voids volume of the column. The chromatographs showed tailing of the main peaks which indicated reversible sorption, i.e. the material was not being separated purely on a size / molecular weight basis. The appearance of a high molecular weight fraction in the rotary evaporated water coincided with the ultracentrifugation and ultrafiltration findings.

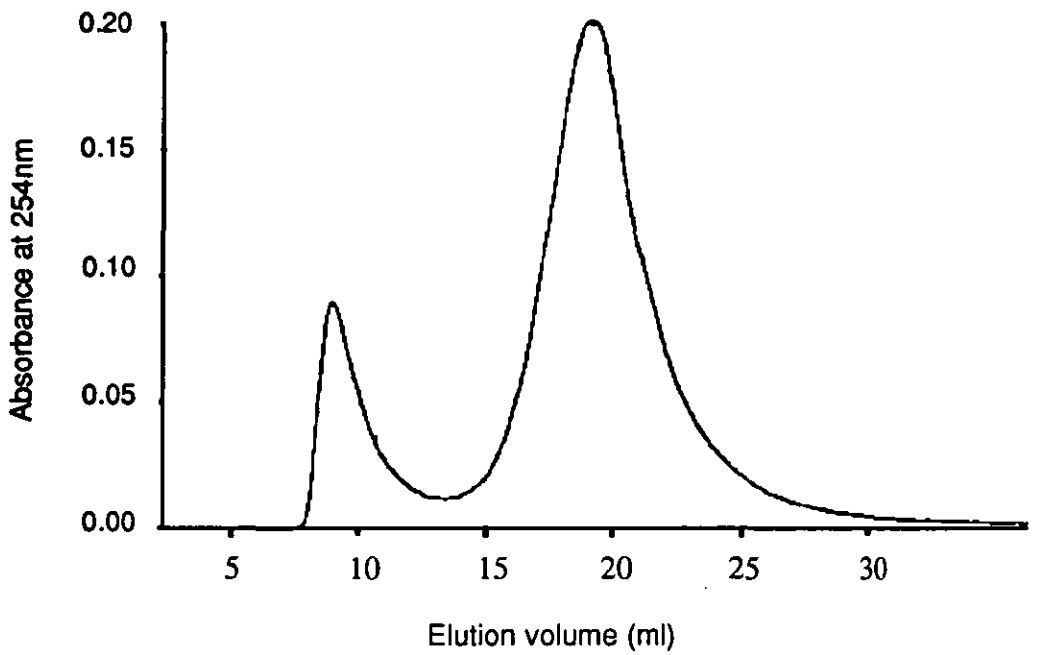

Figure 3.12 Gel filtration of x4 water

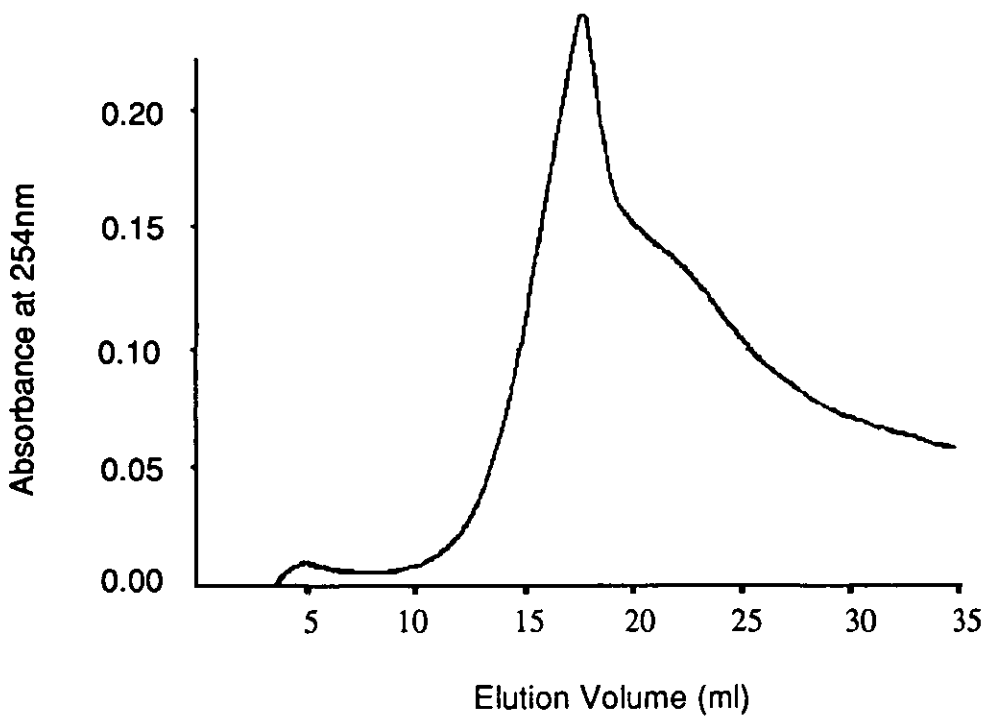

Figure 3.13 Gel filtration of sodium humate

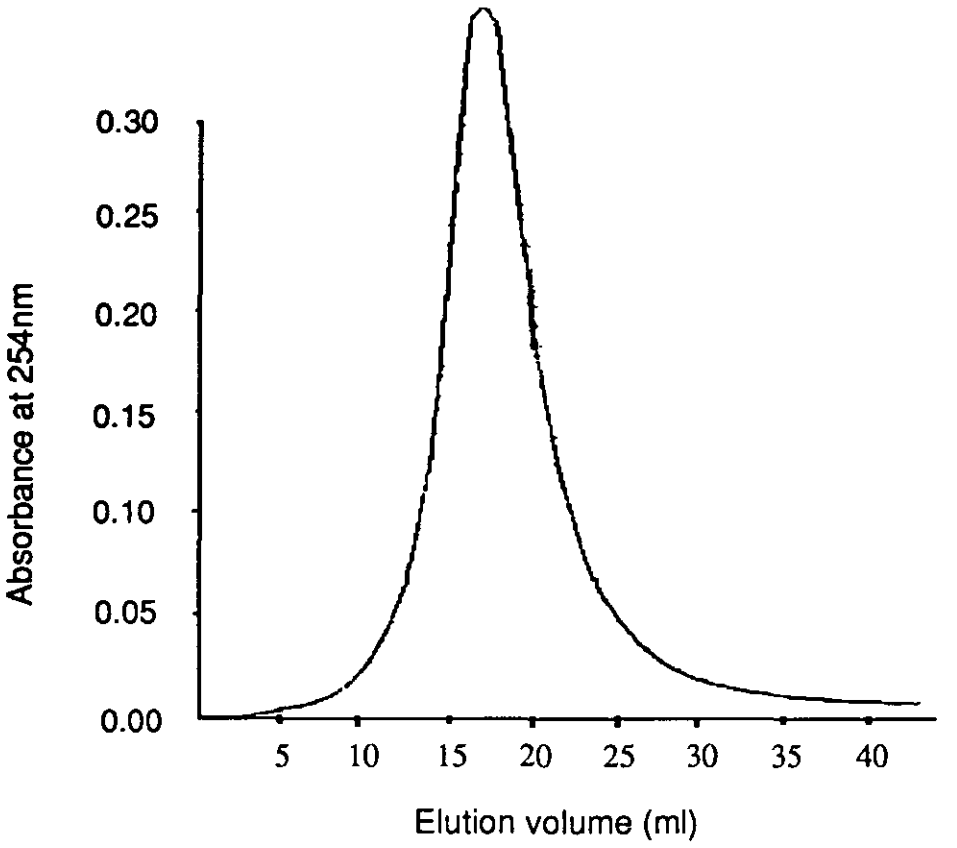

Figure 3.14 Gel filtration of FA

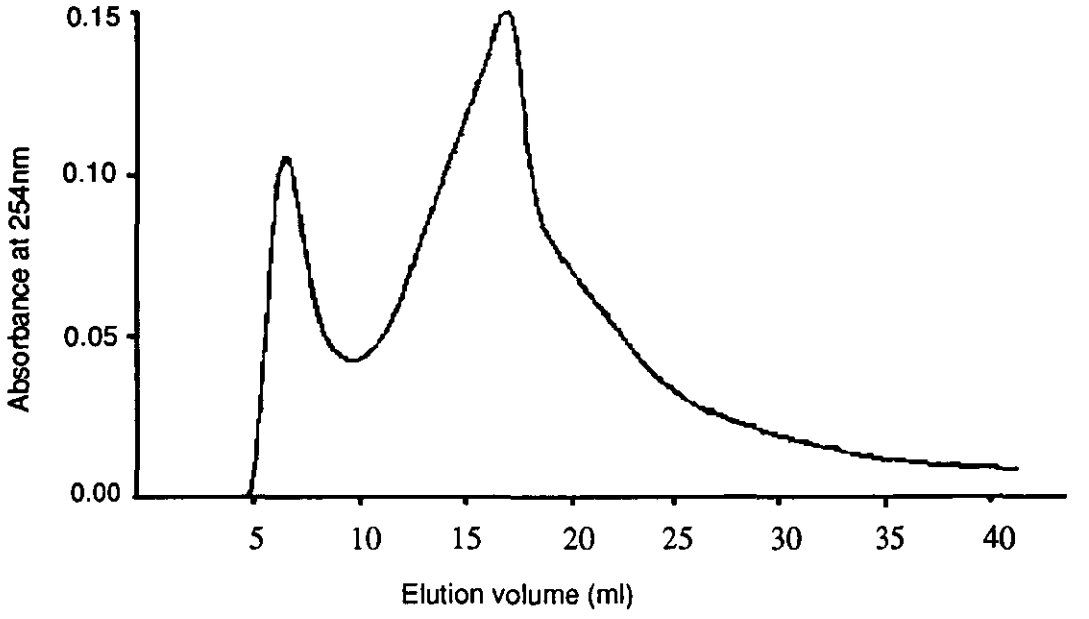

Figure 3.15 Gel filtration of HA

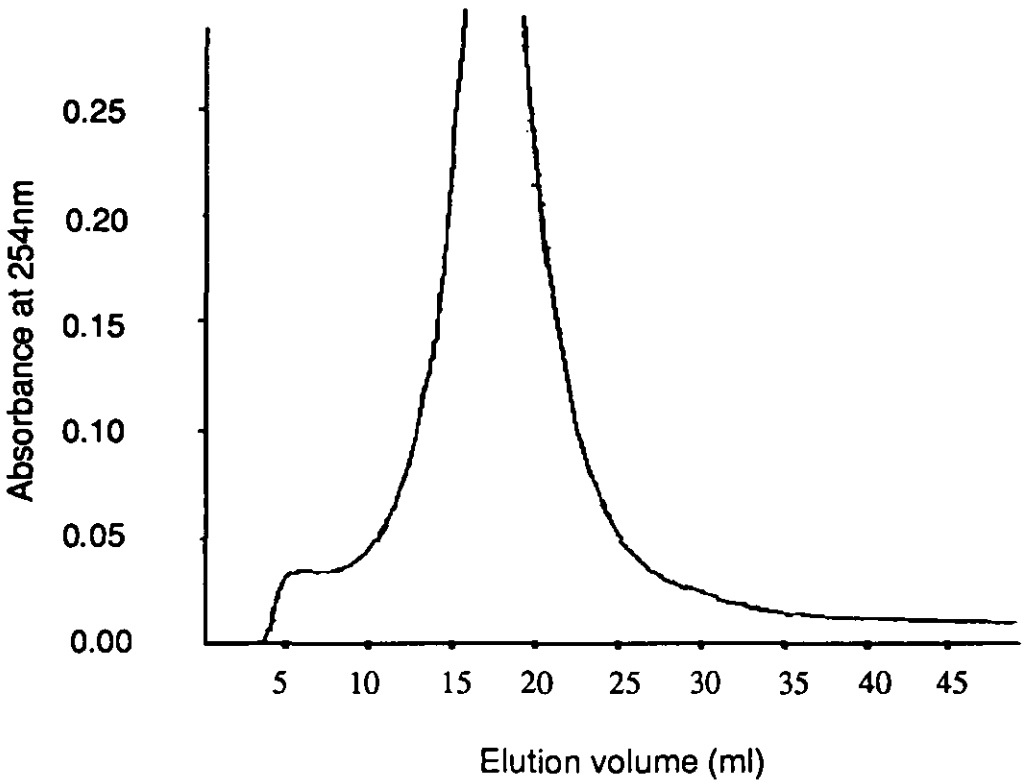

Figure 3.16 **Gel filtration of HA/FA**

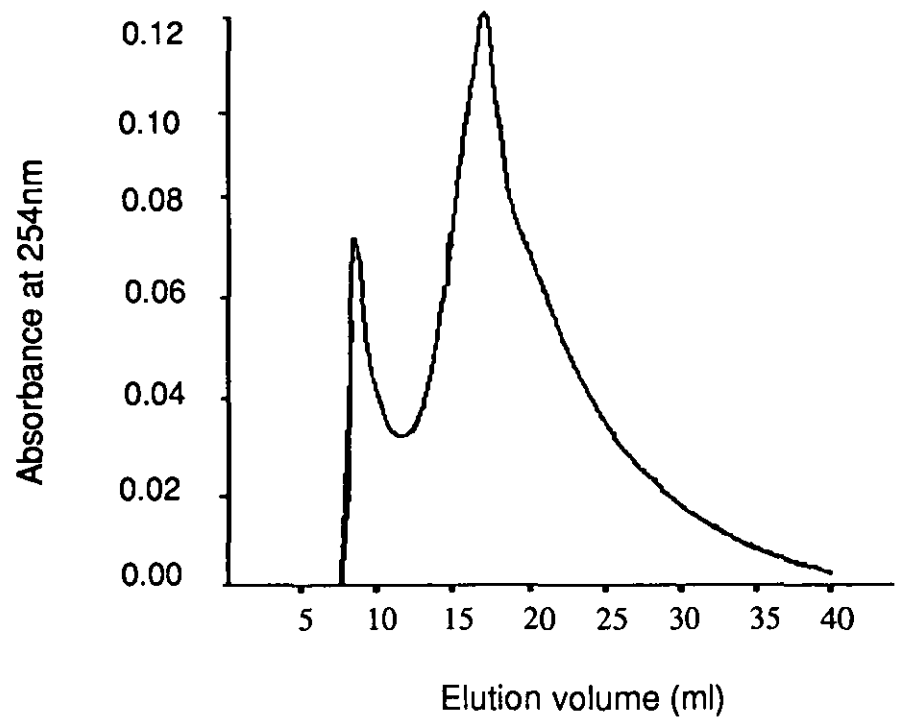

Figure 3.17 **Gel filtration of HA in the presence of phosphate buffer and 1% NaCl**

The experiment was repeated using a mobile phase of 1% sodium chloride and phosphate buffer of pH 6.5 to reduce sorptive effects. A sample of HA was passed through the column and again (Figure 3.17) tailing of the elution peak was observed. This showed that reversible sorption still remained a problem so that the peak maxima positions were late and the molecular weights were underestimated. The in-situ value (1860) was higher than the HA or FA which gave identical results (1646). However the in-situ main peak result agreed with the HA/FA result.

3.7 DISCUSSION OF SIZE DISTRIBUTION RESULTS

The values obtained for molecular weights and sizes were highly dependent on the technique. However, the trends discovered are summarised below:

Technique

Ultracentrifugation (imm diln)	HA	>NaA	>In situ	>FA	>HA/FA
Ultracentrifugation (bulk)	HA	>NaA	>HA/FA	>In-situ	>FA
Ultrafiltration	In situ	>NaA	>HA	>HA/FA	>FA
Size exclusion	In situ	= NaA	>HA	=FA	>NaA
Fluorescence (Plechanov technique)	NaA	>HA	>In situ	>HA/FA	>FA
E_2/E_3	NaA	>HA	>HA/FA	>In situ	>FA

Broadly similar trends can be seen in the ultracentrifugation (bulk), fluorescence and E_2/E_3 techniques. Gel chromatography suffered from adsorption problems and the ultrafiltration method could not be calibrated with suitable molecular weight standards.

3.8 ELEMENTAL ANALYSIS

Solid samples of HA, FA and NaA, prepared as described in Chapter 2, (2.7), were sent to Butterworth's Laboratory for elemental CHNO and Ash analyses.

3.8.1 Discussion of elemental analysis results

The results of the elemental analyses are presented in Table 3.8.

Table 3.8 Elemental Analysis

	%C	%H	%N	%O	%Ash	H/C
HA	46.46	4.02	1.46	42.96	5.1	1.038
FA	16.95	1.37	0.66	61.32	19.7	0.97
NaA	50.42	4.06	1.26	38.86	5.4	0.966

The elemental compositions of the humic acid and the elemental ratios are similar to previously reported results, see Steelink (69). However, the fulvic acid results are rather lower than those which have been previously published for fulvic acid analyses.

3.9 TOTAL ACIDITY

The classical indirect $Ba(OH)_2$ method was employed initially.

3.9.1 Experimental

100 mg of NaA was weighed into a 100 ml ground glass stoppered conical flask. 20 ml of a saturated solution of $Ba(OH)_2$ was added to the flask and the air in the flask was displaced with nitrogen. The flask was then shaken at room temperature for 24 hours. The suspension was filtered and the residue washed thoroughly with HPLC water which had been degassed with nitrogen for 3 hours. The filtrates and washings were titrated potentiometrically under an inert atmosphere, using a pH electrode, with standard 0.1M hydrochloric acid. The volume of acid required to convert the solution to a pH of 8.4 was noted.

To calculate the total acidity, the following formula, which can easily be derived from first principles, was used:

$$\text{Total acidity (mmol g}^{-1}) = \frac{(Vb - Vs) \times M \times 10^3}{\text{Wt of sample (mg)}}$$

where Vb = titration volume of blank (ml)

Vs = titration volume of sample (ml)

M = molarity of acid

Using the formula the acidity of NaA was found to be 3.14 mmol g^{-1}.

Figure 3.18 shows the typical titration results.

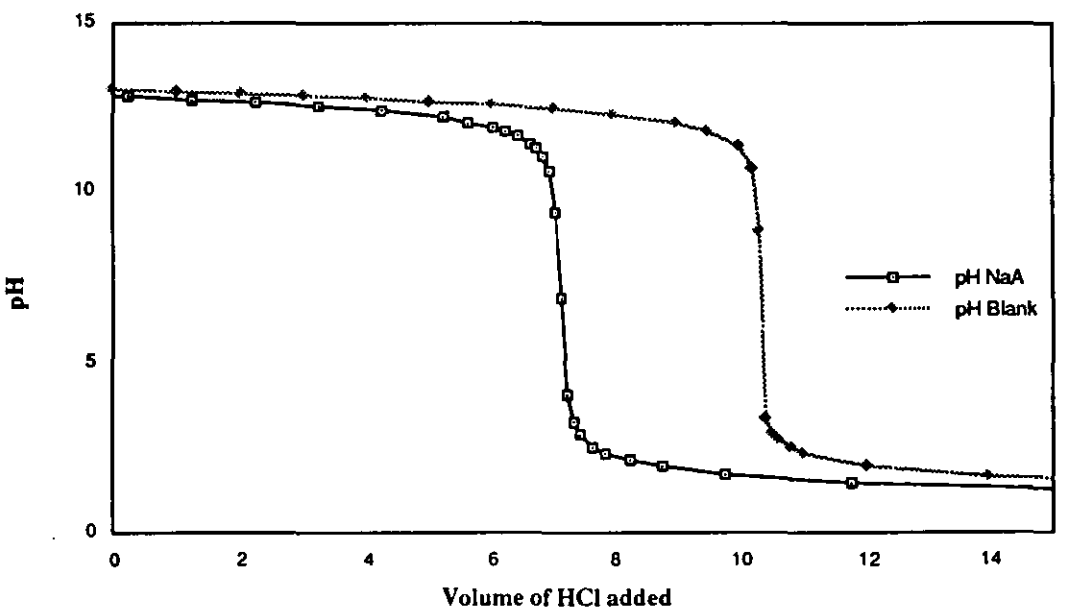

Fig 3.18 pH titration of sodium aldrich humate

The acidity found for the sodium humate is close to that obtained by Peachy and Williams (68) for the same material.

3.9.2 Acidity of natural materials – direct titration

The $Ba(OH)_2$ method could not be applied to the extract solutions which had been previously adjusted to pH 6.3, and had lost their inherent acidity, so the direct titration method reported by Borggaard (70) was employed. The humic or fulvic solution was mixed with NaOH solution, after equilibration excess HCl was added, then the mixture titrated with NaOH.

3.9.3 Experimental

50 ml of a solution of reprecipitated AHA (196 mg in 1 litre of 0.1M NaCl) was placed in a titration vessel and 2 ml of 0.1M sodium hydroxide solution was added. The mixture was left to equilibrate for one hour under a helium atmosphere with continual stirring, then 3 ml of 0.1M hydrochloric acid was added and the mixture was left stirring for a further two hours. The mixture was titrated potentiometrically (each reading being taken on a quiescent solution) with freshly prepared 0.1M sodium hydroxide solution. The temperature was constant throughout the experiment at 18°C. The first derivative (dpH/dV) of the titration curve is shown in Figure 3.19. The acidity of the solution was calculated from the volume difference between the two peaks which represented the end points of the titration for the initial excess hydrochloric acid (pH 3.4) and the humic material (pH 10). The procedure was repeated using the various extract solutions and the x4 water sample.

3.9.4 Discussion of direct titration results

The results are shown in Table 3.9

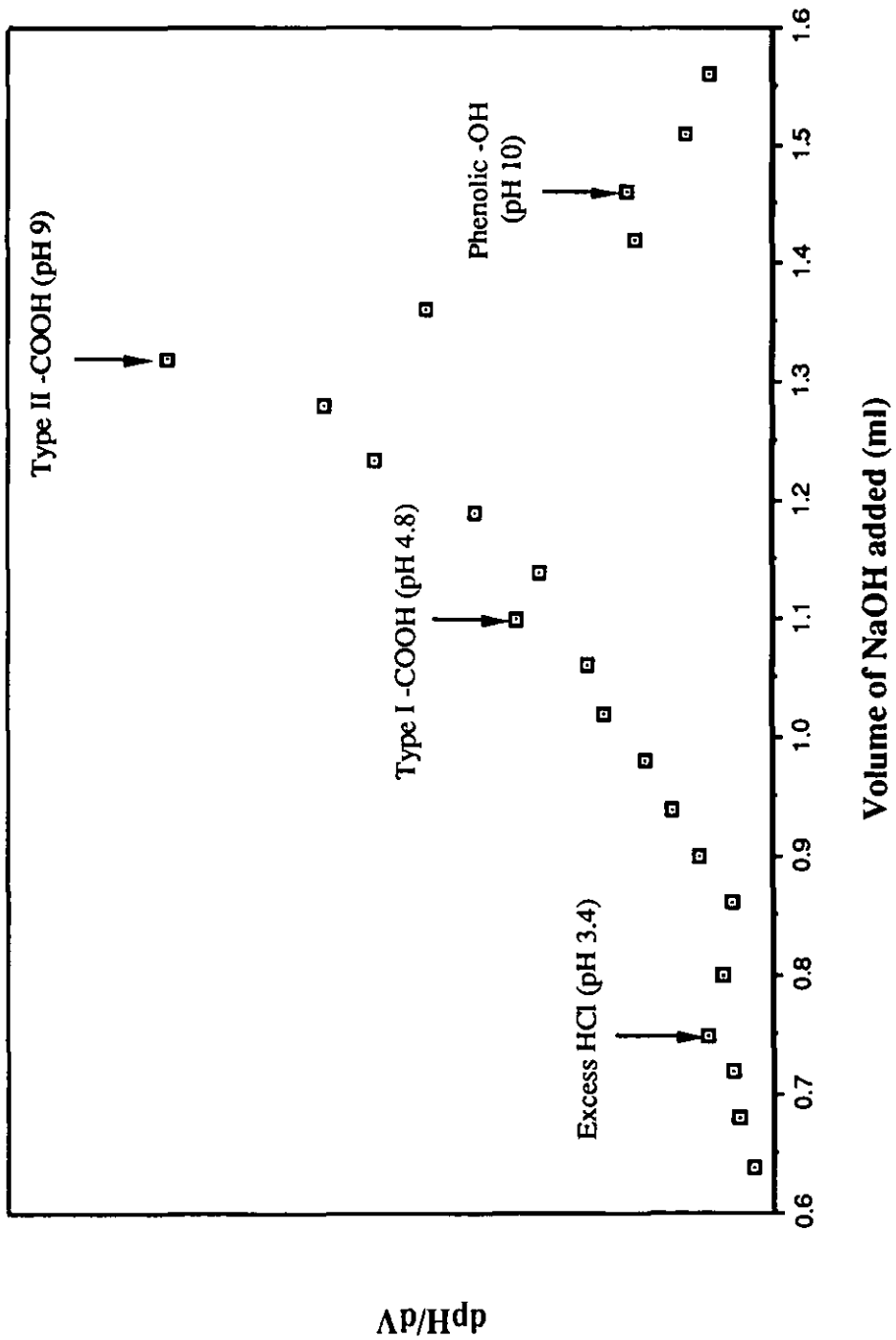

Fig 3.19 Direct titration of Aldrich sodium humate

Table 3.9 The amounts of COOH and Phenolic-OH expressed as mmol g^{-1} of humic (fulvic) material (assuming 50% TOC)

Material	Total COOH (mmol g^{-1})	Phenolic-OH (mmol g^{-1})	Total proton capacity (mmol g^{-1})
FA	8.60	5.97	14.57
HA	7.03	3.96	10.99
HA/FA	10.95	2.74	13.69
AHA	5.56	1.83	7.39
x4 water	11.02	10.15	21.17

These results show that the extracted humic acid has a lower proton capacity than the extracted fulvic acid. This confirms previously published observations. Both extracted acids have apparently lower capacities than the in-situ material. The highest proton capacity was observed from protonated Aldrich humate.

Calculation of the expected proton capacity for the in-situ material is shown below

$$= \frac{(69 \times 14.57) + (31 \times 10.99)}{100}$$

$$= 13.46 \text{ mmol } g^{-1}$$

The measured value is 57% higher than the calculated value, but this is not surprising as the x4 water contains acidic species other than humic materials, eg acidic metal aquo ions.

3.10 CONCLUSIONS

The techniques used to characterise the materials under investigation were validated using NaA and, in general, the results obtained compared favourably with published results.

The in-situ material was found to be composed of 69% fulvic acid and 31% humic acid, assuming negligible contribution from other dissolved organics.

The ultraviolet and visible absorption spectra of all materials were similar. No absorption maxima were observed, the absorption simply increased as the wavelength of the absorbed radiation decreased. The absorption at 254nm was shown to be proportional to the TOC up to at least 50 mg l^{-1} which provided a convenient method of measuring TOC in solution. The order of absorptivities, at 254nm, for the various materials was HA > AHA > FA > HA/FA > In-situ. Using the values of the absorption at 254nm of the extracted materials, it was not possible to predict accurately the absorption of the in-situ material.

The fluorescence spectra of all the materials are similar but changes in the wavelength of the maximum intensity of the emitted light were observed. The maximum intensities of fluorescence decreased in the order FA > HA/FA = In-situ > NaA > HA> AHA. Using the intensities of the extracted materials it was possible to predict approximately the intensity of the fluorescence of the in-situ material.

Conclusions as to whether the size (or molecular weight) of the humic materials changed during extraction and dissolution are difficult to make because of variations in the data obtained from the different techniques. The molecular weights derived by size exclusion chromatography must be used with caution due to sorption of the humic material onto the gel and lack of suitable calibration

standards. However, a general conclusion is that the size ranges of the in-situ material and HA/FA mixture lie in between those observed for the extracted HA and FA materials.

The direct determination of total proton capacities of the extracted material showed that they increased in the order AHA < HA < HA/FA < FA.

Overall the characterisation studies showed that the in-situ materials were similar. Also, the parallel studies (107) on the complexation properties of the in-situ and extracted HA and FA conducted by another member of the research group demonstrated no major effects on extraction.

Chapter Four

Determination of the stability constants of metal and humic acid complexes using ion exchange

4.1 REASON FOR WORK

The need to study the transportation of toxic metals and radionuclides through the geosphere and biosphere is becoming ever more important with the advent of radioactive waste repositories and land fill sites. Both sites will eventually become exposed to groundwater so the uptake of environmental pollutants and the transportation capacities of humic and fulvic material need to be evaluated.

The humates transport metal ions by complexing with them thus converting the positively charged metal ion into a negative complex, and possibly preventing binding to negative clay particles. The negative complexes, being water soluble, may therefore be transported from a waste site by groundwater movements.

For these systems to be modelled accurately, stability constants of metal humate complexes need to be known. The present methods for measuring stability constants are generally slow, expensive and labour intensive. Therefore there is a need for a fast, cheap, reliable method to be developed.

4.2 CHOICE OF MEASURING TECHNIQUE

In general the methods employed for determining the parameters [M], [S] and [MS] can be divided into two groups. Those which separate the components of a mixture before analysis and those which analyse the components of the mixture without separation.

The two approaches are discussed separately below.

4.2.1 Methods based on direct physical separation

The principle methods used in the separation technique are those which are based on differences in

i) charge characteristics

ii) redox properties

iii) size

In general a solution of humic material is titrated with the metal ion being studied, under specified conditions of pH, ionic strength, temperature etc. The system is allowed to reach equilibrium after each addition, i.e the concentration of [M], [S] and [MS] are constant. The 'free' and 'bound' metal species are then separated utilising a technique that is based on one of the properties mentioned and the concentration of one or all of the species is then measured.

The method used to separate the species must do so rapidly so as to eliminate any effects of kinetic instability which would lead to dissociation of any bound species and thus gives an underestimate of metal complexation.

Techniques that fall into this category include dialysis (71)(72), voltammetry (73)(74), size exclusion chromatography (75)(76), ultrafiltration (54)(77) and ion exchange (78).

4.2.2 Direct methods without separation

The humic material is titrated as before and the solution is allowed to reach equilibrium. Then some property of the system that is related to either the 'free' [M] or the 'bound' [MS] is measured without separation of the components. The techniques need to be suitably selective and sensitive for this method to work.

As there is no disturbance of the position of equilibrium with this method there is no problem with the kinetic instability of the formed complex.

The techniques in this category include UV- visible spectroscopy (84)(85)(86), ion selective electrodes (87)(88), fluorescence spectrophotometry (89)(90) and ion exchange (Schubert's method (91)).

4.3 ION EXCHANGE

Ion exchangers are generally utilized in one of two ways, namely batch wise or packed in a column, the choice of method is dependent on the application.

In batch wise operations the resin is added to a suitable container with the solution system being studied. The system is allowed to establish an equilibrium, and once the reaction is complete the treated solution is separated from the resin by filtration or decantation. The remaining solution is then analysed. Certain resin reactions are very efficient but require large excesses of resin, and it is the column method that is usually employed in most laboratory applications of ion exchange.

In column operations the resin is held in a column and the solution system of interest flows through the column. The quantitative exchange is more easily achieved using the column method than the batch wise method. An ion exchange column can be considered to be a series of levels on which equilibrium conditions are reached. As the solution system passes down the column, the reaction is pushed forward, due to equilibrium requirements of each successive level.

4.4 CHOICE OF RESIN

The choice of resin depends on the charges of the entities which are to be measured or extracted. In this study the following basic equilibrium will be studied

$$M^+ + S^- \rightleftharpoons M\text{-}S$$

and the concentration of the free metal ion and bound complexed metal will be used to determine the extent of metal complexation. In these studies, the aqueous metal is expected to be cationic and thus a cation exchange resin was chosen to carry out this work. A strong cation resin was chosen as the kinetics of complexation

between the free metal and the resin are likely to be rapid and only one type of site is present on the strong resin. Groupings such as sulphonic, $-SO_3H$, and methylene sulphonic, $-CH_2SO_3H$, confer strongly acidic properties on the resin.

Cation exchange resins are generally used in two forms, the free acid or hydrogen form, and the salt form, often sodium or ammonium. The acid form will complex cations and release an equivalent amount of protons into solution, whereas the sodium form will release an equivalent amount of sodium etc. The exchange potentials for cations on strongly acid resin are influenced by numerous factors, the most important being molecular size, valency and concentration. In dilute solutions exchange potentials increase with increasing valency as shown below in table 4.1.

Table 4.1 Exchange potential for 0.1M chloride solutions at 25°C

$Th^{4+} > Fe^{3+} > Al^{3+} > Ba^{2+} > Pb^{2+} > Sr^{2+} > Ca^{2+} > Co^{2+} = Ni^{2+} = Cu^{2+} > Zn^{2+} = Mg^{2+} > Mn^{2+} > Ag^{+} > Cs^{+} > Rb^{+} > NH_4^{+} = K^{+} > Na^{+} > H^{+} > Li^{+} > Hg^{2+}$.

The opposite trend is observed in concentrated solutions. This phenomenon is utilized in water softening process. Cation exchange resins are commercially available from many companies. The resin chosen for this work was the commercially available Dowex 50 W-X4 strong cation exchange resin.

4.5 Dowex 50 W-X4

This is a sulphonated polystyrene resin, cross linked with 4% DVB. This grade consisted of spherical particles of 100 – 200 mesh. There is a volume increase of about 8% on conversion from the sodium to the H^+ form. This resin has good thermal stability up to 150°C and is resistant to the action of solvents and reducing agents. It also has excellent resistance to attrition and is almost white in colour. The operational pH range of Dowex 50W-X4 is 1 – 14. The exchange capacity of the resin is theoretically 1.7 meq ml^{-1} wet and 4.8 meq ml^{-1} dry.

4.6 THE SCHUBERT METHOD

To determine stability constants using the Schubert method an aqueous solution of metal ion at trace levels is allowed to reach equilibrium with a cation exchange resin both in the presence and absence of humic acid.

4.6.1 In the absence of humic acid

$$M + Res \rightleftharpoons M\text{-}Res$$

therefore,

$$K = \frac{[M - Res]}{[M][Res]} \qquad (4.1)$$

where [M – Res] is the concentration of the metal bound to the resin,

[M] is the free metal in solution and

[Res] is the concentration of free resin sites, taken as constant to give the distribution coefficient Do

$$Do = \frac{[M - Res]}{[M]} \qquad (4.2)$$

4.6.2 In the presence of humic acid

$$M + Res \rightleftharpoons M\text{-}Res \qquad (4.3)$$

$$M + S \rightleftharpoons M\text{-}S \qquad (4.4)$$

In the presence of humic acid and resin these two equilibria must be satisfied simultaneously.

The stability constant β of equation 4.4 is,

$$\beta = \frac{[M-S]}{[M][S]} \qquad (4.5)$$

Now the distribution coefficient, D is,

$$D = \frac{[M-Res]}{[M]\,sol} \qquad (4.6)$$

where [M]sol is the total concentration of M in solution.

therefore,

$$[M]sol = [M] + [M\text{-}S]$$

$$= [M] + \beta [M] [S]$$

$$= [M](1 + \beta[S]) \qquad (4.7)$$

substituting in D and Do gives

$$\frac{Do}{D} = 1 + \beta[S] \qquad (4.8)$$

taking $\log_{10}$ gives

$$\log(Do / D - 1) = \log[S] + \log \beta \qquad (4.9)$$

therefore plotting $\log(Do / D - 1)$ versus $\log[S]$ gives a straight line whose intercept is $\log \beta$.

There are two ways to interpret the data:

1. Individual β values can be calculated at each experimental plot from

$$\log \beta = \log (Do / D - 1) - \log[S]$$

or

2. A single β can be estimated from the intercept of the line.

The standard Schubert method is to keep the metal concentration constant at trace levels while varying the humic concentration and this generates one log β value. A proposed modification is to keep the humic concentration constant at 50 mg l^{-1} and to vary the metal concentration in the range 1 x10^{-4}M to 1 x10^{-9}M. This change in method needs a revision of the interpretation of the results.

4.7 INTERPRETATION OF DATA BY SCATCHARD PLOTS

The humic functional groups are regarded as ligands, the stoichiometry of which are 1 site : 1 metal ion.

$$M + S \rightleftharpoons MS$$

therefore,

$$K = \frac{[MS]}{[M][S]}$$

$$[S] = [MS]_{max} - [MS] \qquad (4.10)$$

where $[MS]_{max}$ is the maximum concentration of complex that can be formed under the conditions.

therefore,

$$K = \frac{[MS]}{[M]\left([MS]_{max} - [MS]\right)} \qquad (4.11)$$

but a single K value is an unsatisfactory model for humic acid because a range of K's would be expected due to the heterogeneity of the humics' functional groups. A closer approximation is to use two classes of site labelled strong and weak (^{s}S and ^{w}S).

Therefore the complexation is represented by two co-existing equilibria,

eg $M + {}^{s}S \rightleftharpoons M^{s}S$ $\qquad$ $M + {}^{w}S \rightleftharpoons M^{w}S$

$$sK = \frac{[M^{s}S]}{[M][{}^{s}S]} \qquad (4.12) \qquad wK = \frac{[M^{w}S]}{[M][{}^{w}S]} \qquad (4.13)$$

therefore,

$$[MS]_{max} = [M^{s}S]_{max} + [M^{w}S]_{max}$$

the strong site concentration is therefore,

$$[{}^{s}S] = [M^{s}S]_{max} - [M^{s}S] \qquad (4.14)$$

and the weak site concentration is therefore,

$$[{}^{w}S] = [M^{w}S]_{max} - [M^{w}S] \qquad (4.15)$$

Combining equations 4.12 and 4.14 , & 4.13 and 4.15 with rearranging gives,

$$[M^{s}S] / [M] = {}^{s}K([M^{s}S]_{max} - [M^{s}S]) \qquad (4.16)$$

and $$[M^wS] / [M] = {}^wK([M^wS]_{max} - [M^wS]) \quad (4.17)$$

since $$[MS] = [M^sS] + [M^wS]$$

$$[MS] / [M] = {}^sK[M^sS]_{max} - {}^sK[M^sS] + {}^wK[M^wS]_{max} - {}^wK[M^wS] \quad (4.18)$$

${}^sK[M^sS]_{max}$ and ${}^wK[M^wS]_{max}$ are constant, therefore to establish ${}^sK$ and ${}^wK$ experimentally a plot [MS] / [M] versus [MS] is derived.

The graph should show two distinct slopes, the early slope giving $-{}^sK$ and the later slope giving $-{}^wK$. This is assuming the metal binds preferentially to the strong sites and that $-{}^sK[M^sS]$ is constant when the strong sites have been bound.

This approach is comparable to that used by Scatchard in 1949 (20).

4.8 EXPERIMENTAL

4.8.1 Initial experiments

The Dowex 50W-X4 strong cation exchange resin was pretreated to remove any impurities in the supplied resin. The process involved packing approximately 50g of resin into a large glass chromatographic column and washing the resin with numerous bed volumes of reagents in the following sequence, concentrated hydrochloric acid, distilled water, 1M sodium chloride, distilled water, 0.1M Sodium EDTA, distilled water, 0.1M sodium hydroxide, distilled water. The resin was then washed with the buffer to be used in the experiment.

The pretreated resin was packed into plastic columns of 1.2cm i.d. and 5.7cm in length to a depth of 4.4cm. The resin was held in place by two clean glass wool plugs.

4.8.2 Verification of columns ability to extract free metal from solution

The ability of the column to extract free europium was checked using a stock of ^{152}Eu tracer solution. The working stock of ^{152}Eu tracer was prepared by adding 10µl of an Amersham supplied stock of radioactive ^{152}Eu 251MBq ml^{-1} and 0.538 mg ml^{-1} of inactive Eu carrier to 10ml of HPLC grade water. The concentration of Eu in the working stock was therefore

$$= \frac{0.01}{10.00} \times \frac{0.538}{152} \quad \text{mol } l^{-1}$$

$$= 3.539 \times 10^{-6} \text{ mol } l^{-1}$$

A 0.5 ml aliquot of the working stock was added to 4.5 ml of sodium acetate (0.01M pH 6.8) and shaken (solution "a"). A 0.5 ml aliquot of the working stock was washed onto the top of the small resin packed column. The column was washed with 5ml of sodium acetate buffer (0.01M, pH 6.8) and the effluent from the column collected (solution "b"). A 0.5 ml sample was taken from both solutions "a" and "b" and the samples were gamma counted in a Philips 4800 automatic gamma counter. The experiment was repeated a further five times. The results were corrected for background and dilution. The results are shown in table 4.2.

Table 4.2 Repetitions for column verification of free metal

Sample	Eu in sample/cpm	Total activity recovered/cpm	% ^{152}Eu passing through the column
1	2506	71	2.83
2	2594	73	2.81

3	2640	66	2.50
4	2585	65	2.51
5	2611	78	2.98
6	2675	67	2.50

4.8.3 Results and discussion of initial column verification

average counts of ^{152}Eu in sample = 2602 ± 192 cpm

average counts of ^{152}Eu in sample recovered = 70 ± 26 cpm

Values are quoted with $2\,\sigma_{n-1}$ error

$$\text{Thus \% eluted from column} = \frac{70}{2602} \times 100\ \%$$

$$= 2.69 \pm 1.02\ \%$$

Values are quoted with quotient errors

Thus 2.69 % of the activity added to the column is eluted and 97.31 % is retained. As there is no competing or complexing ligand present the column should retain 100% of the added ^{152}Eu tracer. This was considered to be an experimentally acceptable value so the verification process was continued.

4.8.4 Verification of columns ability to exclude complexed metal in solution

The column was washed thoroughly with Sodium EDTA until no activity was present in the effluent. The column was then pretreated again using the procedure outlined earlier.

1ml of the working stock was added to 1ml of 0.1M sodium EDTA and the solution was left for 2 days to equilibrate. A 0.5 ml aliquot of the working stock was added to 4.5 ml of sodium acetate (0.01M, pH 6.8) and shaken (solution "c"). A 0.5 ml aliquot of the working stock was washed onto the top of the small resin packed column. The column was washed with 5ml of sodium acetate buffer (0.01M, pH 6.8) and the effluent from the column collected (solution "d"). A 0.5 ml sample was taken from both solutions "c" and "d" and the samples were gamma counted in a Philips 4800 automatic gamma counter. The experiment was repeated a further five times. The results are shown in table 4.3.

Table 4.3 Repetitions for column verification Eu-EDTA complexes

Sample	Eu in sample/cpm	Total activity recovered/cpm	% ^{152}Eu passing through the column
1	918	882	96.07
2	930	893	96.02
3	898	871	96.99
4	910	877	96.37
5	928	887	95.58
6	895	869	97.09

average counts of ^{152}Eu in sample = 913 ± 70 cpm

average counts of ^{152}Eu in sample recovered = 880 ± 48 cpm

Values are quoted with $2\,\sigma_{n-1}$ error

$$\text{Thus \% eluted from column} = \frac{880}{913} \times 100\,\%$$

$$= \quad 96.38 \pm 9.07\ \%$$

4.8.5 Results and discussion of initial column verification

Eu complexes with EDTA according to the following

$$Eu + EDTA \rightleftharpoons Eu\text{-}EDTA$$

the stability constant is given by

$$K = \frac{[Eu\text{-}EDTA]}{[Eu]\,[EDTA]}$$

the stability constant between Eu and EDTA has a value of 1.949×10^{17} (88)

therefore the Eu bound is given by

$$1.949 \times 10^{17} = \frac{x}{([Eu]_t - x)(0.05 - x)}$$

therefore

$$1.949 \times 10^{17} = \frac{x}{(1.769 \times 10^{-6} - x)(0.05 - x)}$$

Solving for x gives

$$x = 1.765 \times 10^{-6} = [Eu\text{-}EDTA]$$

therefore % Eu bound is

$$\%\ Bd = \frac{1.765 \times 10^{-6}}{1.769 \times 10^{-6}} = 99.77\ \%$$

the mass balance shows that for this system approximately 100% of the Eu will be bound to EDTA so 100% of the activity added to the column should pass through the column unretained. The experimental results show that 96.38 % of ^{152}Eu passes through the column. This verified the usefulness of the column for separating bound and free metal. Ten columns containing the cation resin were prepared for use with metal humate complexation experiments.

4.9 EUROPIUM COMPLEXATION EXPERIMENTS

4.9.1 Preparation of europium solutions for column experiments

Solutions of europium chloride were prepared in HPLC grade water ranging from 1×10^{-2} to 1×10^{-4} mol l^{-1} from the Analytical Reagent grade salt europium chloride ($EuCl_3.6H_2O$). Aldrich humic acid solutions were prepared from a sample of AHA made up to contain 51 mg l^{-1} in triply distilled water . The working stock of ^{152}Eu tracer solution was made by adding 10µl of stock Amersham solution containing 251 MBq ml^{-1} and 0.538 mg ml^{-1} Eu to 10ml of HPLC grade water. Hence the Eu concentration in the working stock.

$$= \frac{0.01}{10.00} \times \frac{0.538}{152} \quad \text{mol } l^{-1}$$

$$= 3.539 \times 10^{-6} \text{ mol } l^{-1}$$

The total concentration of Eu (active + inactive) in the final samples was calculated from the volume of inactive and active Eu added, and the final volume of solution. For example:

Concentration of Eu present in 5ml sample of AHA containing 12.5µl of inactive Eu 1×10^{-4} mol l^{-1} and 25µl of Eu active + carrier

Concentration of inactive Eu is $\frac{0.0125}{5.0375} \times 10^{-4}$ mol l^{-1}

$= 2.481 \times 10^{-7}$ mol l^{-1}

Concentration of active Eu + carrier present

$$= \frac{0.025 \times 3.539 \times 10^{-6} \times 1000}{5.0375 \times 1000} \text{ mol } l^{-1}$$

$= 1.756 \times 10^{-8}$ mol l^{-1}

$\therefore$ total concentration

$= 2.656 \times 10^{-7}$ mol l^{-1}

The composition of all the samples are shown in table 4.4

Table 4.4 Composition of Eu equilibrium samples

Volume of sample /(ml)	Amount of inactive $EuCl_3$ solution added	Amount of radioactive Eu-152 solution added /(µl)	Total concentration of Eu /(mol l^{-1})
5.00	12.5 µl of 1.00×10^{-4} mol l^{-1}	25	2.656×10^{-7}
5.00	25.0 µl of 1.00×10^{-4} mol l^{-1}	25	5.137×10^{-7}
5.00	37.5 µl of 1.00×10^{-4} mol l^{-1}	25	7.618×10^{-7}
5.00	50.0 µl of 1.00×10^{-4} mol l^{-1}	25	10.099×10^{-7}
5.00	12.5 µl of 1.00×10^{-3} mol l^{-1}	25	2.498×10^{-6}
5.00	25.0 µl of 1.00×10^{-3} mol l^{-1}	25	4.979×10^{-6}
5.00	37.5 µl of 1.00×10^{-3} mol l^{-1}	25	7.460×10^{-6}
5.00	50.0 µl of 1.00×10^{-3} mol l^{-1}	25	9.941×10^{-6}
5.00	12.5 µl of 1.00×10^{-2} mol l^{-1}	25	2.482×10^{-5}
5.00	25.0 µl of 1.00×10^{-2} mol l^{-1}	25	4.963×10^{-5}

These concentrations of Europium were used in all the Europium experiments for both batch and column methods to ensure consistency.

4.9.2 Preparation of humic solutions for europium complexation experiments

Aldrich Humic acid (51mg) was dissolved in 1 litre of 0.01M Morpholine ethane sulphonic acid (MES) buffer at pH 6.8. Aliquots (5mls) were added to 10 clean glass vials. 12.5µl, 25µl, 37.5µl and 50 µl aliquots of europium chloride solution were added to give the composition shown in the above table 4.4. The procedure was repeated with 0.001M MES buffer.

4.9.3 Results of europium complexation experiments

The results are presented in tables 4.5 and 4.6. The complexation parameters were generated in three ways. The graphs are plotted in accordance with equation 4.18 and are shown in figs 4.1 to 4.4. The stability constants were taken from the slopes of the generated curves. The percentage complexation and metal totals were input into a biological ligand analysis program (EBDA) that had been modified to allow the program to perform non-linear regression analysis on the experimental data. This also gave the complexation parameters for the experimental results. All the generated complexation parameters are shown along with literature values in tables 4.24 and 4.25,

Table 4.5 Eu-AHA (0.01M MES pH6.3)

$[M]_T$ Total Eu concentration /(mol l^{-1})	Percentage of Eu-AHA bound /(%)	[MS] Eu-AHA complex /(mol l^{-1})	[M] Eu-free /(mol l^{-1})	[MS]/[M]
2.656×10^{-7}	90.91	2.414×10^{-7}	2.414×10^{-8}	10
5.137×10^{-7}	92.36	4.744×10^{-7}	3.924×10^{-8}	12.87
7.618×10^{-7}	96.85	7.378×10^{-7}	2.399×10^{-8}	30.75
1.010×10^{-6}	87.95	8.883×10^{-7}	1.217×10^{-7}	7.29
2.498×10^{-6}	76.60	1.913×10^{-6}	5.845×10^{-7}	3.27
4.979×10^{-6}	62.84	3.128×10^{-6}	1.850×10^{-6}	1.69
7.460×10^{-6}	50.26	3.749×10^{-6}	3.710×10^{-6}	1.01
9.941×10^{-6}	39.74	3.950×10^{-6}	5.990×10^{-6}	0.659
2.482×10^{-5}	25.58	$6..48 \times 10^{-6}$	1.847×10^{-5}	0.344
4.963×10^{-5}	18.67	9.265×10^{-6}	4.036×10^{-5}	0.229

Table 4.6 Eu-AHA (0.001 MES pH 6.3)

$[M]_T$ Total Eu concentration /(mol l^{-1})	Percentage of Eu-AHA bound /(%)	[MS] Eu-AHA complex /(mol l^{-1})	[M] Eu-free /(mol l^{-1})	[MS]/[M]
2.656×10^{-7}	94.10	2.50×10^{-8}	1.567×10^{-8}	15.949
5.137×10^{-7}	93.00	4.78×10^{-7}	3.596×10^{-8}	13.286
7.618×10^{-7}	92.80	7.07×10^{-7}	5.485×10^{-8}	12.889
1.010×10^{-6}	95.30	9.62×10^{-7}	4.747×10^{-8}	20.277
2.498×10^{-6}	88.30	2.21×10^{-6}	2.923×10^{-7}	7.547
4.979×10^{-6}	85.50	4.26×10^{-6}	7.220×10^{-7}	5.897
7.460×10^{-6}	80.70	6.02×10^{-6}	1.440×10^{-6}	4.181
9.941×10^{-6}	76.00	7.56×10^{-6}	2.386×10^{-6}	3.167
2.482×10^{-5}	59.30	1.47×10^{-5}	1.010×10^{-5}	1.457
4.963×10^{-5}	32.50	1.61×10^{-5}	3.350×10^{-5}	0.482

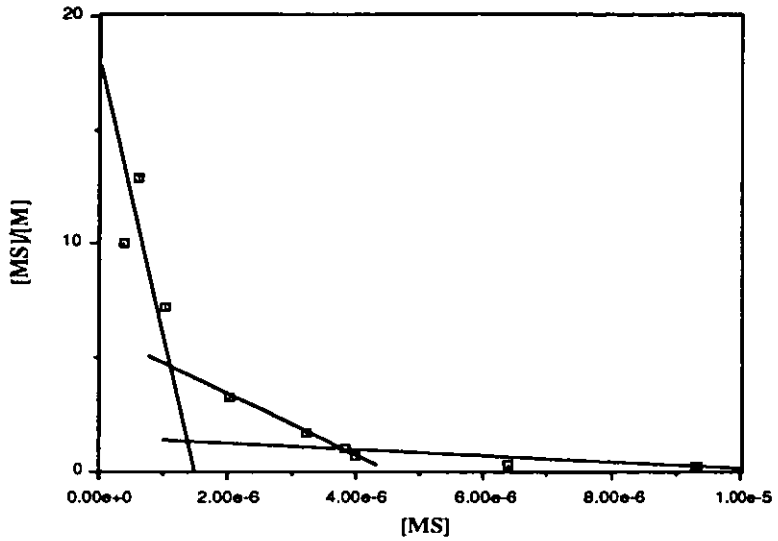

Fig 4.1 Scatchard plot of Eu-AHA (0.01M MES pH 6.3)

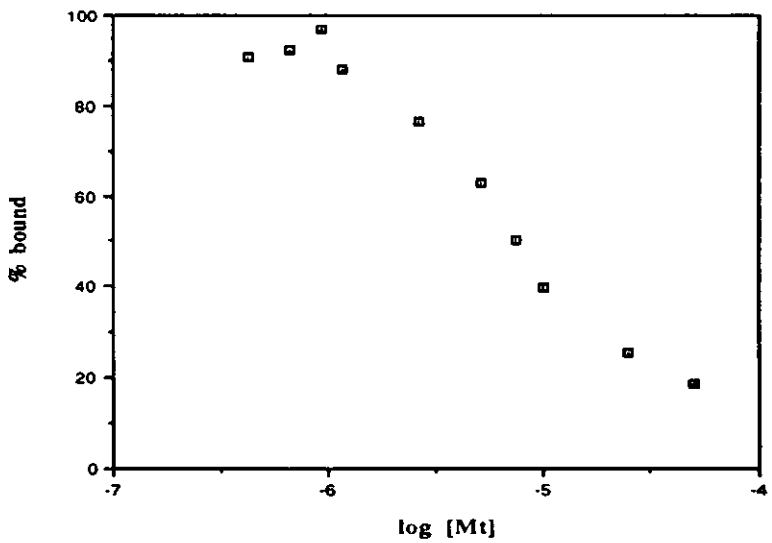

Fig 4.2 Europium percentage bound for the Eu-AHA system (0.01M MES pH 6.3)

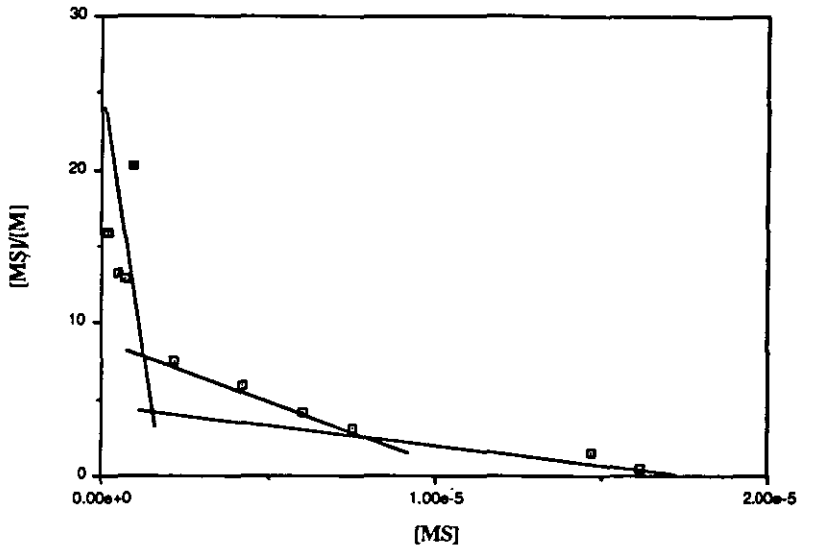

Fig 4.3 Scatchard plot of Eu-AHA (0.001M MES pH 6.3)

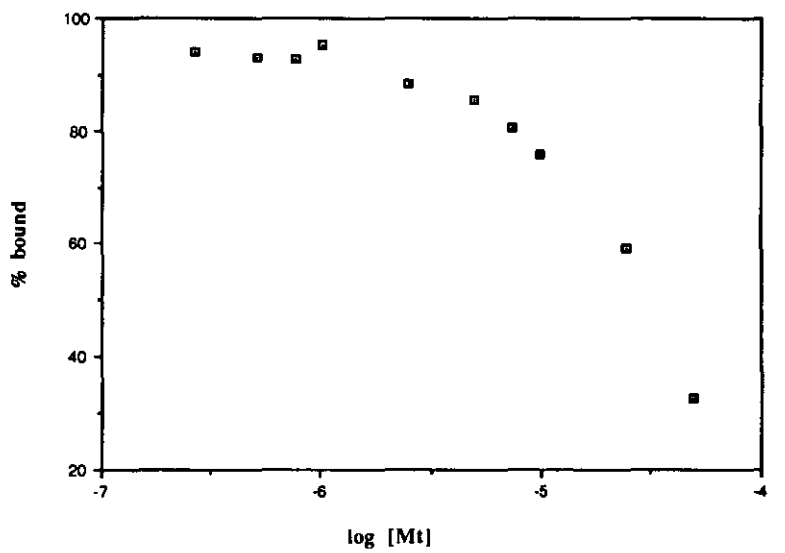

Fig 4.4 Europium percentage bound for the Eu-AHA system (0.001M MES pH 6.3)

4.10 NICKEL COMPLEXATION EXPERIMENTS

4.10.1 Preparation of nickel solutions for complexation experiments

Solutions of nickel nitrate were prepared, having concentration ranging from 1×10^{-1} to 1×10^{-5} mol l^{-1} using Analytical Reagent grade nickel nitrate ($Ni(NO_3)_2 \cdot 6H_2O$). Radioactive ^{63}Ni solution was prepared by diluting 135 µl of carrier free stock $NiCl_2$ solution (37 MBq ml^{-1}, supplied by Amersham International) to 5 ml using HPLC grade water.

The total concentration of nickel in each mixture was calculated from the amount of inactive nickel and the amount of ^{63}Ni.

The amount of radioactive ^{63}Ni added to each mixture was calculated from the amount of the stock taken, and the size of the aliquot taken from the prepared working stock, ie 135 µl of original Amersham stock contained

$$\frac{0.135}{100} \times 37 \text{ MBq} = 5.00 \text{ MBq}$$

a 25 µl aliquot of the prepared nickel working stock was added to each vial, this contained

$$\frac{0.025}{5.00} \times 5 \text{ MBq} = 0.025 \text{ MBq}$$

Now

$$\frac{-dN}{dt} = \frac{0.693 \times N}{t_{1/2}}$$

where N = number of radioactive atoms present at time T

$t_{1/2}$ = half life, ie 100 years for ^{63}Ni

$\therefore$ the number of moles of ^{63}Ni present (n) in 25 µl is given by

$$n = \frac{(\frac{-dN}{dt}) \times t_{1/2}}{0.693 \times L}$$

L = Avogadro Constant = 6.023×10^{23} atoms $mole^{-1}$

$\therefore$ the ^{63}Ni content in a 25 µl aliquot $= \frac{25 \times 10^{3} \times 100 \times 365 \times 24 \times 60 \times 60}{0.693 \times 6.023 \times 10^{23}}$

$= 1.889 \times 10^{-10}$ moles

The composition of the samples used in the experiments are detailed below. The mixtures were left for 7 days to equilibrate. The composition of the sample is shown in table 4.7 below

Table 4.7 Composition of Ni equilibrium samples

Volume of sample (ml)	Amount of inactive $Ni(NO_3)_2$ solution added	Amount of radioactive ^{63}Ni solution added (µl)	Total concentration of Ni /(mol l^{-1})
5.00	50 µl of 1×10^{-5} mol l^{-1}	25	8.692×10^{-8}
5.00	25 µl of 1×10^{-5} mol l^{-1}	25	1.357×10^{-7}
5.00	50 µl of 1×10^{-4} mol l^{-1}	25	5.325×10^{-7}
5.00	25 µl of 1×10^{-4} mol l^{-1}	25	1.022×10^{-6}
5.00	50 µl of 1×10^{-3} mol l^{-1}	25	4.988×10^{-6}
5.00	25 µl of 1×10^{-3} mol l^{-1}	25	9.889×10^{-6}
5.00	50 µl of 1×10^{-2} mol l^{-1}	25	4.995×10^{-5}
5.00	25 µl of 1×10^{-2} mol l^{-1}	25	9.811×10^{-5}
5.00	50 µl of 1×10^{-1} mol l^{-1}	25	4.927×10^{-4}
5.00	25 µl of 1×10^{-1} mol l^{-1}	25	9.805×10^{-4}

These concentrations of nickel were used in all the nickel experiments both batch and column method to ensure consistency.

4.10.2 Preparation of humic solutions for nickel complexation experiments

Aldrich Humic acid (51mg) was dissolved in 1 litre of 0.01M Morpholine ethane sulphonic acid (MES) buffer at pH 6.8. Aliquots (5mls) were added to 10 clean glass vials. 25µl and 50 µl aliquots of nickel nitrate solution were added to give the composition shown in the earlier table 4.7. The procedure was repeated with 0.001M MES buffer.

4.10.3 Results of nickel complexation experiments

The results are presented in tables 4.8 and 4.9. The complexation parameters were generated in three ways. The graphs are plotted in accordance with equation 4.18 and are shown in figs 4.5 to 4.8. The stability constants were taken from the slopes of the generated curves. The percentage complexation and metal totals were input into a biological ligand analysis program (EBDA) that had been modified to allow the program to perform non-linear regression analysis on the experimental data. This also gave the complexation parameters for the experimental results. All the generated complexation parameters are shown along with literature values in tables 4.26 and 4.27.

Table 4.8 Ni-AHA 0.01 M pH 6.3

$[M]_T$ Total Ni concentration /(mol l^{-1})	Percentage of Ni-AHA bound /(%)	[MS] Ni-AHA complex /(mol l^{-1})	[M] Ni-free /(mol l^{-1})	[MS]/[M]
8.692×10^{-8}	88.60	7.701×10^{-8}	9.909×10^{-9}	7.772
1.357×10^{-7}	85.20	1.156×10^{-7}	2.008×10^{-8}	5.757
5.325×10^{-7}	81.36	4.332×10^{-7}	9.926×10^{-8}	4.365
1.022×10^{-6}	84.20	8.605×10^{-7}	1.615×10^{-7}	5.329
4.988×10^{-6}	86.70	4.325×10^{-6}	6.634×10^{-7}	6.519
9.889×10^{-6}	46.70	4.618×10^{-6}	5.271×10^{-6}	0.876
4.955×10^{-5}	25.54	1.266×10^{-5}	3.689×10^{-5}	0.343
9.811×10^{-5}	16.02	1.572×10^{-5}	8.239×10^{-5}	0.191
4.927×10^{-4}	8.00	3.942×10^{-5}	4.533×10^{-4}	0.087
9.805×10^{-4}	14.50	1.422×10^{-4}	8.383×10^{-4}	0.170

Table 4.9 Ni-AHA 0.001 M pH 6.3

$[M]_T$ Total Ni concentration /(mol l^{-1})	Percentage of Ni-AHA bound /(%)	[MS] Ni-AHA complex /(mol l^{-1})	[M] Ni-free /(mol l^{-1})	[MS]/[M]
8.692×10^{-8}	90.01	7.824×10^{-8}	8.682×10^{-9}	9.011
1.357×10^{-7}	89.77	1.218×10^{-7}	1.387×10^{-8}	8.782
5.325×10^{-7}	79.19	4.217×10^{-7}	1.108×10^{-7}	3.805
1.022×10^{-6}	79.77	8.153×10^{-7}	2.067×10^{-7}	3.944
4.988×10^{-6}	59.86	2.986×10^{-6}	2.002×10^{-6}	1.491
9.889×10^{-6}	44.14	4.365×10^{-6}	5.524×10^{-6}	0.790
4.955×10^{-5}	21.16	1.049×10^{-5}	3.906×10^{-5}	0.268
9.811×10^{-5}	14.19	1.392×10^{-5}	8.419×10^{-5}	0.165
4.927×10^{-4}	11.15	5.493×10^{-5}	4.378×10^{-4}	0.125
9.805×10^{-4}	13.80	1.353×10^{-4}	8.452×10^{-4}	0.160

4.11 DEF INTERPRETATION OF RESULTS FOR THE EUROPIUM AND NICKEL COMPLEXATION EXPERIMENTS

This DEF procedure as outlined in section 1.6.3.2 was carried out for the europium and the nickel experimental data obtained in the previous complexation experiments. The results are presented in tables 4.10 to 4.13 and in graphs, figures 4.9 to 4.16. The computer generated data fitted curve equations are shown on the DEF derivation plots and these equations were differentiated as part of the DEF calculation.

Table 4.10 DEF data for Eu-AHA (0.01M MES pH 6.3)

[Ms]/TOC	log *K'
2.01×10^{-4}	5.401
1.11×10^{-4}	6.143
7.58×10^{-5}	6.671
5.64×10^{-5}	7.112
4.41×10^{-5}	7.505
3.56×10^{-5}	7.870
2.94×10^{-5}	8.214
2.48×10^{-5}	8.544
2.12×10^{-5}	8.863
1.83×10^{-5}	9.174
1.59×10^{-5}	9.478
1.40×10^{-5}	9.777

4.11 DEF INTERPRETATION OF RESULTS FOR THE EUROPIUM AND NICKEL COMPLEXATION EXPERIMENTS

This DEF procedure as outlined in section 1.6.3.2 was carried out for the europium and the nickel experimental data obtained in the previous complexation experiments. The results are presented in tables 4.10 to 4.13 and in graphs, figures 4.9 to 4.16. The computer generated data fitted curve equations are shown on the DEF derivation plots and these equations were differentiated as part of the DEF calculation.

Table 4.10 DEF data for Eu-AHA (0.01M MES pH 6.3)

[Ms]/TOC	log *K'
2.01×10^{-4}	5.401
1.11×10^{-4}	6.143
7.58×10^{-5}	6.671
5.64×10^{-5}	7.112
4.41×10^{-5}	7.505
3.56×10^{-5}	7.870
2.94×10^{-5}	8.214
2.48×10^{-5}	8.544
2.12×10^{-5}	8.863
1.83×10^{-5}	9.174
1.59×10^{-5}	9.478
1.40×10^{-5}	9.777

Table 4.11 DEF data for Eu-AHA (0.001M MES pH 6.3)

[Ms]/TOC	log *K'
3.35×10^{-4}	------
3.29×10^{-4}	4.865
2.92×10^{-4}	5.640
2.39×10^{-4}	6.233
1.83×10^{-4}	6.778
1.32×10^{-4}	7.306
9.06×10^{-5}	7.831
5.88×10^{-5}	8.360
3.63×10^{-5}	8.898
2.14×10^{-5}	9.446
1.20×10^{-5}	10.00
6.49×10^{-6}	10.58

Table 4.12 DEF data for Ni-AHA (0.01M MES pH 6.3)

[Ms]/TOC	log *K'
4.35×10^{-4}	5.112
1.14×10^{-4}	6.176
5.05×10^{-5}	6.891
2.76×10^{-5}	7.466
1.70×10^{-5}	7.963
1.13×10^{-5}	8.411
7.94×10^{-6}	8.827
5.79×10^{-6}	9.219
4.36×10^{-6}	9.592
3.37×10^{-6}	9.952

Table 4.13 DEF data for Ni-AHA (0.001M MES pH 6.3)

[Ms]/TOC	log *K'
3.67×10^{-4}	5.197
9.45×10^{-5}	6.269
4.12×10^{-5}	6.990
2.24×10^{-5}	7.567
1.37×10^{-5}	8.067
9.04×10^{-6}	8.518
6.31×10^{-6}	8.936
4.59×10^{-6}	9.329
3.44×10^{-6}	9.704
2.65×10^{-6}	10.06
2.08×10^{-6}	10.41
1.67×10^{-6}	10.75

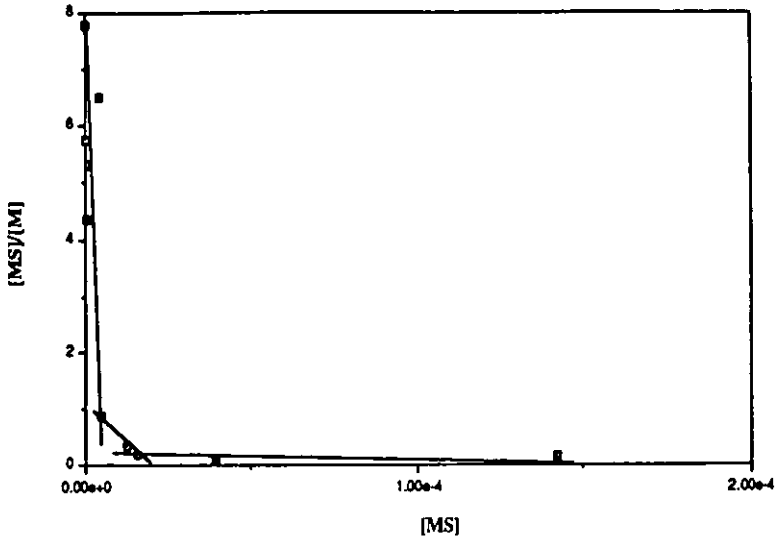

Fig 4.5 Scatchard plot of Ni-AHA (0.01M MES pH 6.3)

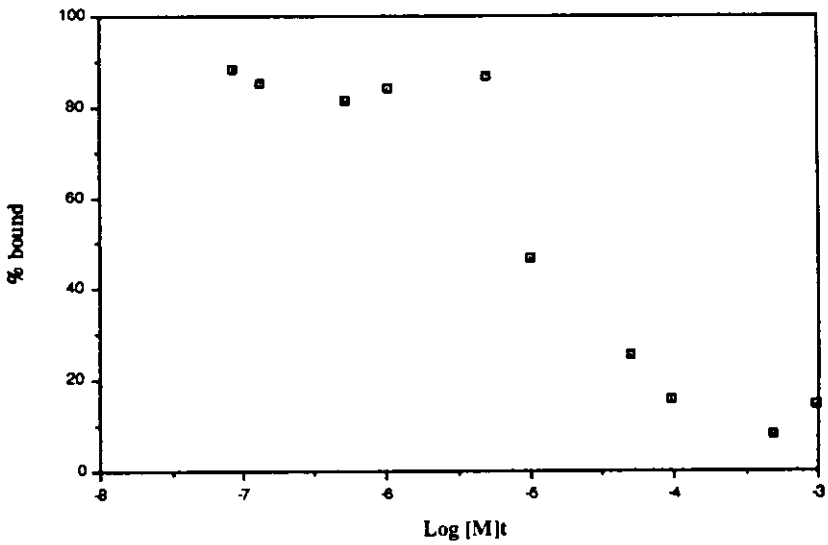

Fig 4.6 Nickel percentage bound for the Ni-AHA system (0.01M MES pH 6.3)

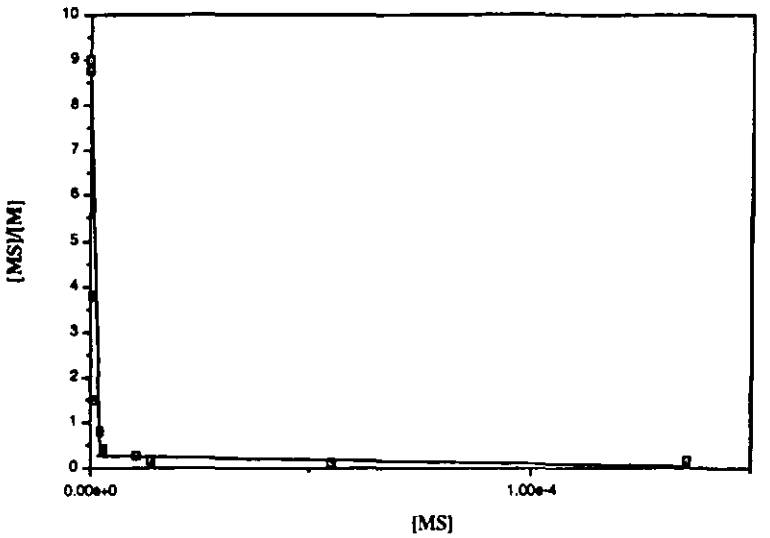

Fig 4.7 Scatchard plot of Ni-AHA (0.001M MES pH 6.3)

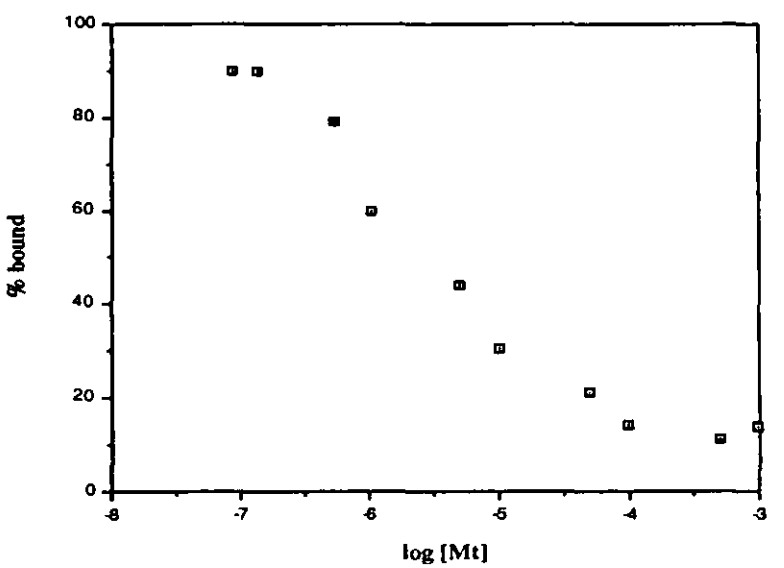

Fig 4.8 Nickel percentage bound for the Ni-AHA system (0.001M MES pH 6.3)

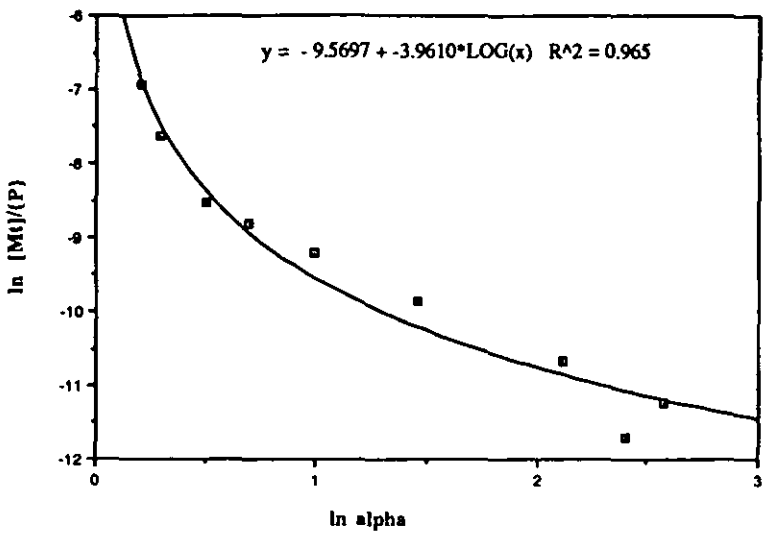

Fig 4.9 Derivation curve for DEF Analysis of Eu-AHA (0.01M MES pH 6.3)

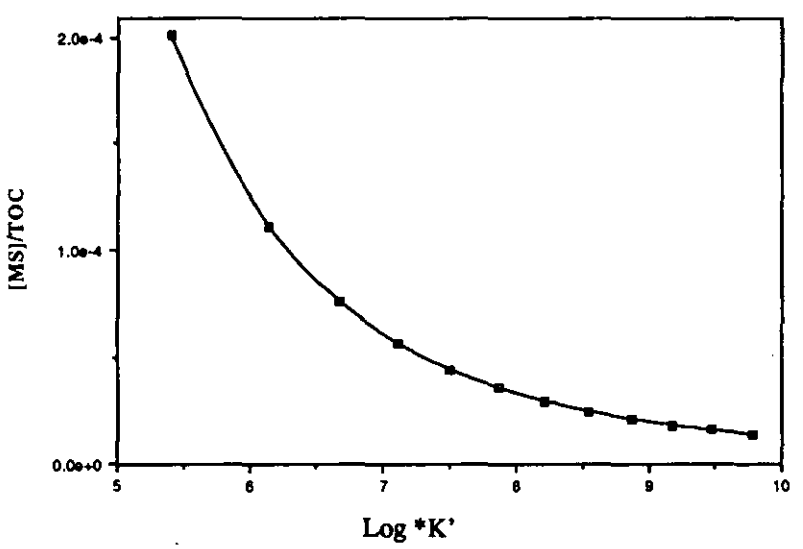

Fig 4.10 DEF curve of Eu-AHA (0.01M MES pH 6.3)

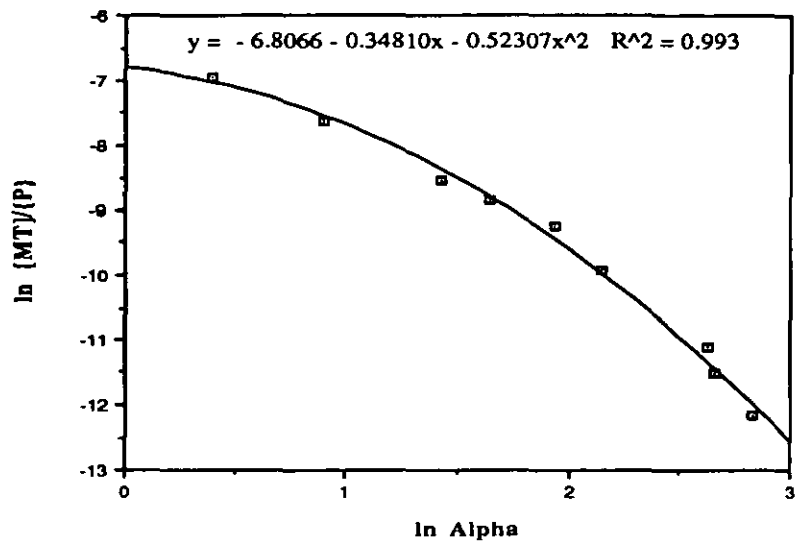

Fig 4.11 Derivation curve for DEF Analysis of Eu-AHA (0.001M MES pH 6.3)

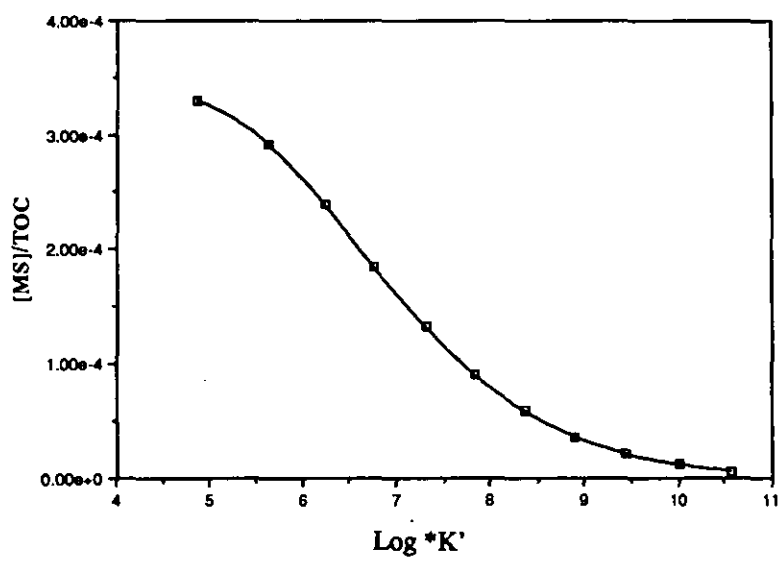

Fig 4.12 DEF curve of Eu-AHA (0.001M MES pH 6.3)

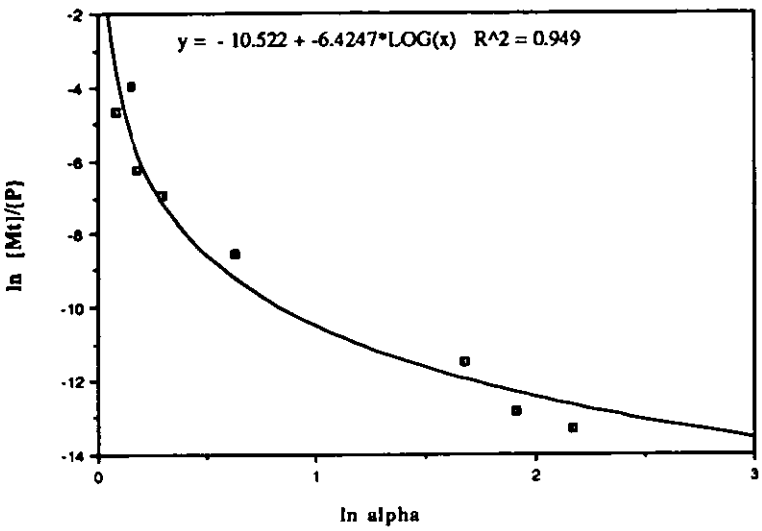

Fig 4.13 Derivation curve for DEF Analysis of Ni-AHA (0.01M MES pH 6.3)

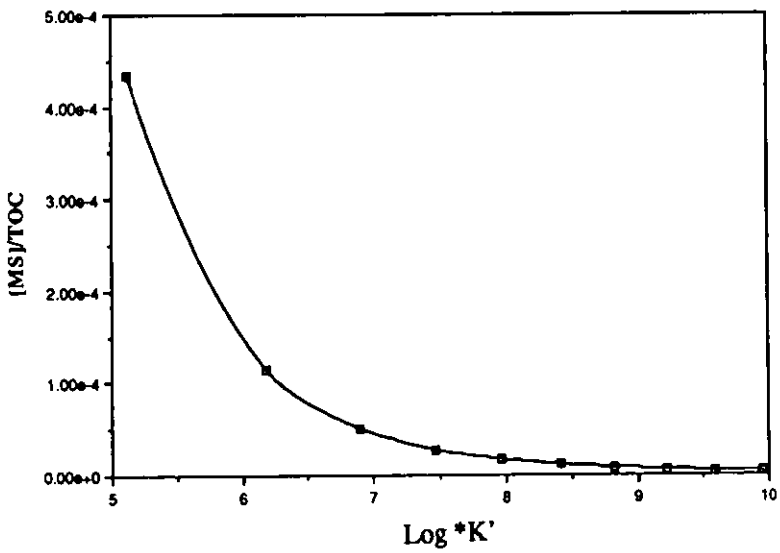

Fig 4.14 DEF curve of Ni-AHA (0.01M MES pH 6.3)

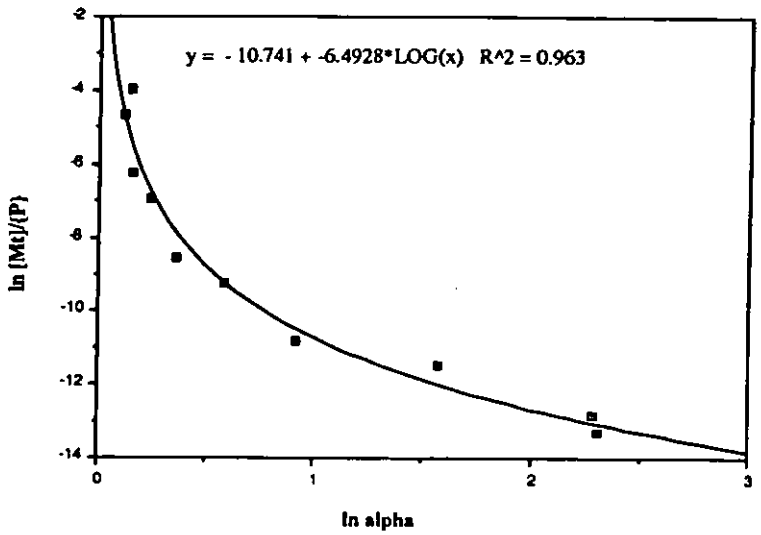

Fig 4.15 Derivation curve for DEF Analysis of Ni-AHA (0.001M MES pH 6.3)

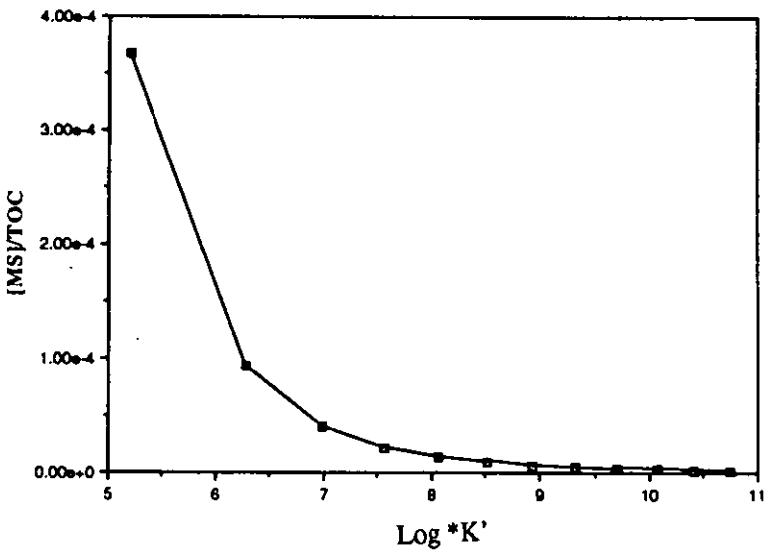

Fig 4.16 DEF curve of Ni-AHA (0.001M MES pH 6.3)

4.12 INTRODUCTION TO BATCH EXPERIMENTS

In batch wise operations the resin is added to the solution system being studied. The system is allowed to establish equilibrium and, once the reaction is complete, the treated solution is separated from the resin by filtration or decantation. The remaining solution is then analysed for metal remaining in solution. Batch wise ion exchange follows the equations used by Schubert (1948) and the theory is explained in 4.6 of this chapter.

4.13 EUROPIUM COMPLEXATION EXPERIMENTS

4.13.1 Preparation of europium solutions for batch experiments

Aldrich Humic acid (51mg) was dissolved in 1 litre of 0.01M Morpholine ethane sulphonic acid (MES) buffer. The pH was then adjusted to 6.8 using dilute NaOH. A similar solution was prepared using 0.001M MES.

The cationic resin was pretreated by placing 50g of the resin into a large glass chromatographic column and washing with numerous bed volumes of reagents in the following sequence: concentrated hydrochloric acid, distilled water, 1M sodium chloride, distilled water, 0.1M Sodium EDTA, distilled water, 0.1M sodium hydroxide and finally distilled water. The resin was then oven dried to constant weight over two days.

Aliquots of the humic acid solution (5mls) were added to ten clean glass vials. In addition 12.5µl, 25µl, 37.5µl and 50 µl aliquots of inactive europium chloride solution, along with 25µl of active ^{152}Eu, were added to the vial to give the composition shown in table 4.14. The procedure was repeated with 0.001M MES buffer. The vials were then left overnight for the contents to equilibrate. Approximately 0.025g of the pre-prepared resin was then added to each vial. The

solutions were then left for five days to reach equilibrium. After this time, 0.5ml of the supernatent was sampled and gamma counted to give the activity remaining in solution. The total activity was determined by placing 25µl of ^{152}Eu into 5ml of distilled water. After 2 days, a 0.5ml sample of this solution was gamma counted to calculate the total activity in the 5 ml solution.

Table 4.14 Composition of Eu equilibrium samples

Volume of sample /(ml)	Amount of inactive $EuCl_3$ solution added	Amount of radioactive ^{152}Eu solution added /(µl)	Total concentration of Eu /(mol l^{-1})
5.00	12.5 µl of 1.00 x10^{-4} mol l^{-1}	25	2.656 x10^{-7}
5.00	25.0 µl of 1.00 x10^{-4} mol l^{-1}	25	5.137 x10^{-7}
5.00	37.5 µl of 1.00 x10^{-4} mol l^{-1}	25	7.618 x10^{-7}
5.00	50.0 µl of 1.00 x10^{-4} mol l^{-1}	25	1.009 x10^{-6}
5.00	12.5 µl of 1.00 x10^{-3} mol l^{-1}	25	2.498 x10^{-6}
5.00	25.0 µl of 1.00 x10^{-3} mol l^{-1}	25	4.979 x10^{-6}
5.00	37.5 µl of 1.00 x10^{-3} mol l^{-1}	25	7.460 x10^{-6}
5.00	50.0 µl of 1.00 x10^{-3} mol l^{-1}	25	9.941 x10^{-6}
5.00	12.5 µl of 1.00 x10^{-2} mol l^{-1}	25	2.482 x10^{-5}
5.00	25.0 µl of 1.00 x10^{-2} mol l^{-1}	25	4.963 x10^{-5}

The results are discussed in 4.15.

4.14 NICKEL COMPLEXATION EXPERIMENTS

4.14.1 Preparation of nickel solutions for batch experiments

Aldrich Humic acid (51mg) was dissolved in 1 litre of 0.01M Morpholine ethane sulphonic acid (MES) buffer. The pH was then adjusted to 6.8 using dilute NaOH. A similar solution was prepared using 0.001M MES.

The cation resin was pretreated as described in 4.13.1

Aliquots from the humic acid solution (5mls) were added to ten clean glass vials. In addition 25µl and 50 µl aliquots of inactive nickel nitrate solution and 25µl of radioactive ^{63}Ni were added to give the composition shown in table 4.15. The procedure was repeated with 0.001M MES buffer. The vials were then left overnight for the contents to equilibrate. Approximately 0.025g of the pre-prepared resin was then added to each vial. The solutions were then left for five days to reach equilibrium. After this time, 1ml of the supernatent was sampled and beta counted to give the activity remaining in solution. The total activity was determined by placing 25µl of ^{63}Ni into 5ml of distilled water. After 2 days, a 1ml sample of this solution was beta counted to calculate the total activity in the 5 ml solution.

Table 4.15 Composition of Ni equilibrium samples

Volume of sample /(ml)	Amount of inactive $Ni(NO_3)_2$ solution added	Amount of radioactive Ni-63 solution added /(μl)	Total concentration of Ni /(mol l^{-1})
5.00	50 μl of 1 x10^{-5} mol l^{-1}	25	8.692 x10^{-8}
5.00	25 μl of 1 x10^{-5} mol l^{-1}	25	1.357 x10^{-7}
5.00	50 μl of 1 x10^{-4} mol l^{-1}	25	5.325 x10^{-7}
5.00	25 μl of 1 x10^{-4} mol l^{-1}	25	1.022 x10^{-6}
5.00	50 μl of 1 x10^{-3} mol l^{-1}	25	4.988 x10^{-6}
5.00	25 μl of 1 x10^{-3} mol l^{-1}	25	9.889 x10^{-6}
5.00	50 μl of 1 x10^{-2} mol l^{-1}	25	4.995 x10^{-5}
5.00	25 μl of 1 x10^{-2} mol l^{-1}	25	9.811 x10^{-5}
5.00	50 μl of 1 x10^{-1} mol l^{-1}	25	4.927 x10^{-4}
5.00	25 μl of 1 x10^{-1} mol l^{-1}	25	9.805 x10^{-4}

The results are discussed and presented in 4.15 below.

4.15 INTERPRETATION OF RESULTS FOR THE NICKEL AND EUROPIUM HUMATE BATCH EXPERIMENTS

In the absence of the humic ligand the distribution coefficient, Do, is given by:

$$Do = \frac{[M\text{-}RES]}{[M]}$$

Where Do is the distribution coefficient

[M-RES] is the metal bound to the resin and

[M] is the metal in solution

If the total activity added to the system is A_{tot} and the amount of activity in the

solution after the equilibration period is A_{sol}, the distribution coefficient can be written in terms of the measured parameters A_{tot} and A_{sol}:

$$Do = \frac{A_{tot}-A_{sol}}{A_{sol}}$$

However in the presence of the humate ligand the two equilibria

$$M + RES \rightleftharpoons M\text{-}RES$$

$$M + nHU \rightleftharpoons M\text{-}HUn$$

are present and must exist simultaneously.

Again the total activity added is A_{tot} and the total activity of the solution after the equilibration period is A_{sol}. We can now calculate all the relevent parameters required to afford the complexation parameters for the system in question. The parameters of interest are [M]f and [M]bd .The free metal [M]f in solution can be calculated from the distribution coefficient in the absence of the humate:

$$[M]f = [M\text{-}RES]/ Do$$

where

$$[M\text{-}RES] = [M]t - [M]sol$$

and

$$[M]sol = (A_{sol} / A_{tot}) \times [M]t$$

The bound value [M]bd can be calculated from the difference:

The bound value [M]bd can be calculated from the difference:

$$[M]bd = [M]sol - [M]f$$

we can now calculate all the relevent complexation parameters.

From the measured activities above and a knowledge of the metal concentrations it is possible to obtain all the data needed to generate the complexation parameters. As with the column ion exchange method, the measurements were subjected to Scatchard and DEF analysis. The results are shown in table 4.16 to 4.23 and in figures 4.17 to 4.32.

Table 4.16 Eu-AHA (0.01M MES pH 6.3) batch

$[M]_T$ Total Eu concentration /(mol l^{-1})	Percentage Eu-AHA bound /(%)	[MS] Eu-AHA complex /(mol l^{-1})	[M] Eu-free /(mol l^{-1})	[MS]/[M]	ln α	ln [M]t/(P)
2.656×10^{-7}	96.53	1.36×10^{-7}	4.88×10^{-9}	27.83	3.998	-12.16
5.137×10^{-7}	95.66	2.32×10^{-7}	1.05×10^{-8}	22.03	3.886	-11.50
7.618×10^{-7}	93.82	2.76×10^{-7}	1.82×10^{-8}	15.18	3.734	-11.11
1.010×10^{-6}	91.83	2.99×10^{-7}	2.66×10^{-8}	11.24	3.635	-10.83
2.498×10^{-6}	90.40	6.52×10^{-7}	6.92×10^{-8}	9.417	3.586	-9.924
4.979×10^{-6}	90.23	1.28×10^{-6}	1.39×10^{-7}	9.239	3.581	-9.234
7.460×10^{-6}	87.24	1.52×10^{-6}	2.23×10^{-7}	6.839	3.512	-8.830
9.941×10^{-6}	86.83	1.97×10^{-6}	2.99×10^{-7}	6.594	3.504	-8.543
2.482×10^{-5}	84.14	4.12×10^{-6}	7.76×10^{-7}	5.307	3.465	-7.628
4.963×10^{-5}	68.07	3.67×10^{-6}	1.72×10^{-6}	2.132	3.360	-6.935

Table 4.17 DEF data for Eu-AHA (0.01M MES pH 6.3) batch

[Ms]/TOC	log *K'
1.11×10^{-4}	6.063
8.76×10^{-5}	6.723
6.49×10^{-5}	7.328
4.59×10^{-5}	7.911
3.13×10^{-5}	8.484
2.05×10^{-5}	9.056
1.31×10^{-5}	9.629
8.09×10^{-6}	10.21
4.87×10^{-6}	10.79
2.85×10^{-6}	11.38
1.63×10^{-6}	11.97

Table 4.18 Eu-AHA (0.001M MES pH 6.3) batch

$[M]_T$ Total Eu concentration /mol^{-1})	Percentage Eu-AHA bound /(%)	[MS] Eu-AHA complex /(mol l^{-1})	[M] Eu-free /(mol l^{-1})	[MS] / [M]	ln α	ln [M]t/(P)
2.656×10^{-7}	97.86	1.70×10^{-7}	3.70×10^{-9}	45.82	3.846	-12.59
5.137×10^{-7}	98.09	3.41×10^{-7}	6.64×10^{-9}	51.34	3.958	-11.89
7.618×10^{-7}	97.13	4.31×10^{-7}	1.27×10^{-8}	33.81	3.550	-11.65
1.010×10^{-6}	95.60	4.60×10^{-7}	2.12×10^{-8}	21.74	3.124	-11.57
2.498×10^{-6}	94.09	9.49×10^{-7}	5.96×10^{-8}	15.91	2.828	-10.83
4.979×10^{-6}	92.61	1.62×10^{-6}	1.29×10^{-7}	12.52	2.605	-10.28
7.460×10^{-6}	90.11	1.94×10^{-6}	2.13×10^{-7}	9.115	2.314	10.07
9.941×10^{-6}	89.77	2.51×10^{-6}	2.86×10^{-7}	8.775	2.280	-9.811
2.482×10^{-5}	87.53	5.28×10^{-6}	7.52×10^{-7}	7.018	2.082	-9.042
4.963×10^{-5}	74.12	4.93×10^{-6}	4.93×10^{-6}	2.864	1.352	-8.945

Table 4.19 DEF data for Eu-AHA (0.001M MES pH 6.3) batch

[Ms]/TOC	log *K'
1.84×10^{-4}	5.142
1.43×10^{-4}	6.304
9.80×10^{-5}	7.208
6.26×10^{-5}	8.049
3.82×10^{-5}	8.865
2.24×10^{-5}	9.671
1.28×10^{-5}	10.47
7.12×10^{-6}	11.28
3.87×10^{-6}	12.09

Table 4.20 Ni-AHA (0.01M MES pH 6.3) batch

$[M]_T$ Total Ni concentration /(mol l^{-1})	Percentage Ni-AHA bound /(%)	[MS] Ni-AHA complex /(mol l^{-1})	[M] Ni-free /(mol l^{-1})	[MS]/[M]	ln a	ln [M]t/([P]
8.692×10^{-8}	92.87	4.296×10^{-8}	3.299×10^{-9}	13.02	2.641	-13.91
1.357×10^{-7}	92.42	6.486×10^{-8}	5.317×10^{-9}	12.19	2.580	-13.49
5.325×10^{-7}	91.79	2.429×10^{-7}	2.173×10^{-8}	11.18	2.500	-12.17
1.022×10^{-6}	90.50	4.263×10^{-7}	4.471×10^{-8}	9.533	2.355	-11.59
4.988×10^{-6}	86.65	1.634×10^{-6}	2.517×10^{-7}	6.491	2.014	-10.20
9.889×10^{-6}	85.50	3.035×10^{-6}	5.145×10^{-7}	5.898	1.931	-9.573
4.955×10^{-5}	72.42	8.157×10^{-6}	3.107×10^{-6}	2.625	1.288	-8.418
9.811×10^{-5}	60.02	9.938×10^{-6}	6.618×10^{-6}	1.501	0.917	-8.033
4.927×10^{-4}	39.41	2.293×10^{-5}	3.526×10^{-5}	0.650	0.501	-6.776
9.805×10^{-4}		-----	-----	-----	-----	----

Table 4.21 DEF data for Ni-AHA (0.01M MES pH 6.3) batch

[Ms]/TOC	log *K'
3.54×10^{-4}	4.758
3.30×10^{-4}	5.770
2.44×10^{-4}	6.528
1.47×10^{-4}	7.273
7.28×10^{-5}	8.049
2.99×10^{-5}	8.873
1.02×10^{-5}	9.755
2.92×10^{-6}	10.70

Table 4.22 Ni-AHA (0.001M MES pH 6.3) batch

$[M]_T$ Total Ni concentration /(mol^{-1})	Percentage Ni-AHA bound /(%)	[MS] Ni-AHA complex /(mol l^{-1})	[M] Ni-free /(mol l^{-1})	[MS]/[M]	ln α	ln [M]t/{P}
8.692×10^{-8}	94.04	4.810×10^{-8}	3.050×10^{-9}	15.77	2.820	-13.81
1.357×10^{-7}	93.96	7.460×10^{-8}	4.790×10^{-9}	15.57	2.808	-13.37
5.325×10^{-7}	92.35	2.590×10^{-7}	2.140×10^{-8}	12.08	2.572	-12.11
1.022×10^{-6}	91.62	4.720×10^{-7}	4.320×10^{-8}	10.94	2.480	-11.50
4.988×10^{-6}	87.82	1.800×10^{-6}	2.500×10^{-7}	7.214	2.106	-10.12
9.889×10^{-6}	86.45	3.300×10^{-6}	5.170×10^{-7}	6.384	1.999	-9.500
4.955×10^{-5}	74.73	9.340×10^{-6}	3.160×10^{-6}	2.957	1.375	-8.315
9.811×10^{-5}	66.14	1.310×10^{-5}	6.680×10^{-6}	1.954	1.083	-7.857
4.927×10^{-4}	46.54	3.150×10^{-5}	3.620×10^{-6}	0.871	0.626	-6.624
9.805×10^{-4}	21.61	2.080×10^{-5}	7.530×10^{-6}	0.276	0.244	-6.274

Table 4.23 DEF data for Ni-AHA (0.001M MES pH 6.3) batch

[Ms]/TOC	log *K'
5.48×10^{-4}	4.581
4.49×10^{-4}	5.611
3.10×10^{-4}	6.390
1.84×10^{-4}	7.134
9.57×10^{-5}	7.885
4.38×10^{-5}	8.660
1.77×10^{-5}	9.467
6.34×10^{-6}	10.31
2.02×10^{-6}	11.19
5.72×10^{-7}	12.12

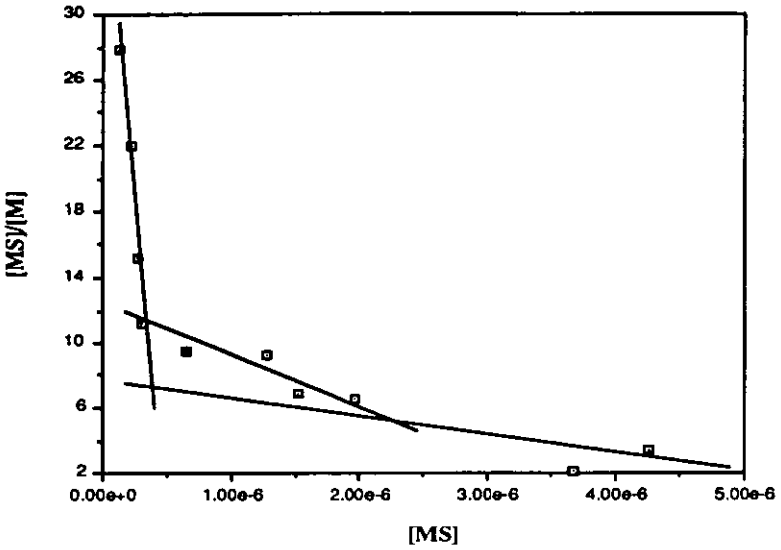

Fig 4.17 Scatchard plot of Eu-AHA (0.01M MES pH 6.3)

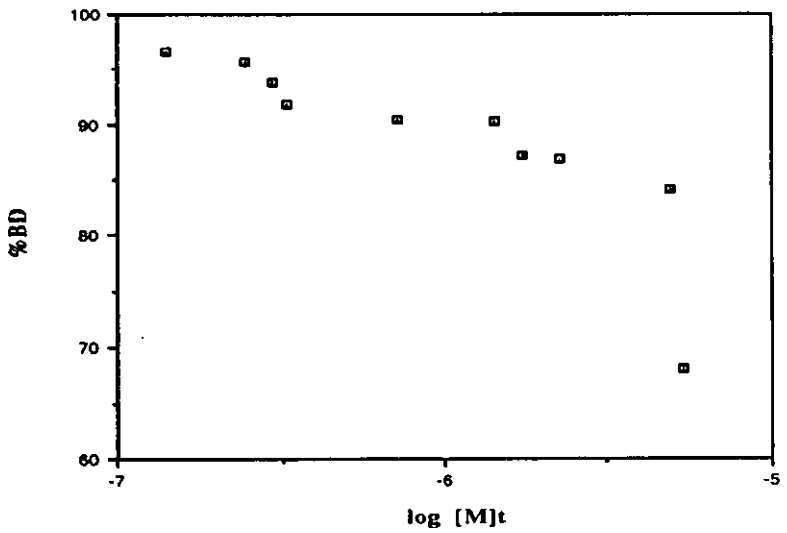

Fig 4.18 Europium percentage bound for the Eu-AHA system (0.01M MES pH 6.3)

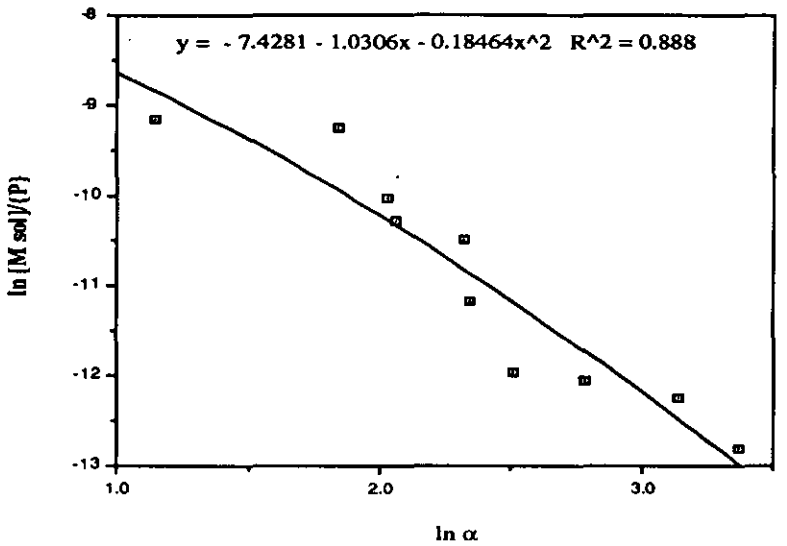

Fig 4.19 Derivation curve for DEF Analysis of Eu-AHA (0.01M MES pH 6.3)

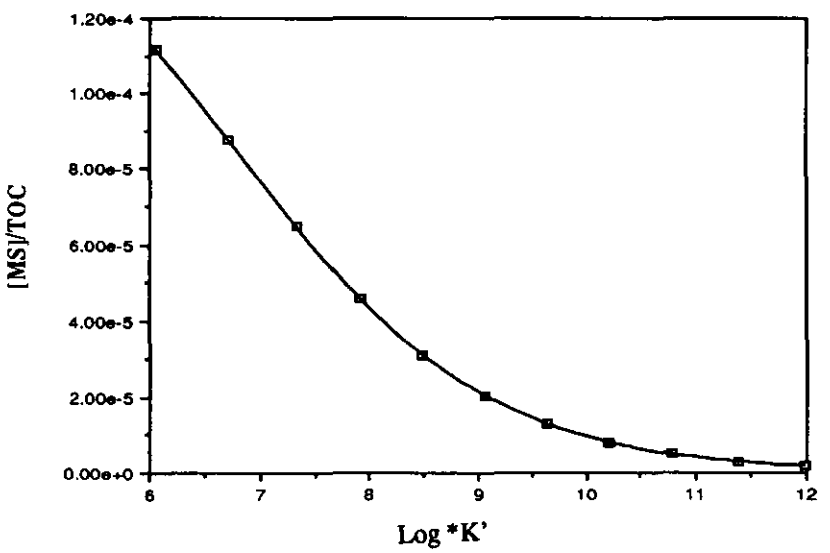

Fig 4.20 DEF curve of Eu-AHA (0.01M MES pH 6.3)

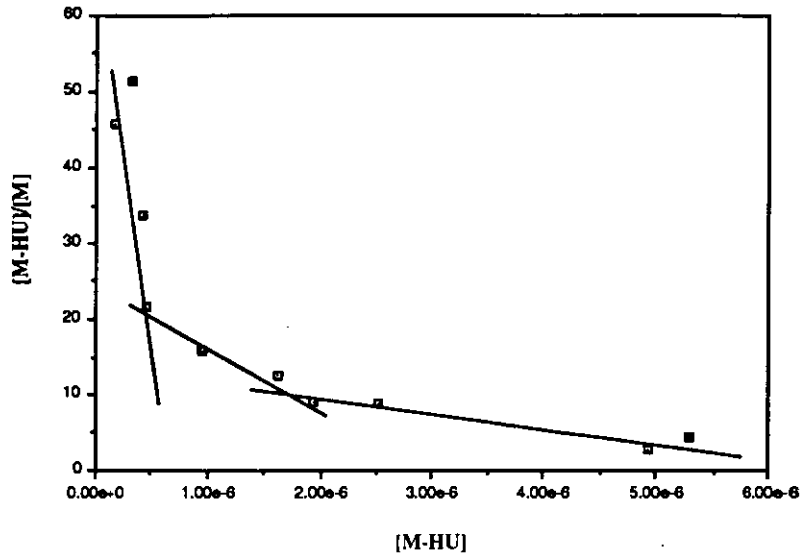

Fig 4.21 Scatchard plot of Eu-AHA (0.001M MES pH 6.3)

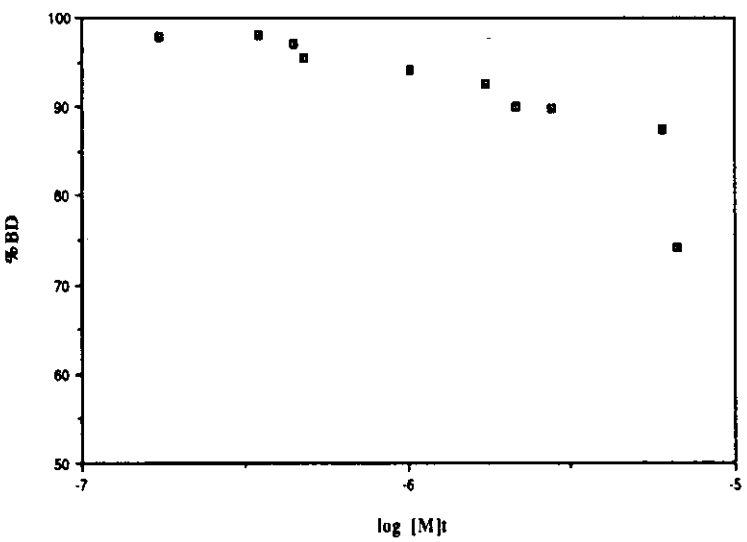

Fig 4.22 Europium percentage bound for the Eu-AHA system (0.001M MES pH 6.3)

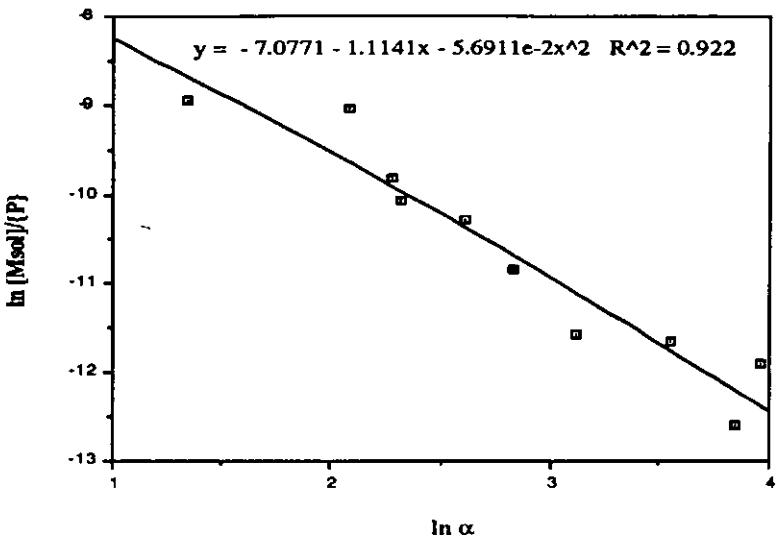

Fig 4.23 Derivation curve for DEF Analysis of Eu-AHA (0.001M MES pH 6.3)

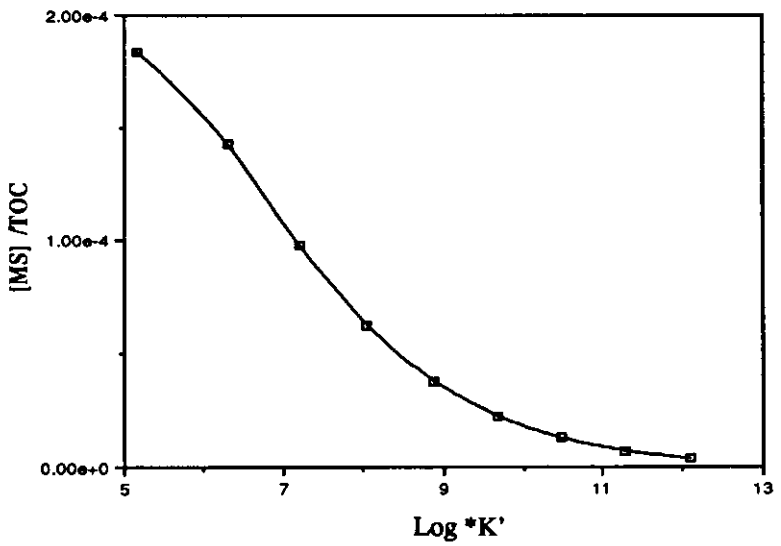

Fig 4.24 DEF curve of Eu-AHA (0.001M MES pH 6.3)

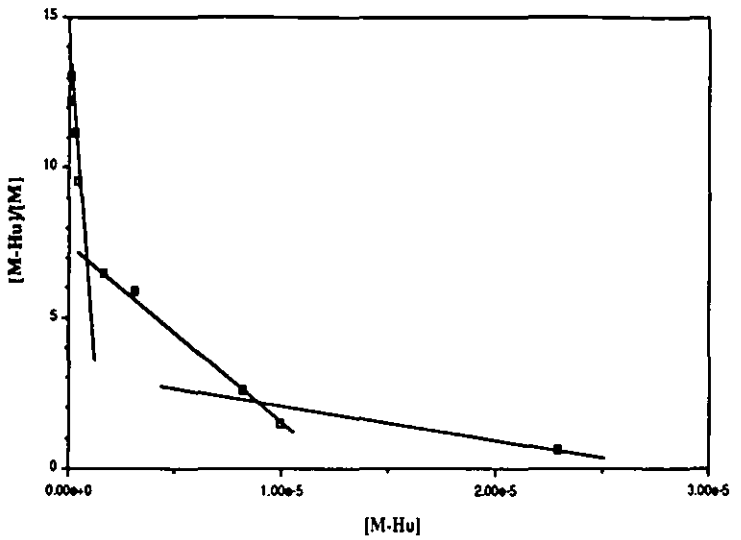

Fig 4.25 Scatchard plot of Ni-AHA (0.01M MES pH 6.3)

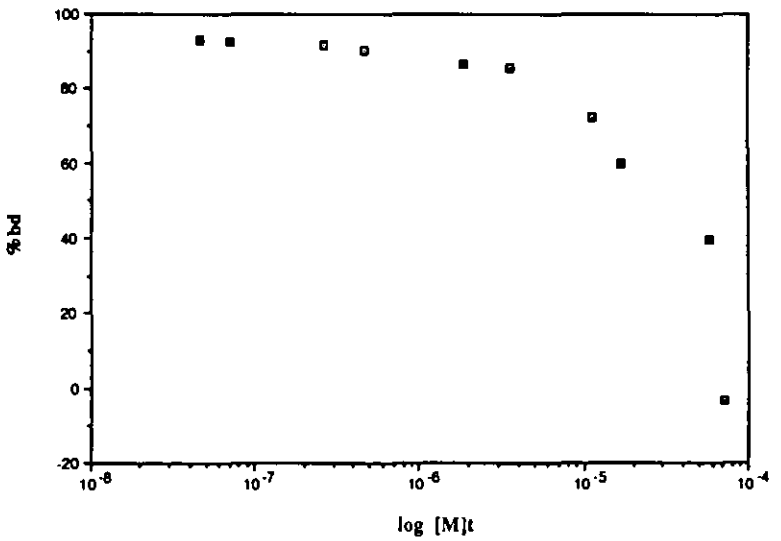

Fig 4.26 Nickel percentage bound for the Ni-AHA system (0.01M MES pH 6.3)

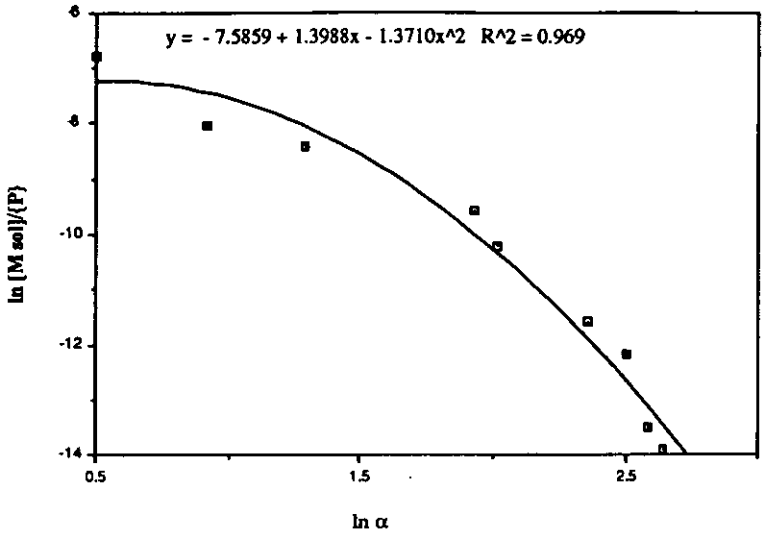

Fig 4.27 Derivation curve for DEF Analysis of Ni-AHA (0.01M MES pH 6.3)

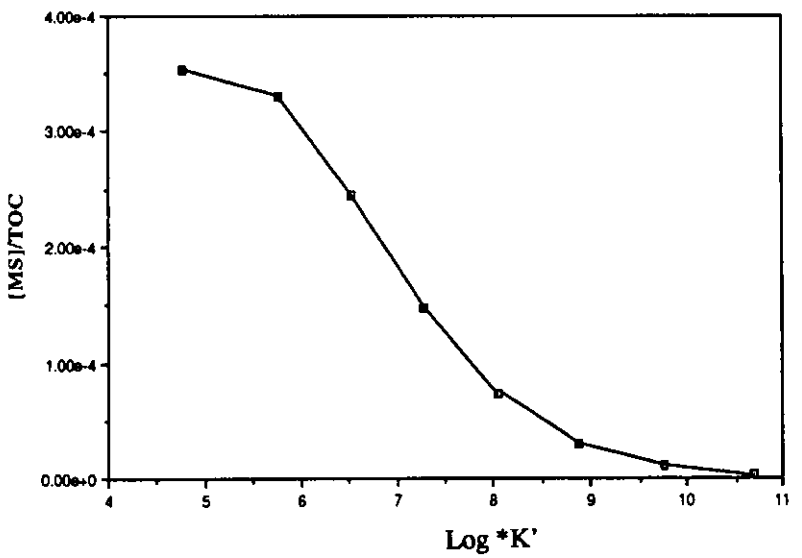

Fig 4.28 DEF curve of Ni-AHA (0.01M MES pH 6.3)

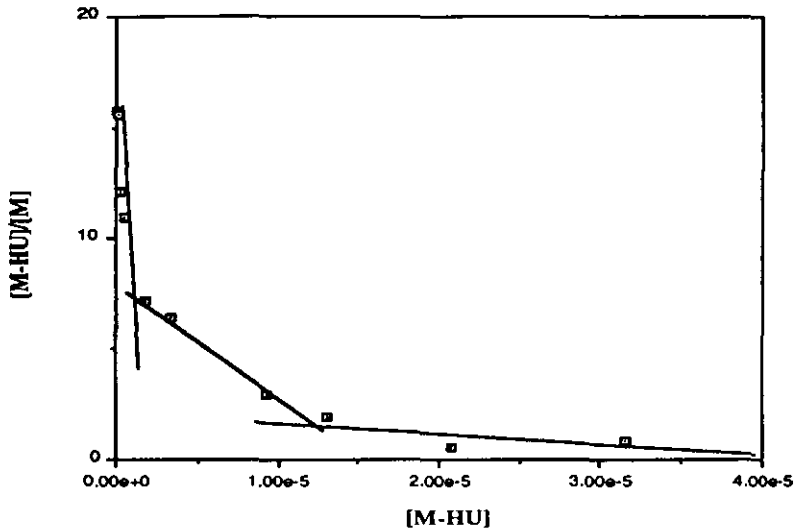

Fig 4.29 Scatchard plot of Ni-AHA (0.001M MES pH 6.3)

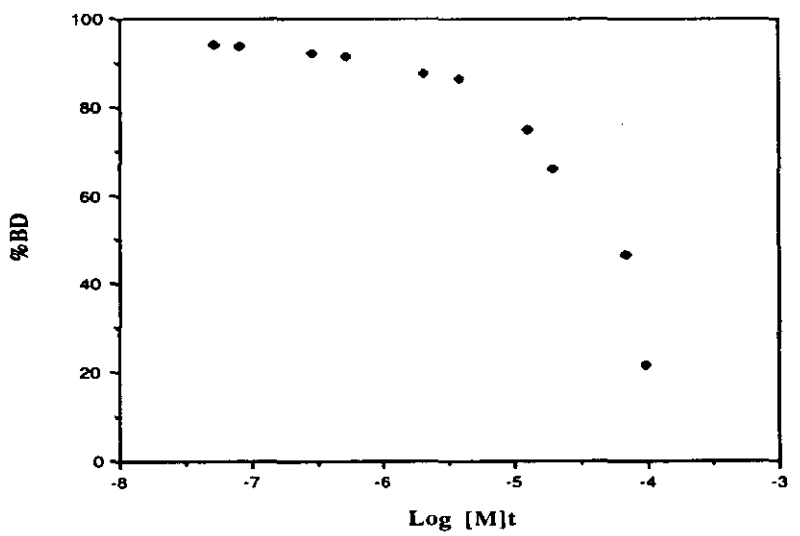

Fig 4.30 Nickel percentage bound for the Ni-AHA system (0.001M MES pH 6.3)

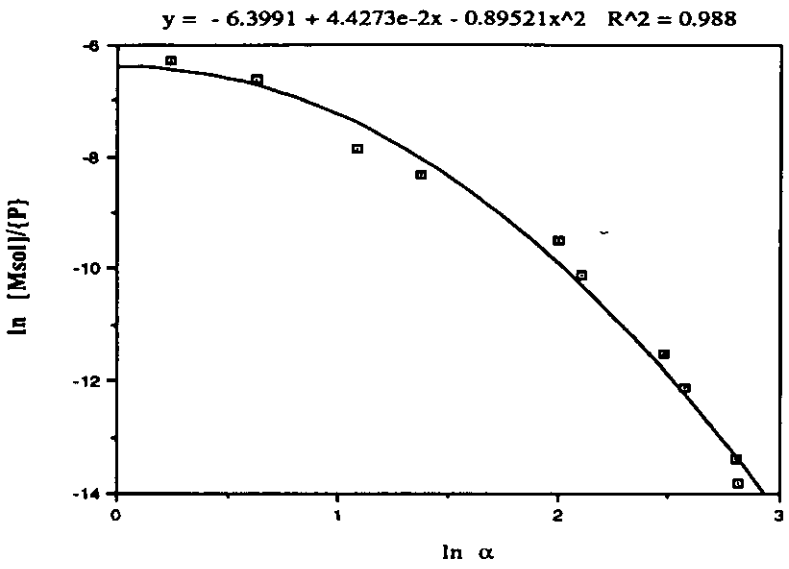

Fig 4.31 Derivation curve for DEF Analysis of Ni-AHA (0.001M MES pH 6.3)

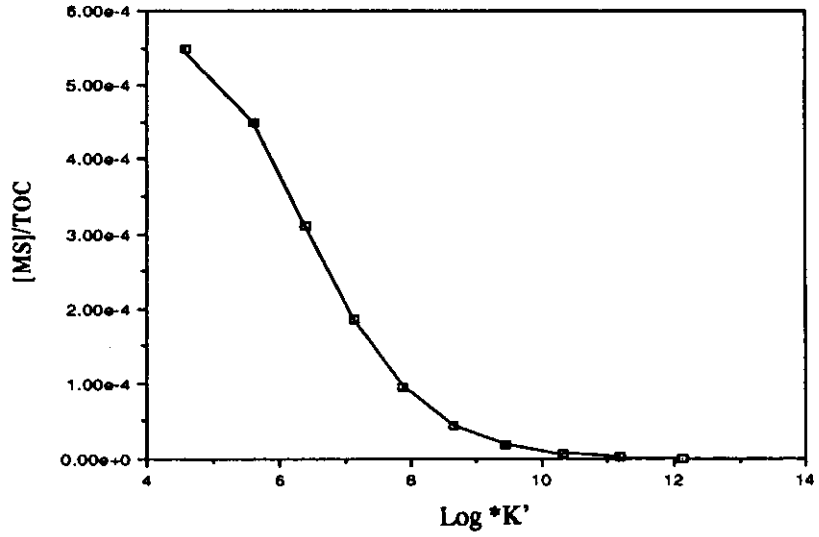

Fig 4.32 DEF curve of Ni-AHA (0.001M MES pH 6.3)

Table 4.24 Complexation parameters for Europium Humate

	Scatchard		EBDA	
Sample	**log ^{1}K**	**log ^{w}K**	**log ^{1}K**	**log ^{w}K**
Column				
Eu (0.01)	6.85	4.94	6.35	4.89
Eu (0.001)	7.00	5.38	6.85	5.46
Batch				
Eu (0.01)	7.78	6.37	7.52	6.02
Eu (0.001)	7.93	6.32	7.75	5.96

Table 4.25 Literature Values for Europium Humate

Sample	**pH**	**I.S**	**log β**	**ref**
HA (Aldrich)	6.0	0.01	7.5	89
HA (Gorleben)	6.0	0.01	8.1	89
HA (Clay)	6.0	0.01	7.5	89

Table 4.26 Complexation parameters for Nickel-Humate

	Scatchard		EBDA	
Sample	**log 'K**	**log "K**	**log 'K**	**log "K**
Column				
Ni (0.01)	6.18	2.22	5.76	2.77
Ni 0.001	6.40	3.50	6.00	2.88
Batch				
Ni (0.01)	6.55	4.31	6.07	4.14
Ni (0.001)	6.63	4.35	6.17	4.01

Table 4.27 Literature Values for Nickel-Humate

Sample	**pH**	**I.S**	**log β**	**ref**
HA (Aldrich)	6.5	0.01	4.37	90
HA (Aldrich)	6.5	0.01	5.17	90

4.16 DISCUSSION AND CONCLUSIONS OF THE COLUMN AND BATCH EXPERIMENTS

To study metal migration through the geosphere accurate stability constants need to be known. For the results obtained using the modified Schubert method it appears that for europium and nickel the majority of metal ions added to the solution are complexed with the humate (over the concentration ranges used). The percentage metal-humate complex formed decreases as the metal concentration increases i.e. as the metal loading increases. This is because the humate is becoming increasingly saturated with metal ions. The nature of the batch technique is such that the analysis is carried out without perturbing the equilibria of the system. This is because the components are analysed without a prior separative stage. In contrast the column system will disturb the equilibria to some extent. The extent to which this occurs is related to the residence time of the material on the ion exchange column. This is minimised to maximise the exchange process without disturbing the equilibria. Choppin et al (91) used this as a justification for 'terrestrial binding', that is binding that occurs at the surface of the macromolecule which arises due to weak electrostatic interactions between the net negative surface potential and the positive metal ion. This binding is not as strong as complexation as bonding does not actually take place. Terrestrial binding is thus dependent on the charge of the metal cation. The batch ion exchange technique gives a higher percentage metal bound than the column technique for both the nickel and the europium systems. The difference for the nickel humate is greater than that for the europium humate and is probably due to the charge difference of the metal ions. The difference only occurs at higher metal concentrations as the molecules sites become increasingly occupied (increased metal loading). This thus hinders the further complexation of metal by the humic material and increases the amount of metal which will be in the terrestrial region. This increased proportion of metal is then available to be stripped off when the system comes into

contact with the cation exchange resin in the dynamic column setup. Complexes of humic substances are subject to the effects of ionic strength in the same way that simple complexes are. It is anticipated that the effects of ionic strength will be more noticeable at low metal concentrations. This is shown by the higher observed stability constants for similar metal concentrations for the DEF experimental data at two different ionic strengths and also the higher observed stability constant for lower ionic strength in the Scatchard analysis, showing that the stability constant decreases with increasing ionic strength. Thus, in general, humic complexes become weaker, i.e more dissociated, as the ionic strength of the solution increases.

The results obtained using the batch technique are probably a more accurate representation of the theoretical levels of metal-humate complex formed. However the column technique results are probably more realistic for the levels of complexation that would occur in the environment as it is likely that a metal-humate complex would come into contact with naturally occurring ion exchangers such as clay and mineral particles. The results indicate that stability constants for metal humates can be rapidly determined using ion exchange.

4.17 COMPARISON AND VALIDATION OF COMPUTER SPECIATION MODELS

As stated in chapter one the ultimate use for stability constants and complexation parameters is not theoretical rhetoric but practical models which will be used to predict metal migration behaviour and also contaminant complexation in the environment. Over the last 2-3 years in the CHEMVAL II project dedicated mathematicians and computer modellers have joined forces with environmental and complexation chemists to improve and implement a more advanced speciation model that has the facility to incorporate naturally occuring organic ligands. It is their ultimate aim to incorporate these models into existing hydraulic transport and water flow models,to predict fully contaminant mobility throughout the geosphere. To this end it is essential that the initial speciation models be validated by comparison with accurate experimental results to assess the predictive power of the models with reference to known systems which contain naturally occuring organic ligands. To this end two current models were acquired and their results to be compared with actual experimental data obtained by ion exchange experiments. The models were as follows :

1) SPOSITOS MODEL (incorporated into PHREEQE)- a discrete ligand model for metal humic/ fulvic acid.

2) MINTEQA2 - a continuous distribution model for metal-DOM interactions.

4.17.1 Validation exercises

For the model comparisons a system comprising of the following conditions was postulated: an increasing amount of europium, within the range $3x10^{-7}$ to $5x10^{-5}$ mol l^{-1}, is added to humic acid 0.05 g l^{-1} at a pH of 6.3 and an ionic strength of 0.01M. The results that were obtained from MINTEQA2 were compared with those obtained from all experiments involving europium and are shown in tables 4.28 and 4.29 and figure 4.33.

An increasing amount of nickel, within the range $1x10^{-8}$ to $1x10^{-3}$mol l^{-1}, is added to humic acid 0.05 g l^{-1} at a pH of 6.3 and an ionic strength of 0.01M. The results that were obtained from MINTEQA2 and Sposito's model were compared with those obtained from all experiments involving nickel and are shown in tables 4.30 and 4.31 and figure 4.34.

4.17.2 Discussion and conclusions on computer speciation models

The major aim was to assess the predictive power of two individual computer speciation programs, which had been derived from one of the two model approaches

i) Continuous distribution model
ii) Discrete ligand model

Each program was asked to predict the amount of metal bound to a humic material (pH 6.3, I.S. 0.01M, T 25°C) over a range of metal concentrations. These predicted values were compared with the results obtained for a similar system that had been determined experimentally by ion exchange. It can be seen from the two graphs, figures 4.33 and 4.34, that neither of the two models correlate with the experimentally observed results exactly. The MINTEQA2 modelled europium results show good agreement with the batch (0.001) data at the low metal concentrations and good agreement with the column (0.001) results at the higher metal concentrations.

The MINTEQA2 modelled nickel results underestimate the percentage bound by approximately 40% at low metal concentration, but the results are closer to the experimentally observed results at higher metal concentration. The Sposito modelled nickel results are closer to the experimentally determined results giving higher predicted values at all metal concentrations although it does not predict either the column or the batch results exactly. The two main factors that effect the predicted binding are 1) the stability constants governing the reactions that are used in the program and 2) the site densities that the model uses for the humic ligand. The stability constants for the MINTEQA2 model are generated assuming a continuous distribution of Log K values from results that were obtained from experimentally observed stability constants for the Suwannee river dissolved organic matter. This means that only the metals that were studied in the Suwannee river project can be determined in the MINTEQA2 model. Unfortunately actinides are absent from this list that comprises fourteen metals. The log K values that are utilised in Sposito's model are found from literature values that are available for the species that are present in the simulated humic mixture. Unfortunately, according to the literature values, it would only be possible for the first row transition metals to be studied as these are the only metals that could provide all the necessary Log K values for the Sposito's mixture model. In consequence, the europium speciation could not be predicted as a full set of Log K values are unavailable for the ligand used in the Sposito's simulated humic acid system. The site densities that are used in the two models differ by an order of magnitude and unfortunately the site densities that are required are difficult to obtain experimentally. Also, for the models to reflect reality realistic site densities are required. In summary the MINTEQA2 model more accurately predicts the europium binding and the Sposito model more accurately predicts the nickel binding. The various merits of the two programs are summarised in table 4.32.

Table 4.28 Predicted Eu-binding using the MINTEQA2 model

Total Eu added [Eu]t /(mol l^{-1})	MINTEQA2 percentage Eu-bound /(%)
3.129×10^{-7}	99.2
5.599×10^{-7}	99.2
8.055×10^{-7}	99.2
1.050×10^{-6}	99.0
2.546×10^{-6}	98.5
5.016×10^{-6}	96.8
7.412×10^{-6}	93.8
9.917×10^{-6}	89.1
2.487×10^{-5}	56.8
4.957×10^{-5}	33.2

Table 4.29 Experimental Eu-AHA binding

Total Eu added $[Eu]_T$ /(mol l^{-1})	Eu (0.01 C) Percentage Eu-bound /(%)	Eu (0.001 C) Percentage Eu-bound /(%)	Eu (0.01 B) Percentage Eu-bound /(%)	Eu (0.001 B) Percentage Eu-bound /(%)
2.656×10^{-7}	90.91	94.10	96.53	97.86
5.137×10^{-7}	92.36	93.00	95.66	98.09
7.618×10^{-7}	96.85	92.80	93.82	97.13
1.010×10^{-6}	87.95	95.30	91.82	95.60
2.498×10^{-6}	76.60	88.30	90.40	94.09
4.979×10^{-6}	62.84	85.50	90.23	92.61
7.460×10^{-6}	50.26	80.70	87.24	90.11
9.941×10^{-6}	39.74	76.00	86.83	89.77
2.482×10^{-5}	25.58	59.30	84.14	87.53
4.963×10^{-5}	18.67	32.50	68.07	74.12

where B and C refer to batch and column experiments see sections 4.9 and 4.13

Table 4.30 Predicted Ni-binding using SPOSITO'S and MINTEQA2 models

Total Ni added $[Ni]_T$ /(mol l^{-1})	SPOSITO'S Percentage Ni-bound /(%)	MINTEQA2 Percentage Ni-bound /(%)
1×10^{-8}	78.3	34.4
5×10^{-8}	78.3	34.3
1×10^{-7}	78.3	34.2
5×10^{-7}	78.0	34.3
1×10^{-6}	77.7	32.3
5×10^{-6}	75.0	26.0
1×10^{-5}	71.6	21.2
5×10^{-5}	46.4	9.5
1×10^{-4}	30.0	6.1
5×10^{-4}	8.46	1.9
1×10^{-3}	4.69	1.1

Table 4.31 Experimental Ni-AHA binding

Total Ni added $[Ni]_T$ /(mol l^{-1})	Ni (0.01 C) Percentage Ni-bound /(%)	Ni (0.001 C) Percentage Ni-bound /(%)	Ni (0.01 B) Percentage Ni-bound /(%)	Ni (0.001 B) Percentage Ni-bound /(%)
8.692×10^{-8}	88.60	89.98	92.87	94.04
1.357×10^{-7}	85.20	89.77	92.42	93.96
5.325×10^{-7}	81.36	79.19	91.79	92.35
1.022×10^{-6}	84.20	60.00	90.50	91.62
4.988×10^{-6}	86.70	44.00	86.65	87.82
9.889×10^{-6}	46.70	30.40	85.50	86.45
4.955×10^{-5}	25.54	21.16	72.42	74.73
9.811×10^{-5}	16.02	14.19	60.02	66.14
4.927×10^{-4}	8.00	11.15	39.41	46.54
9.805×10^{-4}	14.50	13.80	----	21.61

where B and C refer to batch and column experiments see sections 4.10 and 4.14

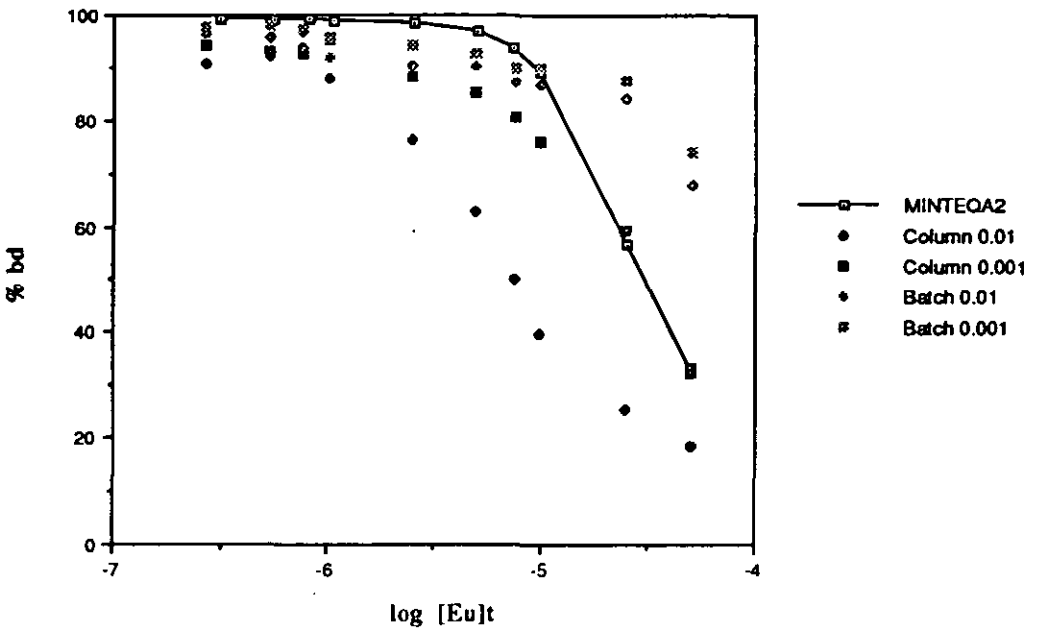

Fig 4.33 Experimental Eu- binding and predicted Eu-binding using the MINTEQA2 model

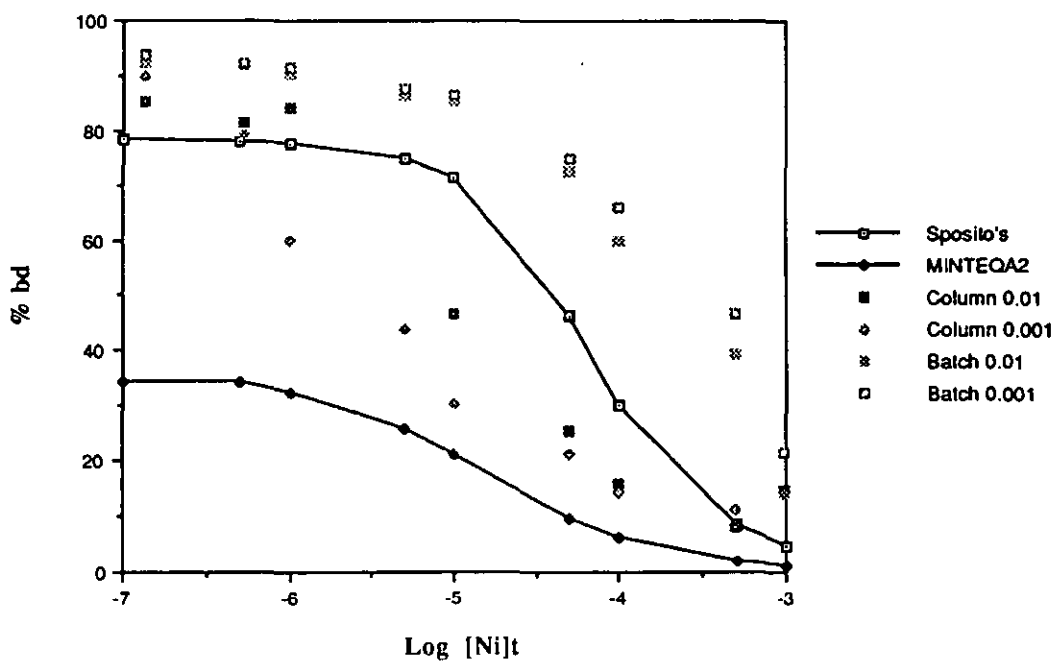

Fig 4.34 Experimental Ni-binding and predicted Ni-binding using SPOSITO'S and MINTEQA2 models

Table 4.32 Comparison of the main features of the models

Feature	Continuous distribution MINTEQA2	Ligand mixture Sposito
Theoretical aspects	Simple continuous distribution model	Arbitary choice of ligands unable to account for for metal loading effects
Database	Limited to TMs and Eu, Ca and Be	Likely to be always restricted to a few TMs
Compatability with speciation codes	Yes	Yes
Adjustable parameters for data fitting	1 (or 2)	0 (or 10)
Site density	5×10^{-3} mol g^{-1}	~ 2×10^{-3} mol g^{-1}
Accomodation of I.S. and pH effects	Limited	Limited
Accomodation of competitve effects	Yes for a limited number of metals	No in practice

Chapter Five

Synchronous Scanning Fluorescence studies of humic acid solutions

5.1 SYNCHRONOUS SCANNING FLUORESCENCE (SF)

The excitation and emission modes of fluorescence measurement involve setting one monochromator to a fixed wavelength and scanning the second monochromator over the desired wavelength range. In excitation fluorescence the emission monochromator is fixed and the excitation monochromator is scanned whilst in emission fluorescence the excitation monochromator is fixed and the emission monochromator is scanned. The two spectra that are produced are then compared in terms of relative shape, energies and wavelength shifts. This gives an indication of the molecular shapes and energy distribution patterns. In the synchronous scanning mode the two monochromators are linked and scanned simultaneously. There are several permutations that are available to the experimenter (92):

(1) Constant wavelength synchronous fluorescence (CW - SF)

(2) Linear variable angle synchronous fluorescence (V.A - SF)

(3) Non- linear variable angle synchronous fluorescence (N.L.V.A-SF)

these are shown schematically in Fig 5.1

(4) Constant energy synchronous fluorescence (CE - SF)

The most common form being the CW-SF mode. This mode usually involves setting the excitation monochromator to pass wavelength λ and the emission monochromator to pass wavelengths $\lambda + \Delta\lambda$. The fluorescence intensity is then recorded as both monochromators are scanned simultaneously, whilst $\Delta\lambda$ is kept constant. In this mode the synchronous fluorescence spectra are generally recorded as fluorescence intensity versus emission wavelength. This technique was introduced in the early 1970's by Lloyd (93,94,95). It was shown (96) that the synchronous fluorescence intensity, I_s, depends on properties of both the normal excitation and emission spectra as well as on the wavelength difference, $\Delta\lambda$. Vo-Dinh (97) has shown that the synchronous fluorescence intensity is given by the following

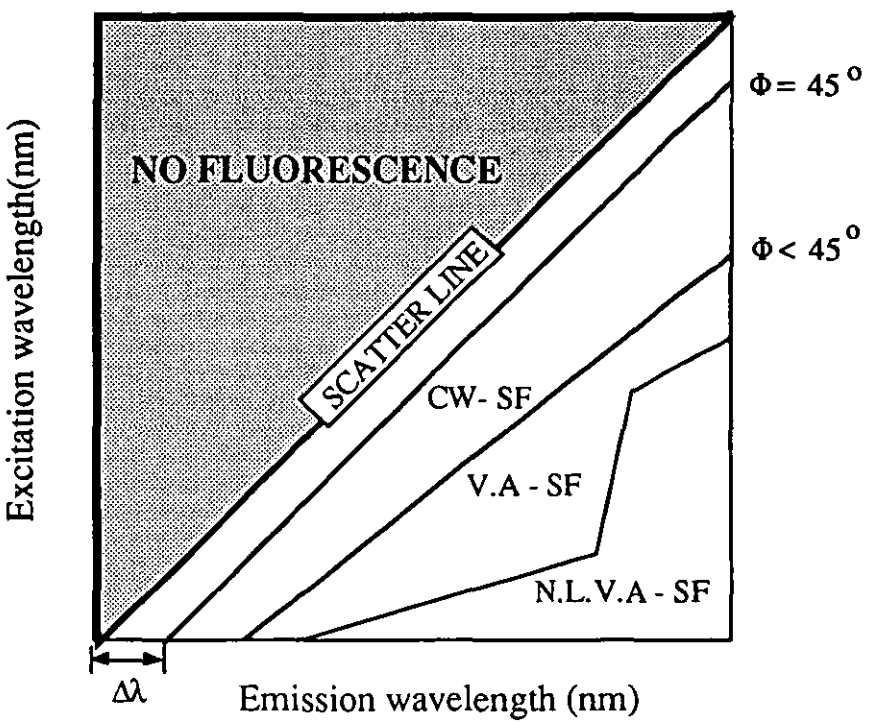

Fig 5.1 Modes of synchronous scanning fluorescence

expression:

$$I_s = Kcd\ Ex(\lambda em-\Delta\lambda)\ Em(\lambda em) \quad (1)$$

Where I_s is intensity of fluorescence signal

K is a constant

c is the concentration of the fluorescent species

d is the sample thickness

Ex(λem-Δλ) and Em(λem) are defined as the intensity distribution patterns

Equation 1 involves two functions i.e. both the excitation and the emission wavelengths, instead of only the one as in conventional fluorescence methods. It is also clear from the expression that the intensity of fluorescence will only be finite if the product Ex(λem-Δλ) Em(λem) is finite, which implies that the synchronous signal will be observed only when fluorescence excitation and emission occur over the Δλ selected. This makes the shape and bandwidth of a synchronous fluorescence spectrum a strong function of the Δλ selected, which ultimately gives the experimenter more control. For example if the Δλ is small , the signal should be finite only in the limited range where the fluorescence excitation and emission bands overlap. As Δλ gets larger, the synchronous fluorescence spectrum extends over a greater spectral range and its shape and bandwidth become dependent on the total wavelength distribution of the molecules' excitation and emission spectra. Synchronous fluorescence spectra obtained at a small Δλ show an effective lowering of bandwidth resulting in spectral simplification and a consequent reduction in spectral overlap (98). Thus the use of the synchronous scanning technique can increase the chance of obtaining a resolved spectral structure by decreasing the two adverse effects that lead to the main diffuseness of the conventional fluorescence spectra i.e. the intrinsic broadness and the often

severe overlapping bands. If $\Delta\lambda$ is large the resulting synchronous spectrum often contains more than one peak for each component of the mixture. Moreover, the spectral pattern that emerges for each component depends on the product Ex(λem-$\Delta\lambda$) Em(λem) for the component, which is often unique for each component in the mixture. As a consequence, the synchronous spectrum obtained with large $\Delta\lambda$ usually contains more detail than the normal excitation or emission spectrum of the mixture. The synchronous fluorescence spectrum thereby becomes a signature or spectral fingerprint for that particular mixture.

5.2 STRUCTURAL AND ENVIRONMENT EFFECTS ON FLUORESCENCE

5.2.1 Structural effects

Fluorescence may be expected generally in molecules that are aromatic or contain multiple conjugated double bonds with a high degree of resonance stability. Both classes of substance have delocalised π- electrons that can be placed in low lying excited singlet states. Fluorescence always involves the lowest energy excited transition. If the molecules possess atoms with lone pairs of electrons, such as oxygen or nitrogen, the electronic transition of lowest energy may involve one of the non-bonding n electrons ($n \rightarrow \pi^*$ transition). Alternatively, the electronic transition of lowest energy may involve the π bonding and the π^*-antibonding orbitals ($\pi \rightarrow \pi^*$ transition). The nature of this transition is a very important factor in determining the fluorescence properties of a particular molecule. Metal chelate fluorescence frequently involves $\pi \rightarrow \pi^*$ transitions in the ligand, but some metal chelates can involve either a transition between two metal energy levels or between a metal energy level and a π energy level in the ligand i.e. a charge transfer transition. The overall fluorescence behaviour of a molecule will primarily depend on the molecular structure, any given change being likely to induce one or more different types of effects. As a result, the overall fluorescence properties must be considered as a cumulative effect of structural changes. Increasing the extension

of the π electron system has the effect of increasing fluorescence and lowering the energy difference between the ground and first excited state, thus shifting the emission wavelength to higher values. Linear ring systems fluoresce at lower wavelengths than non-linear systems. Heteroatom substitution greatly effects the fluorescence of aromatic compounds. Substituents that delocalise the π electrons, such as $-NH_2$, -OH, $-OCH_3$ and $-NHCH_3$ groups, often enhance fluorescence because they tend to increase the transition probability between the lowest excited singlet state and the ground state. Electron withdrawing groups containing -Cl, $-NO_2$ and -COOH can decrease or quench completely the fluorescence. When a fluorescent organic compound complexes with a metal ion of high atomic number the fluorescence efficiency decreases, particularly when the ion is paramagnetic, where an enhanced rate of intersystem crossing is observed at the expense of fluorescence. Increasing structural rigidity has the effect of reducing the degree to which a fluorescent molecule can interact with its medium, which in turn tends to reduce the rate of internal conversion, resulting in an increase in fluorescence.

5.2.2 Environment effects

Environmental factors, such as temperature, nature of solvent, heavy atoms, hydrogen bonding, presence of solutes , pH and metal ions, can strongly influence the fluorescence of a compound by either influencing the rate of one or more processes involving excited states or by perturbing one or more of the energy levels involved in fluorescence. As changes in the structure of a molecule will generally influence the interaction with its environment and vice versa, changes in the environment often effect the structure of the molecule, therein environmental and structural effects are strictly interrelated.

5.3 EXPERIMENTAL

5.3.1 Effect of Δ λ on the synchronous fluorescence spectra of humic acid

Humic acid 12 mg l^{-1} was dissolved in HPLC water and the synchronous fluorescence of the sample was taken with Δλ set to 15, 20, 25, 30, 35, 40, 45, 50, 55, 60, 65, 70, 75, 80, 85, 90, 95 and 100nm. Synchronous fluorescence were recorded for each Δλ. The results are shown in Figures 5.2 to 5.4.

Results and discussion of the effects of Δλ

The CW-SF spectra are clearly more resolved than the EE spectra (shown in chapter 3 Figure 3.9) with a definite peak at 485nm. As the Δλ increases from 15 to 50nm the intensity of the peak at 485 nm increases as shown in Figure 5.4. From Δλ of 35nm a second peak starts to emerge at 300nm which shifts to 350nm and increases in intensity as Δλ increases. The intensity of the peak at 465nm eventually becomes constant whilst the intensity of the peak at 350nm increases and shifts back to 330nm. In particular the main peak shifts from 350nm to 465nm as Δλ decreases.

It was decided that for all subsequent experiments Δλ would be kept constant at 20nm.

5.3.2 Effect of humic acid concentration on the synchronous fluorescence spectra

Humic acid was dissolved in HPLC water to obtain concentrations of 100, 95, 90, 85, 80, 75, 70, 65, 60, 55, 50, 45, 40, 35, 30, 25, 20, 15, 10, 5 and 2 mg l^{-1}. The solutions pH was adjusted to 7 with NaOH and HCl and an ionic strength of 0.1M with sodium chloride. The solutions were immediately scanned in the synchronous fluorescence mode. The results are shown in Figures 5.5-5.6.

Results and discussion of the effects of the concentration of humic on the synchronous fluorescence

The CW - synchronous spectra presented show the effect of concentration on the fluorescence properties of the humic acid. The fluorescence intensity as measured at the peak at 485nm increases steadily up to 80mg l^{-1} and then increases at a slower rate and remains almost unchanged at higher concentrations. This behaviour is attributable to different fluorescence thresholds for different fluorophores in the humic molecule. The overlapping effect of different fluorescent groups and interference, due to self quenching and the inner filter effect at high concentrations, is not present below 15 mg l^{-1}, where the plot of fluorescence intensity versus absorbance shown in figure 5.7 is linear up to that concentration. All subsequent work was carried out on sample with a humic concentration of less than 15mg l^{-1}.

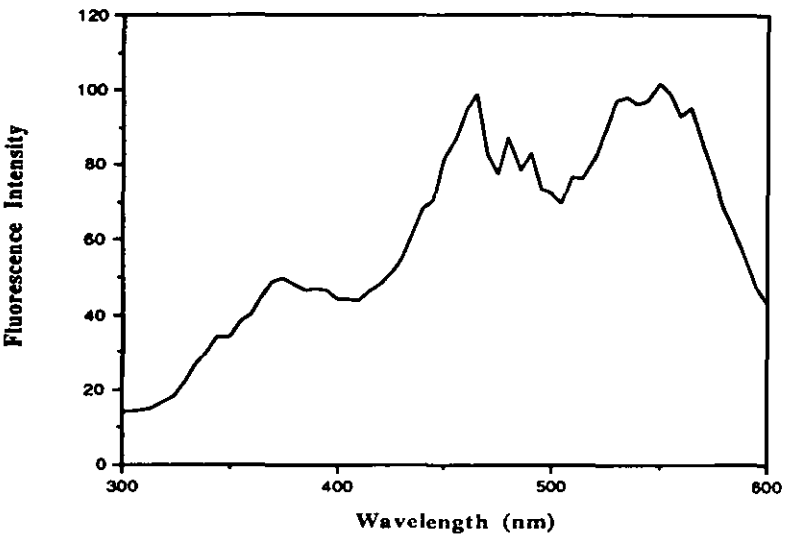

Fig 5.2 Effect of Δλ on the synchronous fluorescence of Humic acid (Δλ 5nm)

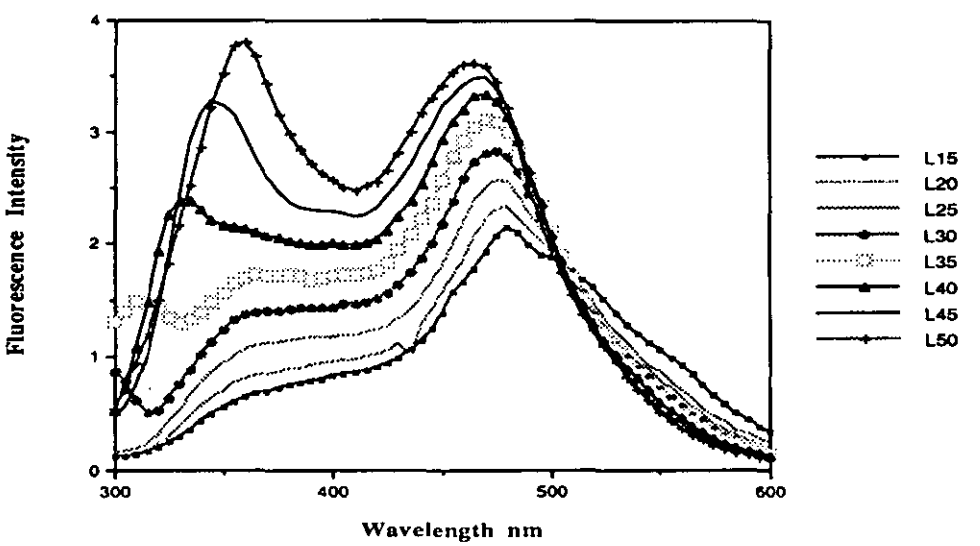

Fig 5.3 Effect of Δλ on the synchronous fluorescence of Humic acid (Δλ 15, 20, 25, 30, 35, 40, 45 and 50nm)

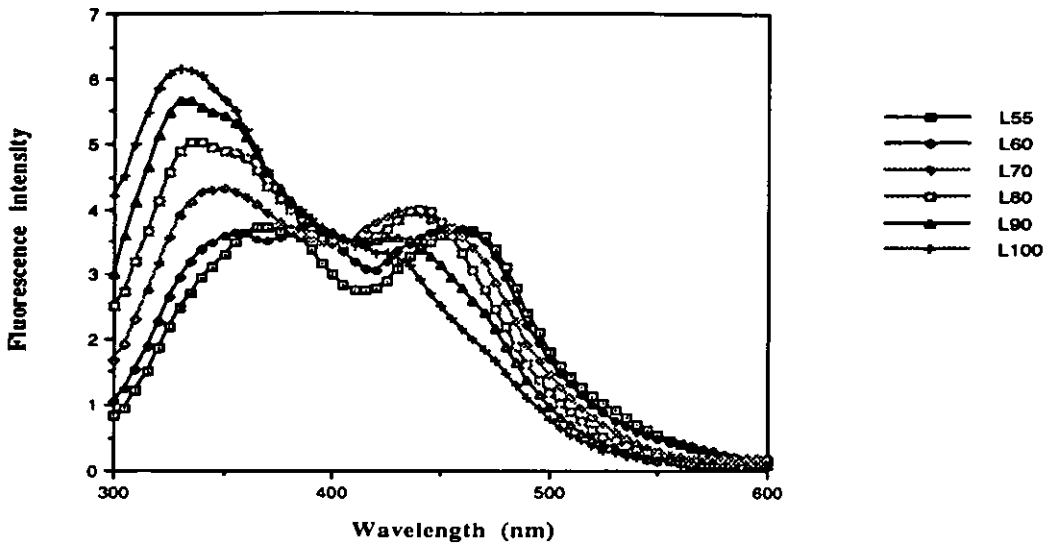

Fig 5.4 Effect of Δλ on the synchronous fluorescence of Humic acid (Δλ 55, 60, 70, 80, 90 and 100nm)

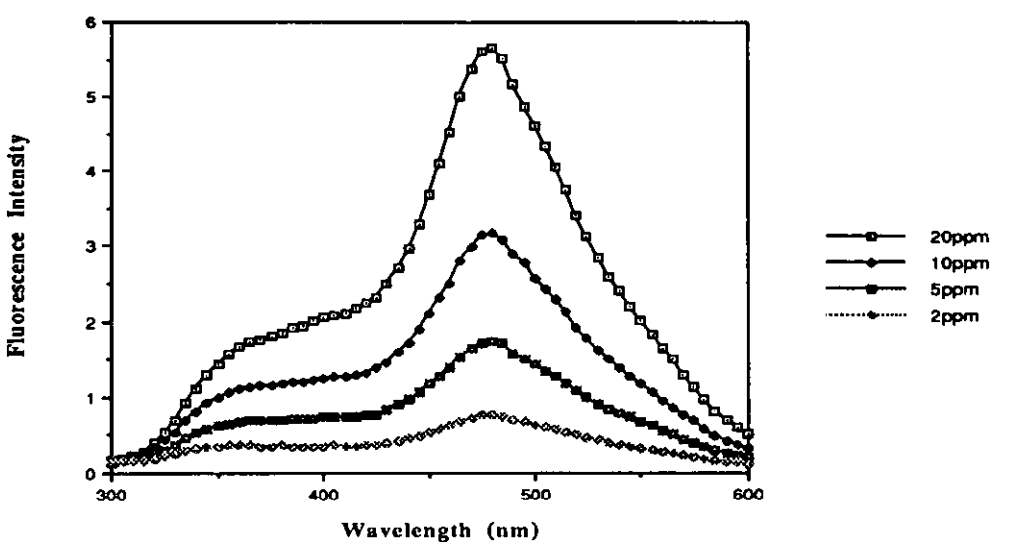

Fig 5.5 Effect of Humic acid concentration on the synchronous fluorescence ([HA] 2, 5, 10 and 20 ppm)

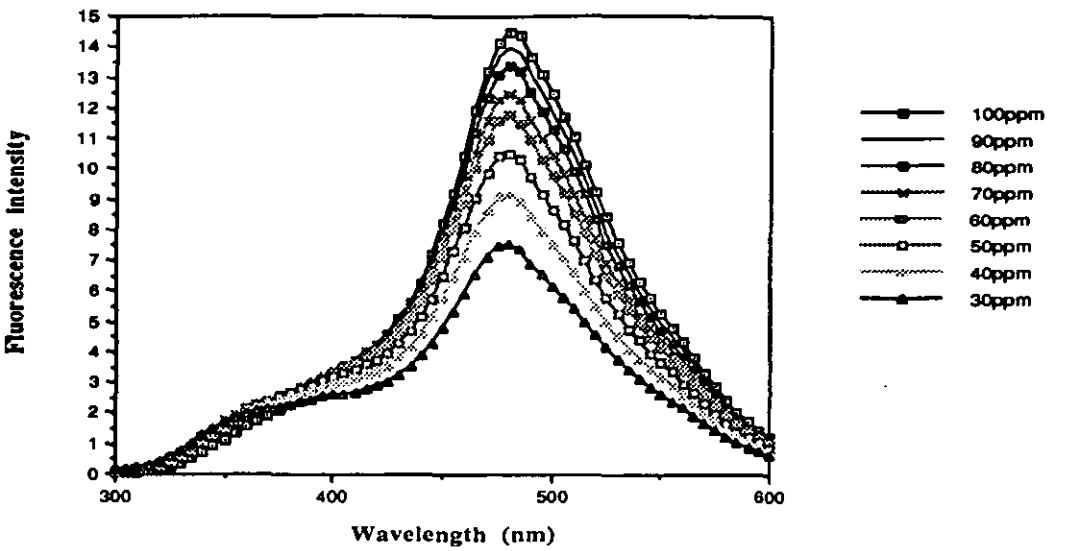

Fig 5.6 Effect of the Humic acid concentration on the synchronous fluorescence ([Ha] 30, 40, 50, 60, 70, 80, 90 and 100 ppm)

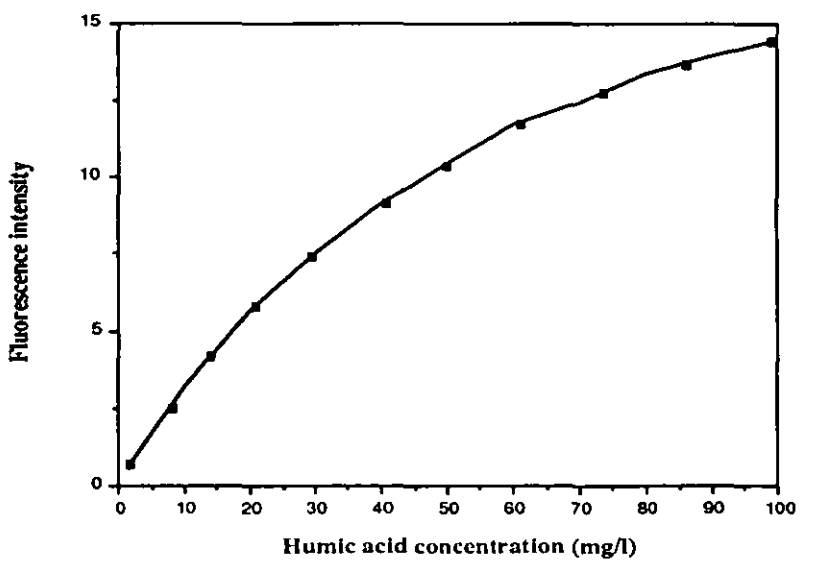

Fig 5.7 Fluorescence intensity versus absorbance for the humic acid solution using synchronous scanning fluorescence

5.3.3 Effect of solution pH on the synchronous fluorescence spectra of humic acid

Humic acid (12mg l^{-1}) was dissolved in HPLC water and 12 aliqouts were placed into glass vials. The pH of each solution was adjusted with sodium hydroxide or hydrochloric acid to produce solutions with a range of pH. The solutions were immediately scanned in the synchronous fluorescence mode. The results are shown in Figures 5.8 to 5.10

Results and discussion of pH effect

As the pH of the solution decreases, the degree of site protonation increases and thus the sites responsible for fluorescence are reduced resulting in the decrease in fluorescence intensity. The fluorescence intensity decreases gradually to a pH of about 7, and this is due to the humic acid being almost totally deprotonated to this point so all the sites responsible for fluorescence are free and thus there is only a gradual change in the intensity. At about pH 7 the degree of site protonation increases so the fluorescence intensity starts to decrease more rapidly. This should continue until a solution pH of 2 is reached at which point the humic would precipitate out of solution. Any observed fluorescence would be due to the conjugated structural features that are only slightly effected by pH. However, at pH 4 the fluorescence spectra show a shift in wavelength of the fluorescence maxima from 485nm to 460nm with an increase in the fluorescence intensity. If the observed effects are due to conformational changes alone then the same effects should be observed with an increase in ionic strength as high ionic strength would cause the molecule to coil up. Therefore, the effects of ionic strength were investigated as reported in 5.3.4. Alternatively, if we acknowledge that at pH 2 the humic acid becomes a precipitate we must also acknowledge that at some time before precipitation the size of the humic materials should be within the colloidal size range and thus the increase in fluorescence intensity and the associated

spectral shift may be due to the light scattering effects of colloidal particles. According to the light scattering theory, as proposed by Raleigh (1871), colloidal particles scatter light to the blue region of the electromagnetic spectrum, i.e. to approximately 450nm. Because of this, the fluorescence of colloidal suspensions was also investigated. A third way to investigate the effect of pH on the fluorescence properties of humic acid was to carry out the experiment on a model molecule. The molecule chosen was 2-hydroxy benzoic acid. This molecule contains a functional grouping believed to be responsible for humic metal binding (16).

5.3.4 Effect of solution ionic strength on the synchronous fluorescence spectra of humic acid

Humic acid (12mg l^{-1}) was dissolved in HPLC water and 12 aliquots were placed into glass vials. Sodium chloride was added to each vial to produce a range of ionic strengths (0.001M to 5M). The solutions were immediately scanned in the synchronous fluorescence mode. The results are shown in Figures 5.11 to 5.12

Results and discussion of ionic strength effects

The fluorescence intensity of the peak at 480nm decreases with increasing ionic strength . The fluorescence decreases rapidly up to an ionic strength of 1M NaCl but from then on the change is slower and appears to be negligible after an ionic strength of 5M. This observation can be accounted for in two ways: salt surpressing the ionization of functional groups on the humic molecule and also a gradual coiling up of the humic macromolecule structure which is flexible and uncoiled at low ionic strength.

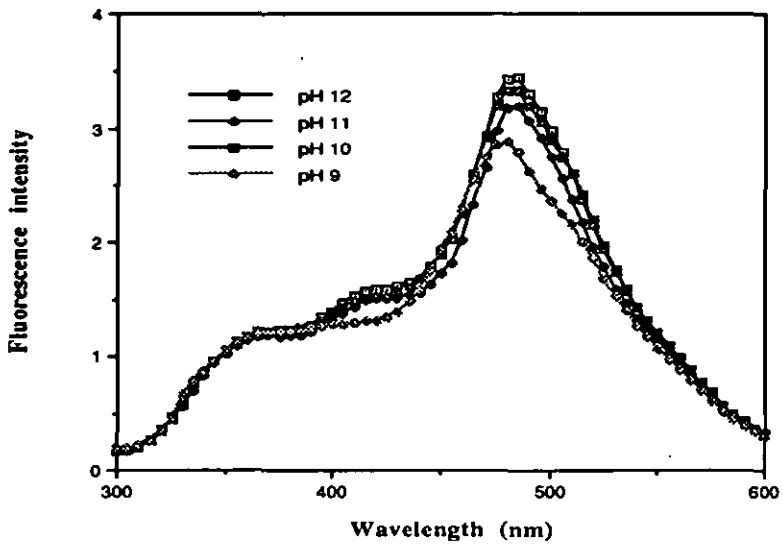

Fig 5.8 Effect of pH on the synchronous fluorescence of Humic acid (pH 12, 11, 10 and 9)

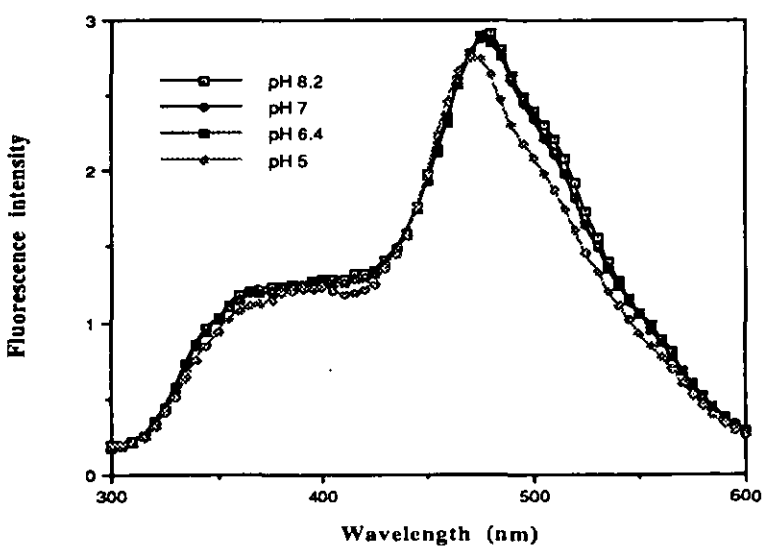

Fig 5.9 Effect of pH on the synchronous fluorescence of Humic acid (pH 8, 7, 6.4 and 5)

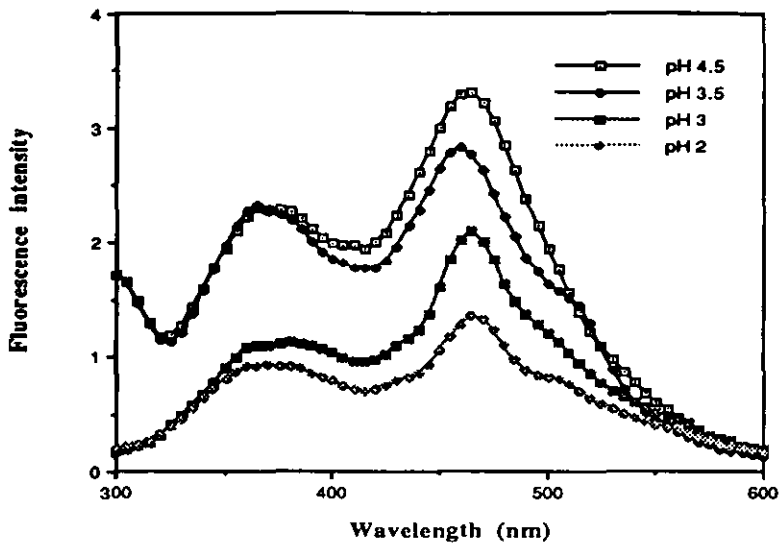

Fig 5.10 Effect of pH on the synchronous fluorescence of Humic acid (pH 4.5, 3.5, 3 and 2)

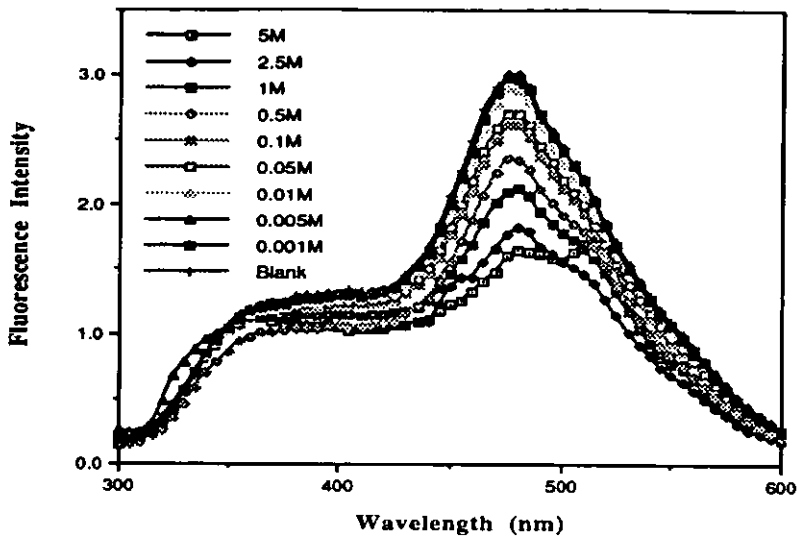

Fig 5.11 Effect of ionic strength on the synchronous fluorescence of Humic acid (I.S.)

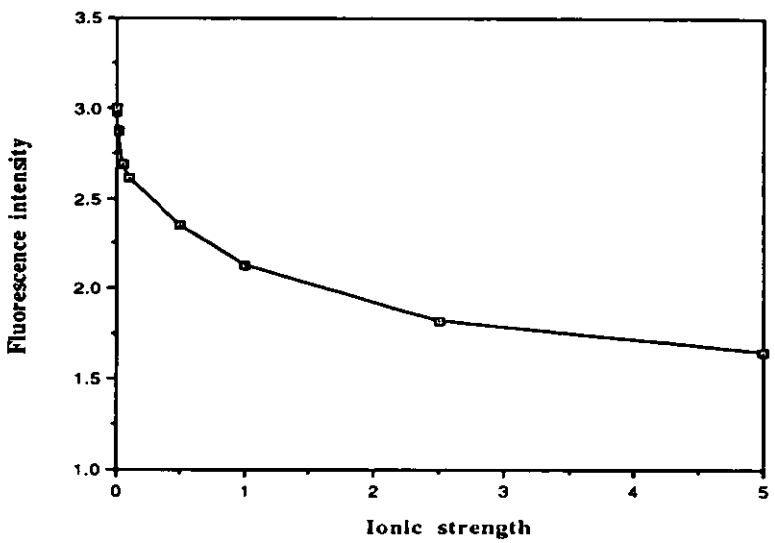

Fig 5.12 Effect of i.s. on the synchronous fluorescence of Humic acid

5.3.5 The synchronous fluorescence of colloidal suspensions

Seven commercially available colloidal suspensions were obtained, each having a different nominal size (as determined by the suppliers). Solutions of the colloidal suspensions were prepared so that each was 100ppm in concentration.
The synchronous fluorescence of the samples was carried out. The results are shown in Figures 5.13 to 5.14.

Composition of colloidal suspensions used

Commercial Name	Chemical name	Shape	Nominal diameter
Titanium dioxide P25	TiO_2	Spherical	21nm
Bindzil (BZ)	SiO_2	Spherical	40nm
Ludox TM (LX)	SiO_2	Spherical	22nm
W30	SiO_2	Spherical	125nm
D30	SiO_2	Spherical	7nm
Bacosol	Al(OH)O	Spherical	129nm
δ-Aluminium oxid C	Al_2O_3	Spherical	13nm

Results and discussion of the synchronous fluorescence of colloidal suspensions

The CW-SF spectra presented show that each colloidal suspension gives a very characteristic spectrum which is due to the scattering of light. Each spectrum shows a peak at 450nm and two shoulders at 370nm and 500nm, although for the smaller particles these two shoulders are weak. Two of the mentioned three regions are definitely present on the humic molecule spectrum i.e. 370nm and 500nm, however the main peak at 450 nm is missing. This peak should be present on all colloidal solution spectra and its absence in the spectra observed from the humic

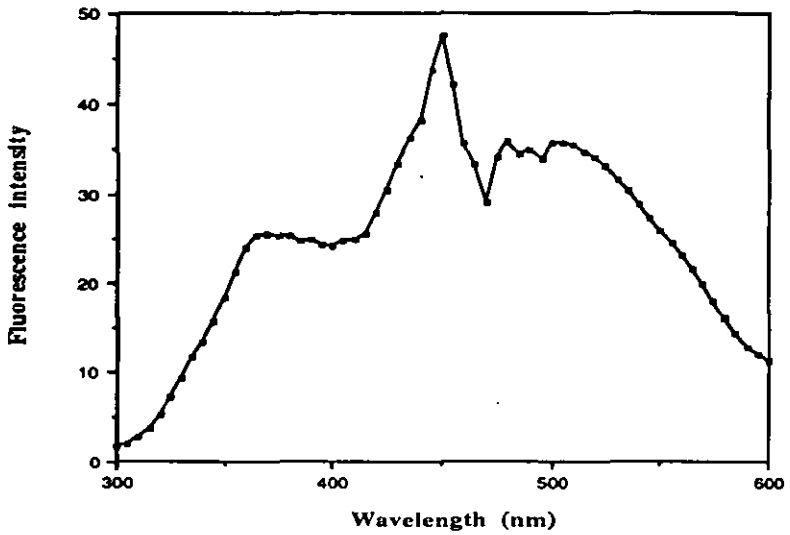

Fig 5.13 Synchronous fluorescence of a colloidal suspension (TiO_2 , 100ppm)

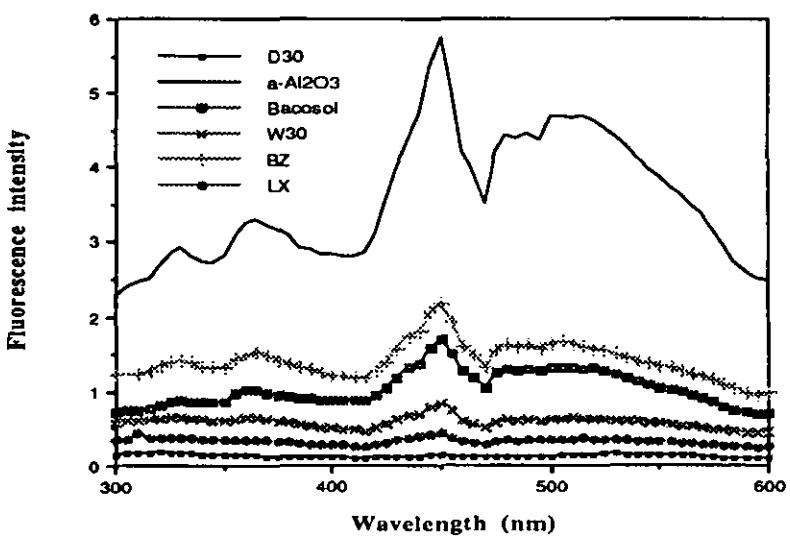

Fig 5.14 Synchronous fluorescence of a colloidal suspension (D30, δ-Al_2O_3, Bacosol, W30, BZ and LX , 100ppm)

solutions suggests that the humic is not acting as a colloidal scatterer.

5.3.6 Effect of solution pH on the synchronous fluorescence spectra of 2-hydroxy benzoic acid

2-hydroxy benzoic acid (1×10^{-4}M) was dissolved in HPLC water and 12 aliquots were placed into glass vials. The pH of each vial was adjusted with sodium hydroxide or hydrochloric acid to produce solutions with a range of pH values. The solutions were immediately scanned in the synchronous fluorescence mode across the same wavelength range as for humic acid with a $\Delta\lambda$ of 20nm. The results are shown in Figure 5.15.

Results and discussion of the effect of pH on the synchronous fluorescence spectra of 2-hydroxy benzoic acid

There are 5 main peaks that can be identified in 2-hydroxy benzoic acid spectra, at 370, 436, 450, 464 and 478 nm. All peaks, except the peak at 350nm, are reduced as pH is lowered from 7 to 2, which is comparable with the peak at the same position on the humic acid spectra. The peak at 350nm is visible at all pH and could represent the aromatic ring on the 2-hydroxy benzoic acid. If the intensity of the peak at 478nm is plotted as a function of pH (see figure 5.16), the point that represents a 50 % reduction in the fluorescence intensity of the 2-hydroxy benzoic acid is equivalent to its first pKa value, as shown in the 2-hydroxy benzoic acid speciation diagram (figure 5.17). This value, as determined by synchronous fluorescence quenching, is 2.85, and may be compared with the actual value of 2.81 (99). The humic pH quenching spectra were examined in the same way, and the decrease of the intensity of the peak at 480nm was plotted against pH, the curve is shown in Figure 5.18. The similarity of the two derived curves (5.16 and 5.18) suggests that the peak at 478nm is indicative of a 2-hydroxy benzoic acid grouping

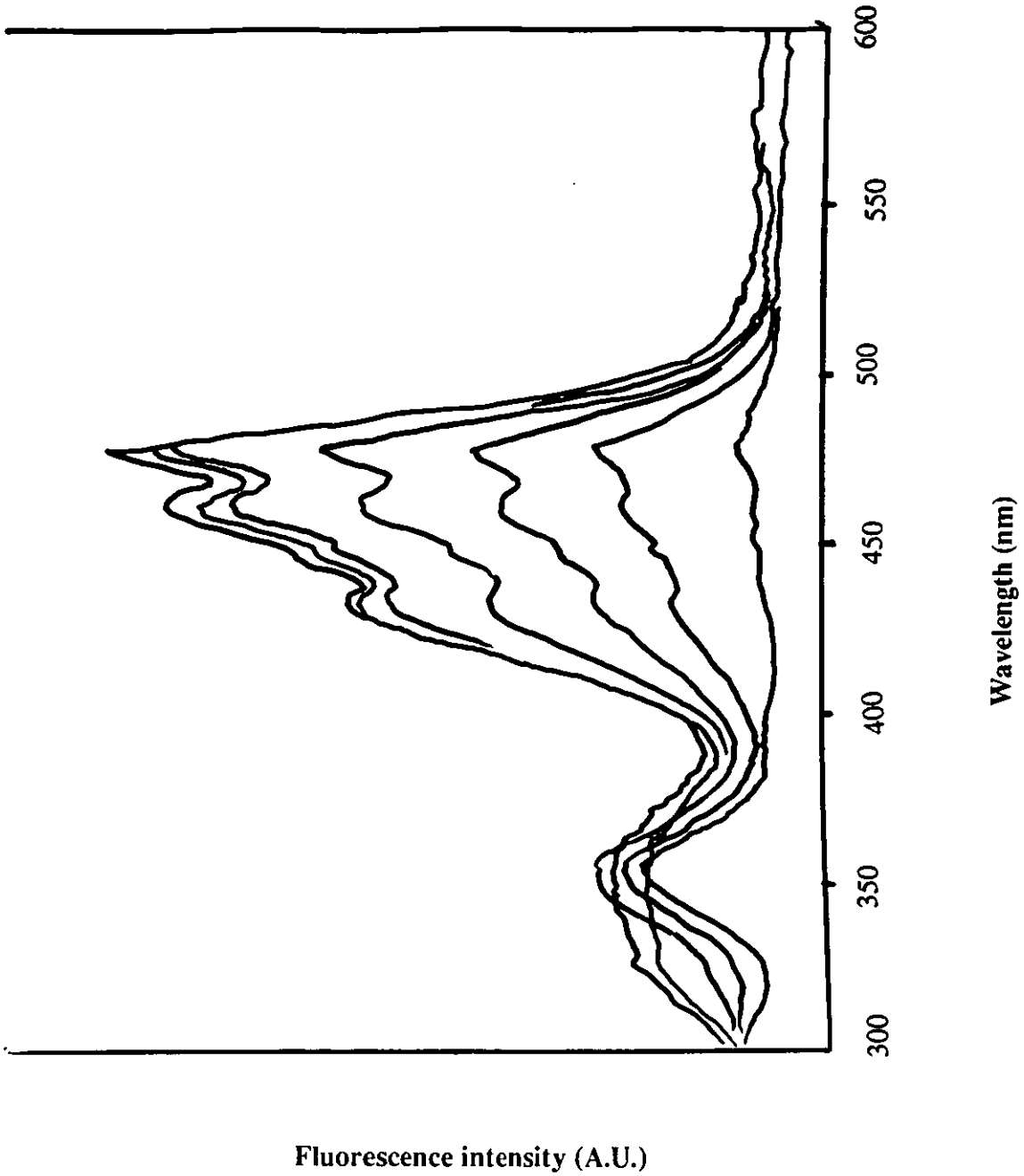

Figure 5.15 Effect of pH on the synchronous spectra of 2-hydroxy benzoic acid

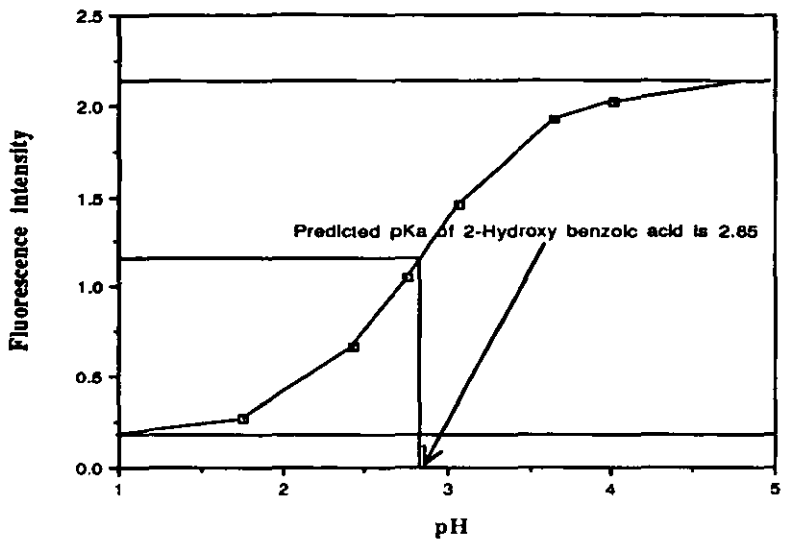

Figure 5.16 Synchronous fluorescence intensity versus pH for 2-hydroxy benzoic acid

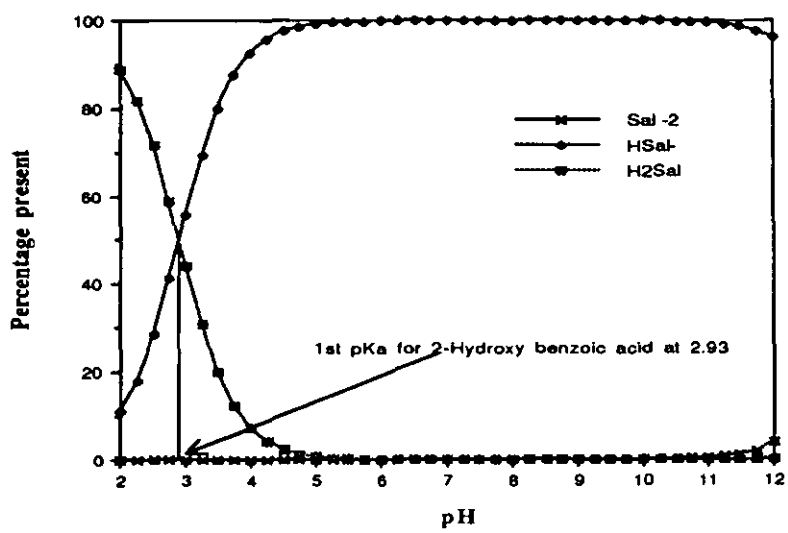

Figure 5.17 Speciation diagram for 2-hydroxy benzoic acid

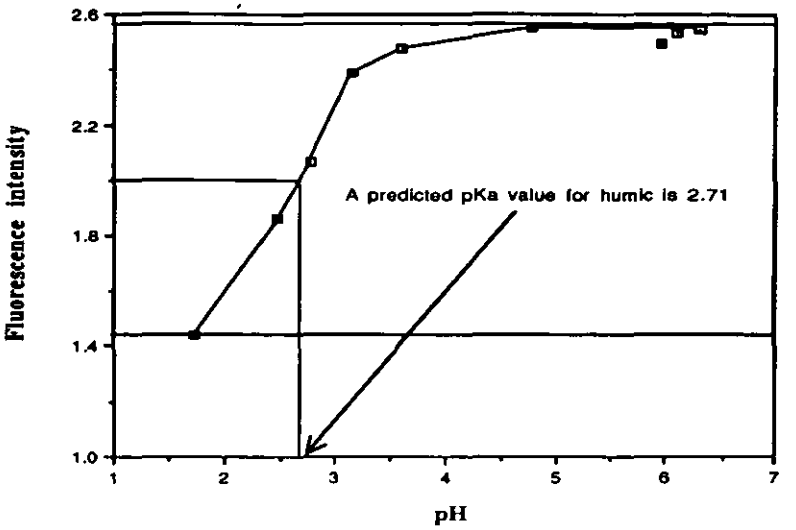

Figure 5.18 Synchronous fluorescence intensity versus pH for humic acid

and that it is this grouping that is responsible for the observed fluorescence of the humic acid molecule.

5.4 FLUORESCENCE MEASUREMENTS OF METAL-HUMATE COMPLEXATION

The quenching of dissolved organic material (DOM) by bound metal ions is the basis of the quantitative metal-DOM binding technique by Weber et al (100-102). Fluorescence quenching of dissolved ligands in solution is useful when solutions of low organic concentrations are involved, but fairly insensitive when low metal concentrations are involved. This is because the low metal concentrations only slightly reduce the free ligand concentration. Changes in the intensity of a single broad peak provide a one dimensional indicator of complexation which cannot differentiate between the cause of quenching e.g the quenching of humate by protons is indistinguishable from that by metals. Synchronous fluorescence is in effect a three dimensional measurement with the λem and λex as the independent variables and I_s as the dependent variable. The high information content of fluorescence is often unrealised because of the broad symmetrical peaks that are obtained from EE fluorescence (103). The use of synchronous fluorescence results in sharper peaks being obtained with greater resolution by cutting diagonally across the EE spectrum (104)(105). In the following the metal binding by humic acid is investigated by synchronous fluorescence to determine whether any new information can be gained on metal-humic binding by the application of this technique. It is important to use metal salts that have the same anion to eliminate any contradicting effect caused by the heavy counter ion.

5.4.1 Metal quenching experiments

Humic acid (12mg) was dissolved in 1 litre of triply distilled water containing 0.01M $NaClO_4$ at a pH of 6.8. Metal salt solutions were prepared by adding the salt to triply distilled water. The following stock metal solutions were prepared:

Copper (ii) Nitrate	$1x10^{-2}$ M
Aluminium (iii) Nitrate	$1x10^{-2}$ M
Nickel (ii) Nitrate	$1x10^{-2}$ M
Calcium (ii) Nitrate	$1x10^{-2}$ M
Europium (iii) Nitrate	$1x10^{-2}$ M
Cobalt (ii) Nitrate	$1x10^{-2}$ M
Zinc (ii) Nitrate	$1x10^{-2}$ M

Aliquots of 1ml of each metal salt solution were added to clean glass vials containing 9ml of the humic acid solution, to give a final metal concentration of $1x10^{-3}$ M, and the solutions were then left for 5 days to reach equilibrium. The synchronous fluorescence spectrum was then recorded for each solution.
Graphs of wavelength versus fluorescence reduction (R) were plotted, where:

$$R = I_{HA\ Blank} - I_{HA\ Metal}$$

where $I_{HA\ Blank}$ is the fluorescence intensity of the humic acid solution alone
$I_{HA\ Metal}$ is the fluorescence intensity of the metal humate solution.

The experiment was repeated using final metal salt solution concentrations of $1x10^{-4}$ M and $1x10^{-5}$ M. The results are shown in Figures 5.19 to 5.25.

Results and discussion on metal quenching

The similarity of the metal quenching spectra (figures 5.19 to 5.25) suggest that the metals bind to similar sites on the humic macromolecule e.g, the copper ion and the cobalt ion, which are present in the same concentrations, both quench the peak at 480 nm, however copper quenches to a greater extent than cobalt. Two possible mechanisms account for the quenching of the humic fluorescence by metals, static quenching by complexation at a fluorescent site on the macromolecule or dynamic quenching whereby the macromolecule is deactivated by collision with ions in solution. Heavy metal ions quench fluorescence by accelerating both the rate of inter system crossing and for paramagnetic ions, the rate of non-radiative processes. These two processes only occur if the metal is associated with the molecule in question. This type of quenching is related to the fraction of ligand sites that are occupied by the metal ion and this is the basis of static quenching. Dynamic quenching is related to the concentration of ions in solution by the Stern-Volmer relationship (106) and increases linearly with metal ion concentration. A plot of the fluorescence reduction against metal concentration would thus be linear for dynamic quenching and non linear for static quenching, as seen in figure 5.26. The degree of quenching is not linearly related to the metal concentration for all the metals except calcium, and the curves that are generated for the other metals reach a plateau at higher metal concentrations. This led to the conclusion that fluorescence quenching is not a collisional mechanism and that a static mechanism gave a better explanation of the experimental results for all the metals except calcium. However the plot of fluorescence reduction against metal concentration for the calcium is linear. This suggests that a collisional mechanism would fit the calcium data with better agreement. Also, it is possible that it is indicative of the strength of the binding between the metal and the humic macromolecule i.e that the order of binding strengths predicted from the degree of fluorescence reduction are Eu > Al > Cu > Co, Ni > Zn > Ca. This is supported by their stability constants between the metal and a humic molecule being Eu 1.3, Al 1.3 > Cu 1.5 > Zn 2.3 >Co, Ni 2.7 > Ca 3.2 (107).

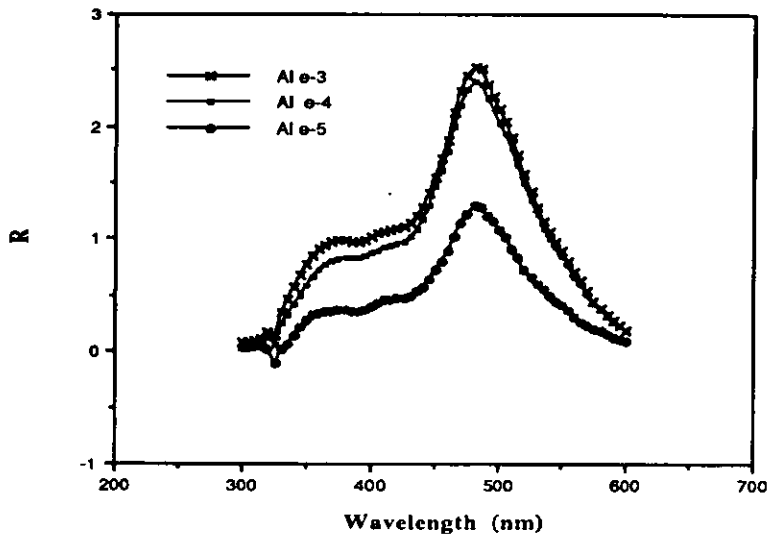

Fig 5.19 Effect of aluminium on the synchronous fluorescence of humic acid

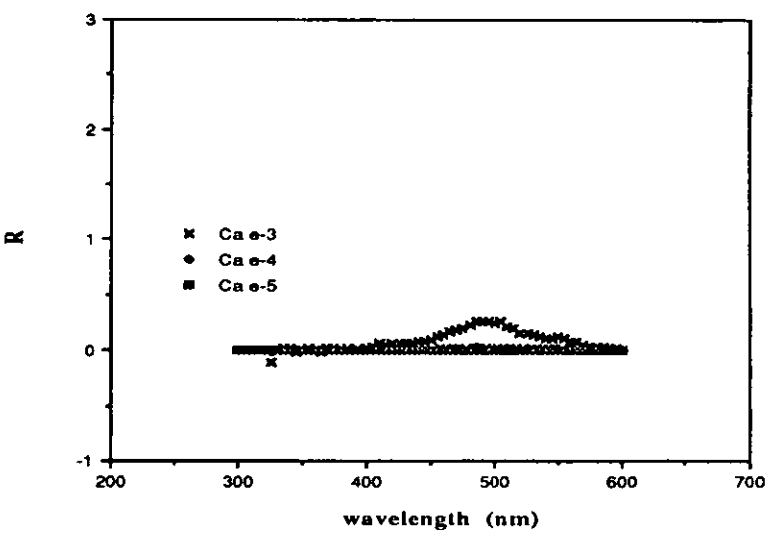

Fig 5.20 Effect of calcium on the synchronous fluorescence of humic acid

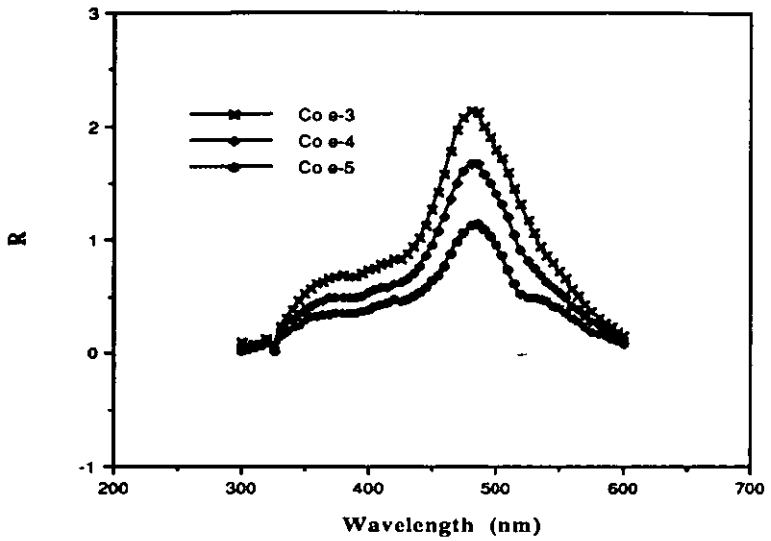

Fig 5.21 Effect of cobalt on the synchronous fluorescence of humic acid

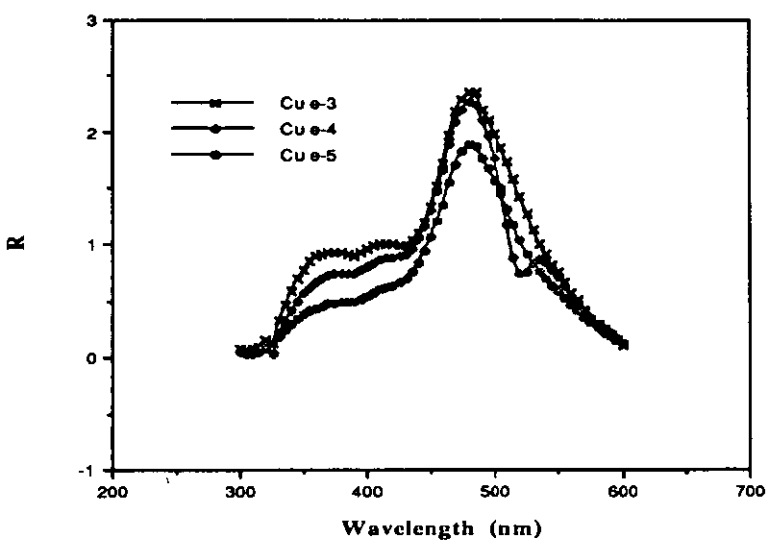

Fig 5.22 Effect of copper on the synchronous fluorescence of humic acid

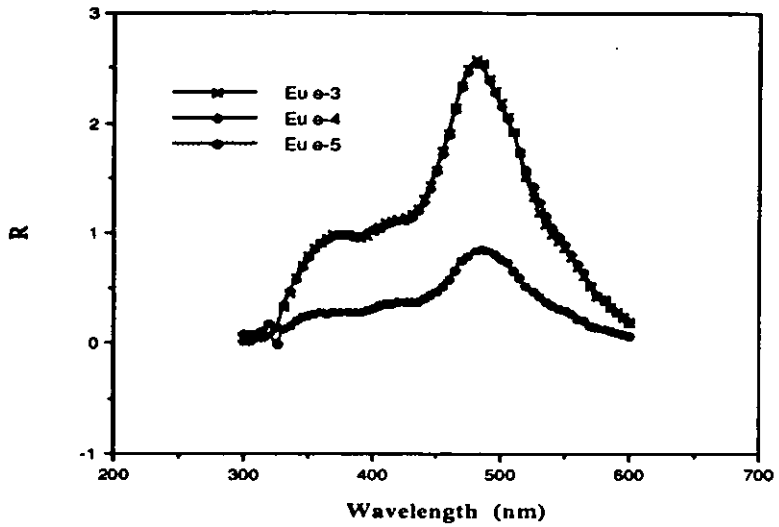

Fig 5.23 Effect of europium on the synchronous fluorescence of humic acid

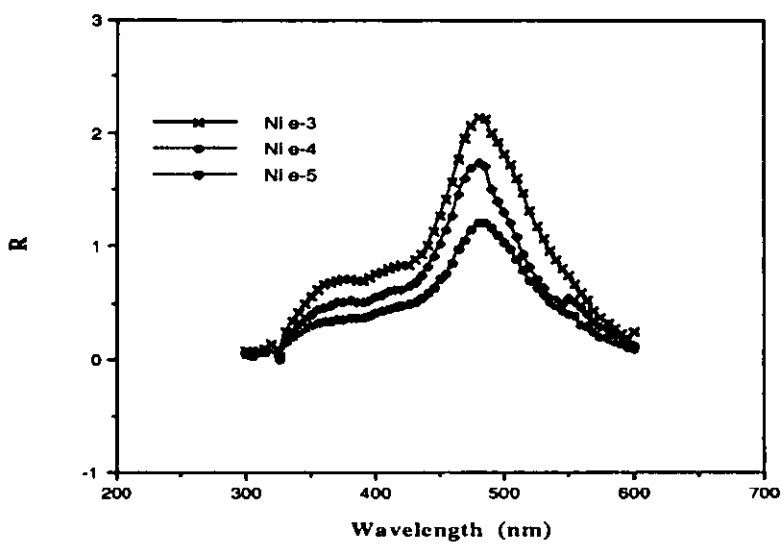

Fig 5.24 Effect of nickel on the synchronous fluorescence of humic acid

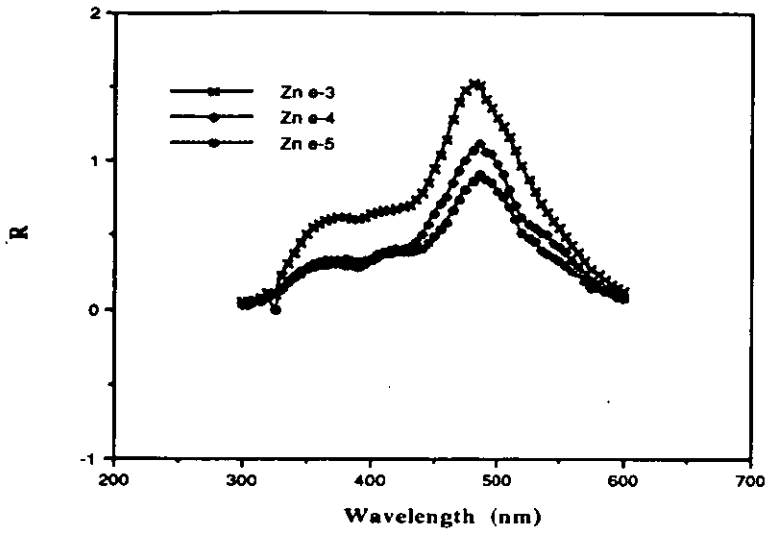

Fig 5.25 Effect of zinc on the synchronous fluorescence of humic acid

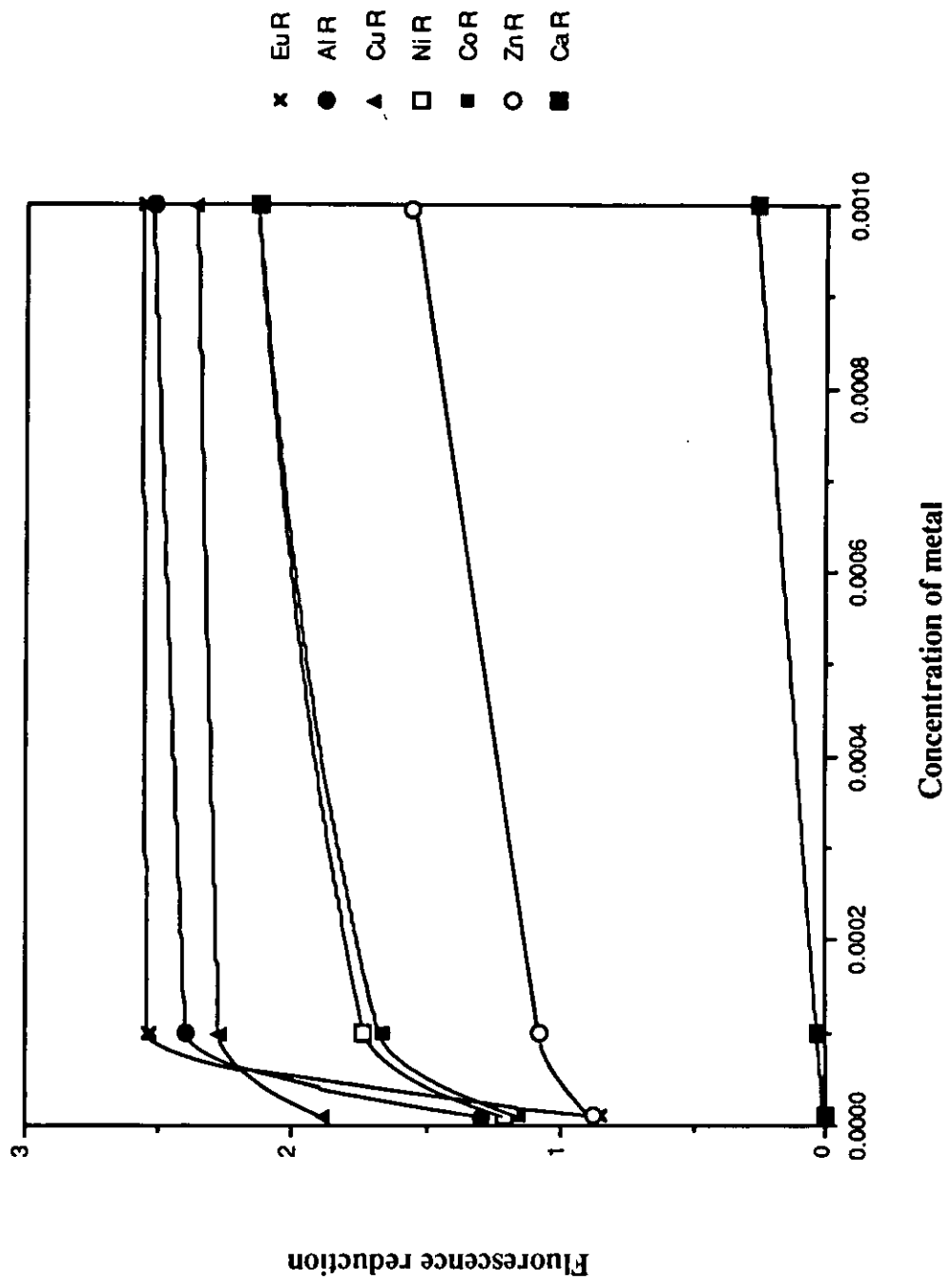

Fig 5.26 Plots of fluorescence reduction against metal concentration

5.5 METAL COMPETITION

An attempt was made to discover whether the fluorescence quenching phenomenon could be used to study calcium / metal competition effects, in the presence of relatively large concentrations of calcium (1×10^{-4} M to 1×10^{-3} M) (12) such as would be present in an environmental water. Calcium competition for binding sites could lead to a reduction in trace metal complexation. Any reduction in trace metal uptake by humic material would be seen as beneficial, since potential transport through the environment would be reduced. Competition for binding sites on a humic material by calcium and a trace metal arise primarily from mass action. Mass action competition occurs when both metals could bind at the same ligand site, but one occupies so many sites that the binding of the second metal is significantly reduced. The way to examine competitive effects within a metal ligand system is to look at the additivity of the spectra. In the absence of interaction between two metals (A and B), the quenching spectrum of the mixture HA+A+B should be simply the sum of the spectra observed from HA+A and HA+B. In the presence of competition, the combined spectrum observed from the mixture will not be simply the sum of the spectra observed from HA+A and HA+B. A realistic calcium concentration (1×10^{-3}M) was used. And, to give the best possible chance of seeing a competitive effect, it was decided to use the highest metal concentration (1×10^{-5}M) as mentioned (108) to ensure a maximum saturation of sites, but avoiding precipitation. The following describes experiments to investigate the competition of calcium and metal for humic binding using the additivity of spectra theory.

5.5.1 Calcium competition experiments

Humic acid (12mg) was dissolved in 1 litre of triply distilled water containing 0.01M $NaClO_4$ at a pH of 6.8. Metal salt solutions were prepared by adding the salt to triply distilled water. See section 5.6.1 for details of salts used.

Aliquots of 1 ml of each metal salt solution (1×10^{-4}M) and 1ml of calcium nitrate solution (1×10^{-2}M) were added to a clean glass vial containing 8ml of the humic acid solution, to give final metal concentrations of 1×10^{-5} M and a calcium concentration of 1×10^{-3} M. The solutions were then left for 5 days to reach equilibrium. The synchronous fluorescence spectrum of each solution was then recorded. The spectra of the metal humate and calcium humate alone were also recorded. Graphs of wavelength versus fluorescence reduction (R) were plotted, where:

$$R = I_{HA\ Blank} - I_{HA\ Metal}$$

where $I_{HA\ Blank}$ is the fluorescence intensity of the humic acid solution alone

$I_{HA\ Metal}$ is the fluorescence intensity of the metal humate solution.

The recorded spectra of the metal humate and calcium humate were used to predict the spectra of the metal humate / calcium humate mixed system. The predicted spectra were then compared with that of the actual spectra of the mixtures. The results are shown in figures 5.27 - 5.32.

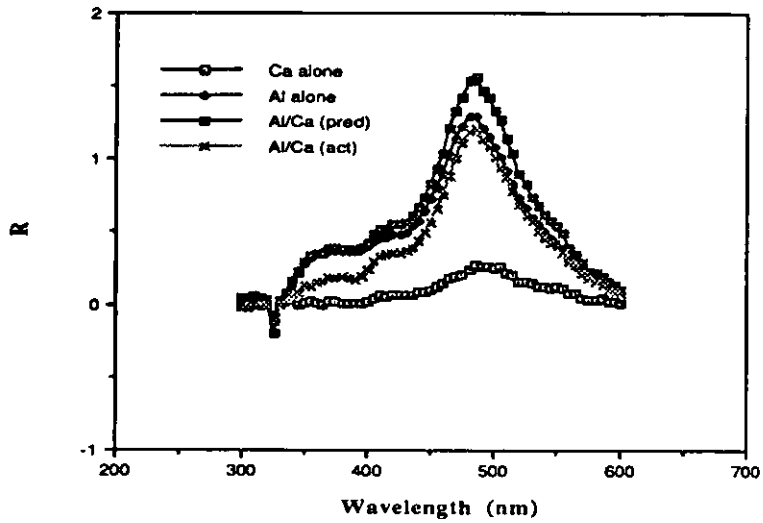

Fig 5.27 Competition for binding of aluminium and calcium to humic acid

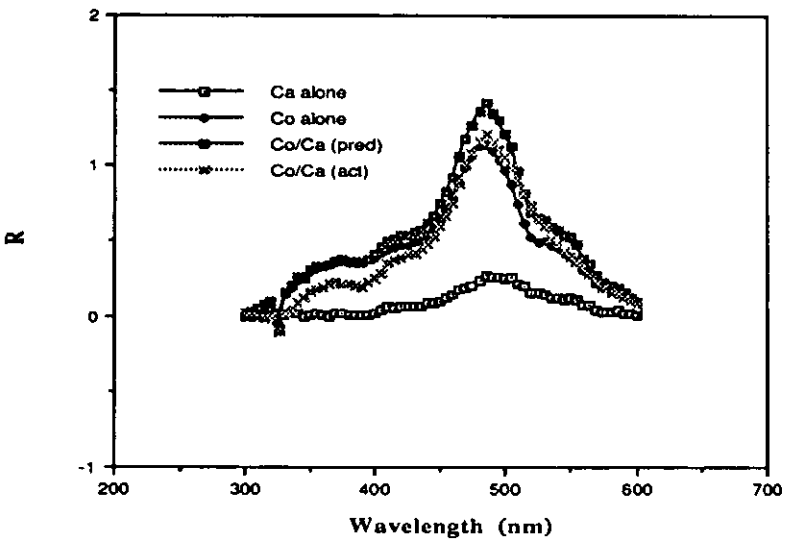

Fig 5.28 Competition for binding of cobalt and calcium to humic acid

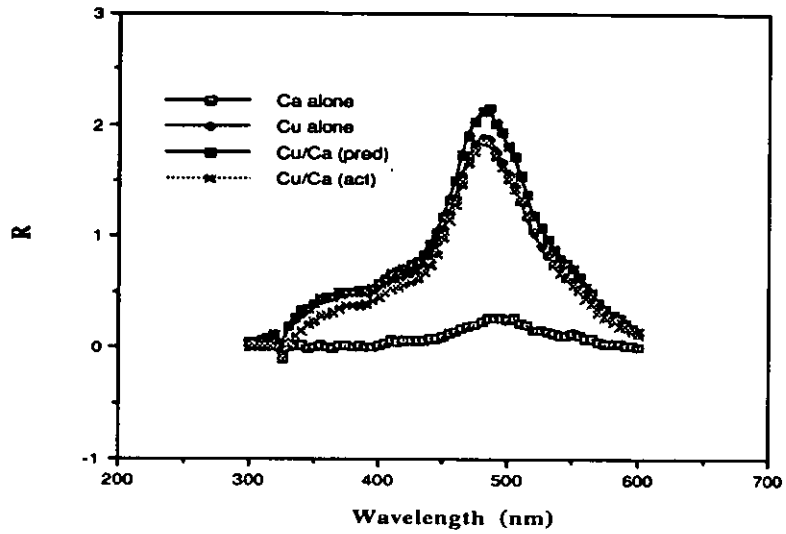

Fig 5.29 Competition for binding of copper and calcium to humic acid

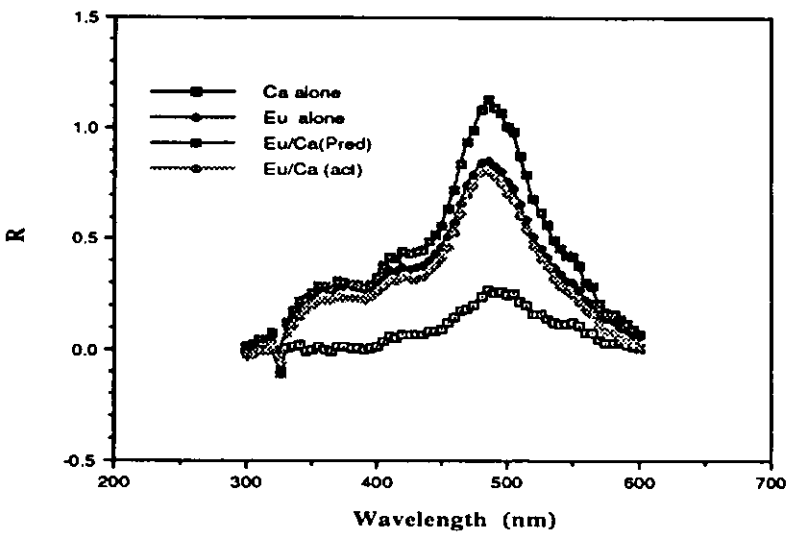

Fig 5.30 Competition for binding of europium and calcium to humic acid

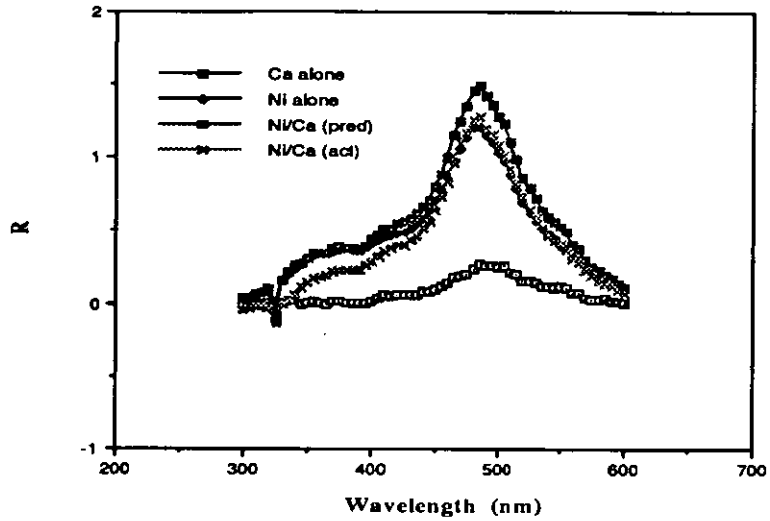

Fig 5.31 Competition for binding of nickel and calcium to humic acid

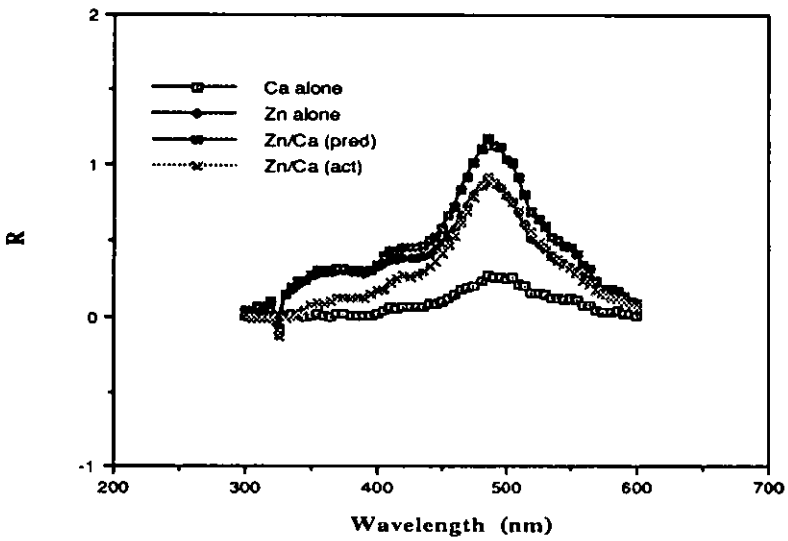

Fig 5.32 Competition for binding of zinc and calcium to humic acid

5.5.2 Results and discussion of metal competition

From the fluorescence spectra of the metal / calcium humate competition reactions it can be seen that the actual spectra of the mixtures are less than the predicted spectra, and the spectra observed for the mixtures are very similar to the spectra of the competing metal cation alone. These observations suggest that under these conditions no fluorescence reduction was observed so calcium competition has no effect on the binding of the competing metal at these concentrations. This was the conclusion was also reached by other workers using different techniques to study calcium competition reactions e.g Maes et al (108) and Moulin et al(108). Also Morel et al (109) studied the competition between calcium and copper by laboriously titrating the three systems involved and found that the predicted data were an overestimation of the actual situation. They also concluded that the effect of calcium as a competing metal was of minor (110) concern. This appears to be the case as the calcium does not cause a change in the synchronous fluorescence spectra of the mixture, as compared to that of the metal alone.

5.6 CONCLUSION ON SYNCHRONOUS SCANNING FLUORESCENCE SPECTROSCOPY

The synchronous scan fluorescence spectra appear more structured and resolved than those of conventional fluorescence methods. Because of the complexity and heterogeneity of the humic material, the synchronous scan represents the summation of the spectra of several different fluorophores present in the HA molecule. Although the identification of the prominent chemical structure responsible for the fluorescence of HA is still an open question, the synchronous spectra is able to identify a number of common fluorescent units. The principle advantages of this non-separative, non-destructive technique are the limited requirements for sample preparation and the ability to study substances in the dissolved and suspended state

at concentrations approaching those typical of the natural environments. Although relatively high metal concentrations have been used in the studies reported herein, fluorescence intensity is proportional to the intensity of the excitation beam, and therefore the quenching effects of lower metal concentrations may be observed by using a more intense, e.g laser , excitation source. With respect to conventional fluorescence methods the synchronous fluorescence method offers the possibility of the operator selecting an experimental parameter, $\Delta\lambda$, which greatly contributes to reducing superimposition interference and to achieve, in principle, spectral separation into individual components. Synchronous fluorescence has been used to demonstrate that the 2-hydroxy benzoic acid grouping is responsible for the major peak observed from humic material and is thus a major site on the humic macromolecule. It is also possible to say that the metal complex with this site and quench the macromolecules fluorescence by a static mechanism. It is also apparent that, under the conditions investigated, calcium has no effect on the binding of the other metals investigated.

Chapter Six

References

REFERENCES

Chapter 1

1. Woodwell G.M., Whittaker R.U., Reiners W.A., Likens G.E., Delwiche C.C. and Botkin D.B., Science 199: 141-146, (1978).

2. Sausore T. de Paris Ann. 12: 162, (1804).

3. Döbereiner J.W., Phyto Cheime. 66-74, (1822).

4. Berzelius J.J., Lehrbuch der Chemie, 3rd ed Dresden and Leipzig, (1839).

5. Leenheer J.A. and Huffman E.W.D. Jr., U.S. Geol. Surv. J. Res. 4: 737-751, (1976).

6. Maillard L.C., Ann. Chem. Phys. 5: 258-317, (1916).

7. Kononova M.M., Soil organic matter, Pergamon, Elmsford NY, (1966).

8. Hobson R.P. and Page H.J., J. Agric. Sci. 22: 297-299; 497-515; 516-526, (1932).

9. Waksman S.A., Williams and Wilkins, Baltimore, M.D. (1936).

10. Flaig W. Coal Sci. (Adv. Chem. Ser.) 55: 64-65, (1966).

11. Thurman E.M., PhD Thesis, University of Colorado. Boulder, (1979).

12. Buffle J.Complexation reactions in aquatic systems.An analytical approach.Ellis Horwood series in analytical chemistry.John wiley and sons.(1988)

13. Guy Robert D. and Chakrabart C.L., Can. J. Chem. 54: 2600-2611, (1976).

14. Rainville D.P., and Weber J.H., Can. J. Chem. 60: 1-5, (1982).

15. Kim, J.I., Handbook of Phys. and Chem. of the Actinides, Vol 4, Eds. Freeman A.J. and Keller C., North Holland Phys. Publ. Amsterdam, Chap. 7.

16. Schnitzer, M., Soil. Sci. Soc. Am. Proc. 33: 75-81, (1969).

17. Gamble D.S., Can. J. Chem. 48: 2662-2669, (1970).

18. Stevenson F.J., Wiley-Interscience, New York, 443, (1982).

19. Perdue E.M and Lytle C.R. In aquatic and terrestial humic materials .Christman R.F and Gjessing E.T.(eds) Ann.Arbor.Science.Michigan 48106.USA. (1982)

20. Scatchard G. Ann.N.Y.Acad .Sci.51:660-672 (1949)

21. Klotz M. Science 217:1247-1249 (1982)

22. Buffle J. .Anal.Chem. 49:216-222 (1977)

23. Cabaniss S.E, Shuamn M.A and Collins B.J.
Kramer C.J.M and Duinker J.C.(eds). Nijhoff/junk. Germany 1984

24. Byrne R.H. Trace metal complexation in high ligand variety media. Mar.Chem.12:15-24 (1983)

25. Mattigod S.V. and Sposito G. ACS. Symposium Series No.93. Chemical Modelling in Aqueous Systems.Ed. E.A.Jenne. ACS.37:837-856 (1979).

26. Altmann R.S and Buffle J.Geochim.Cosmochim.Acta. 52:1505-1519 (1988)

27. Dzombak D.A, Fish W and Morel F.M.M.Environ.Sci .Technol. 20:7:669-675 (1986)

28. Dzombak D.A, Fish W and Morel F.M.M. 2.Environ.Sci .Technol. 20:7:676-683 (1986)

29. Shuman M.S, Collins B.J, Fitzgerald P.J and Olsen D.L.. In aquatic and terrestial humic materials .Christman R.F and Gjessing E.T.(eds) Ann.Arbor.Science. Michigan 48106.USA. (1982)

30. Gamble D.S. .Can.J.Chem.48:2662-2669 (1970)

31. Gamble D.S , Underdown A.W and Langford C.H.
analysis.Anal.Chem. 52:1901-1908 (1980)

32. Buffle J. Natural organic matter and metal-organic reactions in aquatic systems, in metal ions in biological systems. Vol 18.Circulation of metals in the environment.A.Sigel(ed) Marcel Dekker.New York (1984)

33. Altmann R.S. and Buffle J. Geochim et Cosmochim Acta, 52, 1505-1519, (1988).

34. Dzombak D.A., Fish W. and Morel F.M.M. Environ. Sci. Technol. 20, 7, 669-675, (1986).

35. Fish W. Dzombak D.A. and Morel F.M.M. Environ. Sci. Technol. 20, 7, 676-683, (1986).

36. Buffle J. and Altmann R.S. In Aquatic surface chemistry: Chemical processes at the particle-water interface. Stumm W. (ed), J. Wiley & Sons, NY, 351-383, (1987).

37. Ashton J.,Broyd T.W.,Jones M.A.,Knowles N.C.,Liew S.K.,Mawbey C.S.,Read D. and Smith S.L. A directory of computer programs for assessment of radioactive waste disposal in geological formations.CEC report:EUR 14201/1EN (1993)

38. Dobbs J.C., Suseteyo W.,Carreira L.A. and Azarraga.L.A.Anal .Chem.61:1519-1524(1989)

39. PerdueE.M.,ReuterJ.H.andParrish.R.S.Geochim .Cosmochim.Acta. 48:1257-1263(1984)

40 Suseteyo W., Carreira L.A. Azarraga L.A. and Grimm D.M. Fresnius.J.Anal .Chem339:624-635(1991)

Chapter 2

41. Miles C.J., Tuschall J.R. Jr, Brezonik P.L., Anal. Chem. 55: 410-411, (1983).

Chapter 3

42. Schnitzer M., In Soil Biochemistry, Vol. 2. (A.D. McLaren and J. Skkujins, eds.), Marcel Dekker. New York, 60-95 (1971).

43. Schnitzer M., Soil organic matter (M. Schnitzer and S.U. Khan, eds.), Elsevier, New York, 1-64, (1978).

44. Schnitzer M. and Khan S.U., Humic Substances in the Environment. Marcel Dekker. New York, 327, (1972).

45. Ghosh K. and Schnitzer M., J. Soil Sci. 30: 735-745, (1979).

46. Chen Y., Senesi N. and Schnitzer M., Soil Sci. Soc. Am. J. 40: 682-686, (1977).

47. De Haan H., Aquatic and Terrestrial Humic Materials (R.F. Christman and E.T. Gjessing, eds.) Ann. Arbor Science, Michigan, 165-182, (1983).

48. Flaig W., Bectelspacher H., Rietz E., Soil components: Volume 1. Organic Components (J.E. Gieseking, eds.). Springer-Verlag, New York, 1-211 (1975).

49. Ghosh K. and Schnitzer M., Can. J. Soil Sci. 60: 373-379, (1980).

50. See ref. 19, page 184.

51. Ryan D.K. and Weber J., Anal. Chem. 54: 986-990, (1982).

52. Plechanov N., Org. Ceochem. 5: 143-149, (1983).

53. Cross R.A. and Strathmann H., Wiley Interscience, New York, 469-496, (1973).

54. Buffle J., Deladoey P., Haerdi W., Anal. Chim. Acta. 101, 339-357, (1978).

55. Swift R.S. and Posner A.M ., J. Soil. Sci 22: 237-249, (1971).

56. Kolesnikov M.P., So. Soil Sci. 10: 174-181 (1978).

57. Goh K.M. and Williams M.R., J. Soil. Sci. 30: 747-755, (1979).

58. Dannesberg O.H., Bodenkultur, 32: 93-104, (1981).

59. Dawson H.J. et al. Soil. Sci. 132: 191-199, (1981).

60. Archibald W.J., J. Phys. Colloid Chem. 51: 1204, (1947).

61. Cameron R.S. et al. J. Soil Sci. 23: 394-408, (1972).

62. Ritchie G.S.P. and Posner A.M., J. Soil. Sci. 33: 233-247, (1982).

63. Reid P.M., et al. Geochim. Cosmochim. Acta. 54: 131-138, (1989)..

64. Hayes M.H.B. and Swift R.S. The Chemistry of Soil Constituents (D.J. Greenland and M.H.B. Hayes, eds.) Wiley-Interscience, New York, 179-230, (1978).

65. Thurman E.M., 'Organic Geochemistry of Natural Waters', Martinus Nijhoff, D. W. Junk, Dordrecht, The Netherlands, (1985).

66. Stevenson F.J. and Butler J.H.A., Organic Geochemistry (G. Eglinton and
M.T .J. Murphy, eds.) Springer-Verlag, New York, 534-557, (1969).

67. Perdue E.M. et al. Geochim. Cosmochim. Acta 44: 1841-1851, (1980).

68 . Peachey D. and Williams G.M., BGS Report, FLPU 87-5, (1987).

69. Steelink C.. Aiken G.R., McKnight D.M., (eds). Wershaw R.L. Wiley-Interscience, Chap.18 (1985).

70. Borggaard O.K.Acta.Chem.Scand.28:121-122(1974)

Chapter 4

71. Rainville D.P. and Weber J.H.Can.J.Chem:60,1(1982)

72. Truitt R.E. and Weber J.H.Anal.Chem:53,337(1981)

73. Davison W. and Whitfield M.J.Electroanal.Chem:75,763(1977)

74. Turner D.and Whitfield M. in Marine Electrochemistry, Whitfield M and Jagner D.(eds),Chap 2.Wiley.New.York (1981)

75. Dawson H.J.,Hrutfiord B.F.,Zasoski R.J. and Ugolini F.C.Soil. Sci: 132 191(1981)

76. Lindqvist I.Acta.Chem.Scand:28,823(1974)

77. Chian E.S.K.Water.Res:11,225(1977)

78. Weber J.H. and Wilson S.A..Water.Res:9,1079(1975)

79. Campbell P.G.C.,Bisson M.,Gagne R. and TessierA. .Anal. Chem:49. 2358 -2362.(1977)

80. Kim, J.I., Buckau, G., Bryant, E. and Klenze, R. . Radiochim. Acta: 48.135-143.(1989)

81. Tuschall J.R.and Brezonik P.L.Anal.Chim.Acta:149.47.(1983)

82. Buffle J.Greter F.L.and Haerdi W. electrodes.Anal.Chem:49.216-222.(1977)

83. Saar R.A. and Weber J.H. .Can.J.Chem:57 (11).1263-1268.(1979)

84. Cabaniss, S.E. and Schuman, M.S. Fluorescence quenching measurements of copper-fulvic acid binding. Anal. Chem. 60, 2418 - 2421. (1988).

85. Ventry L.S. Ryan D.K Gilbert T.R.Microchemical. Journal.

86. Schubert, J . I.J. Phys and Coll. Chem. 52, 340 - 356.(1948)

87. Kunin R.Ion Exchange Resins.2nd eds John wiley and sons.NewYork: page26

88. Smith and Martell.Critical.Stability.Constants.Plenum press.Newyork. London: Vol 6 (1989)

89. Moulin V.,Tits J. and Ouzounian G..Radiochimica.Acta: 58/59,179-190(1992)

90. Warwick P.,Bennett J.,Riley L.,Zhu D.,Hall A. and Williams G.M. EC Report: EUR15160 EN (1994)

91. Choppin G.R.and Clarke S.Chemical Modelling of Aqueous Systems II.ACS Symposium Series.No.416:40,519-525(1990)

Chapter 5

92 Nguta.C.M.Ph.D thesis.Loughborough University(1990)

93 Lloyd J.B.F.J.Forensic.Sci.Soc.2:83.(1971)

94 Lloyd J.B.F.J.Forensic.Sci.Soc.2:153.(1971)

95 Lloyd J.B.F.J.Forensic.Sci.Soc.2:253.(1971)

96 Passwater R.A.Guide to fluorescence literature.Plenum press.New York.1967

97 Vo-Dinh T.,Anal. Chem.50:396-401, (1978).

98 Rubio S., Gomez-Hens A., Valcarel M., Tatlanta.33: 633-640, (1986)

99 Smith and Martell.Critical.Stability.Constants.Plenum press.Newyork. London: Vol 6 (1989)

100 Saar R.A. and Weber J.H.Anal.Chem.52:2095.(1980)

101 Ryan D.K. and Weber J.H.Anal.Chem.54:986.(1982)

102 Ryan D.K. and Weber J.H.Environ.Sci.Technol.16:866.(1982)

103 Miller J.N.Analyst.109:191.(1984)

104 Lloyd J.B.F.Nature.231:64.(1971)

105 Vo-Dinh T.Appl.Spectrocopy.36:576.(1982)

106 Green S.A., Morel F.M.M. and Blough N.V.Environ.Sci.Technol.:26. 294(1992)

107 Private communications.Radiochemistry.Group.Loughborough University(1994)

108 Kim J.I., Moulin V., Marquard C. and Maes A.Institut Fur Radiochemie 5th progress report (RCM00794) (1994)

109 Morel F.M.M. And Hering J.G.Environ.SCi.Technol:22,1234(1988)

110 Morel F.M.M.Principles of aquatic Chemistry.1st ed.johnwiley and sons:New York,147-180(1983)